The CD8+ memory T cell response following PLGA microparticle immunization

Dissertation zur Erlangung des

akademischen Grades eines Doktors der Naturwissenschaften

(Dr. rer. nat.)

vorgelegt von

MacKerracher, Anna

an der

Universität Konstanz

Mathematisch-Naturwissenschaftliche Sektion

Fachbereich Biologie

Konstanz, 2021

Tag der mündlichen Prüfung: 05. April 2022

1. Referent/Referentin: Prof. Dr. Marcus Groettrup

2. Referent/Referentin: Prof. Dr. Oliver Planz

Table of contents

Abstract

The ongoing COVID-19 pandemic has had an enormous impact on societies and highlights more than ever the need for effective vaccines. High efficacy requires the ability to induce long lasting and functionally efficient memory responses. In this respect the critical role of tissue-resident memory T cells (T_{RM} cells) in offering protection from recurring infections and malignant tumors is becoming increasingly clear. Due to their presence in many barrier tissues, T_{RM} cells are ideally located to rapidly respond to re-encountered pathogens. Moreover, a host of studies has shown that the quantity of T_{RM} cells correlates with increased survival rates in cancer patients. Therefore, vaccination strategies which induce a strong and sustained T_{RM} cell response are particularly promising.

To this end we and others have studied the use of poly-(D,L-lactic-*co*-glycolic) acid microspheres (PLGA MS) as a vaccine delivery system. Various antigens and adjuvants can be encapsulated into these particles for efficient delivery. In aqueous solutions the polymers are slowly hydrolyzed thereby releasing the content and efficiently delivering the antigens to dendritic cells (DCs) in a targeted manner. Since complete hydrolysis in the body takes 30 days, PLGA MS create a depot effect at the site of injection which leads to prolonged antigen presentation by DCs. In past projects we have shown that immunization with these PLGA MS can protect mice from influenza A virus (IAV) infection as well as tumor growth. However, we have hitherto not studied the different $CD8^+$ memory T cell subtypes generated in response to PLGA MS immunization.

In this study we show that a subcutaneous prime followed by an intranasal boost immunization led to a strong T_{RM} cell response in the lungs and airways of mice 6 days after the boost vaccination. Although numbers subsequently declined over time, T_{RM} cells were still detectable 60 days post boost. To study the protection from tumor growth we generated a tumor cell line stably expressing the model antigen ovalbumin (Ova) together with the enzyme luciferase. Using this cell line, we were able to track tumor growth *in vivo* and analyze the antitumor protection induced by immunizing mice with Ova-bearing PLGA MS. We observed that immunized mice were protected from lung metastasis formation when mice were challenged with i.v. injected tumor cells 6 days post boost. By treating mice with an inhibitor of lymphocyte recirculation, we were able to show that the local memory response was sufficient to protect mice from tumor development. Gradually this protective effect decreased, but even when tumor cells were injected 60 days after the boost immunization mice still showed some level of protection.

Furthermore, we looked at the capacity of T_{RM} cells to protect mice from infection with IAV. The currently employed influenza vaccines mainly induce neutralizing antibodies that recognize the surface proteins hemagglutinin and neuraminidase. As these are highly prone to mutation, the

vaccine formulation has to be updated every season. In contrast to antibodies, the majority of the $CD8^+$ T cell response is directed at internal virus proteins which are highly conserved and far less susceptible to mutation. A vaccine that induces long-lasting T_{RM} cell populations could potentially alleviate the problems associated with the current influenza vaccines.

We found that the $CD8^+$ T_{RM} cells induced by PLGA MS immunization protected mice from high viral titers, body weight loss and death induced by infection with a recombinant IAV. While mice immunized with antigen-bearing PLGA MS showed significantly reduced symptoms of IAV infection when they were infected 6 days after the boost, this effect was strongly diminished when the infection occurred after 30 days.

Taken together, these results show that the ability of PLGA MS to induce a strong protective T_{RM} cell response further supports their use as a potent vaccination strategy.

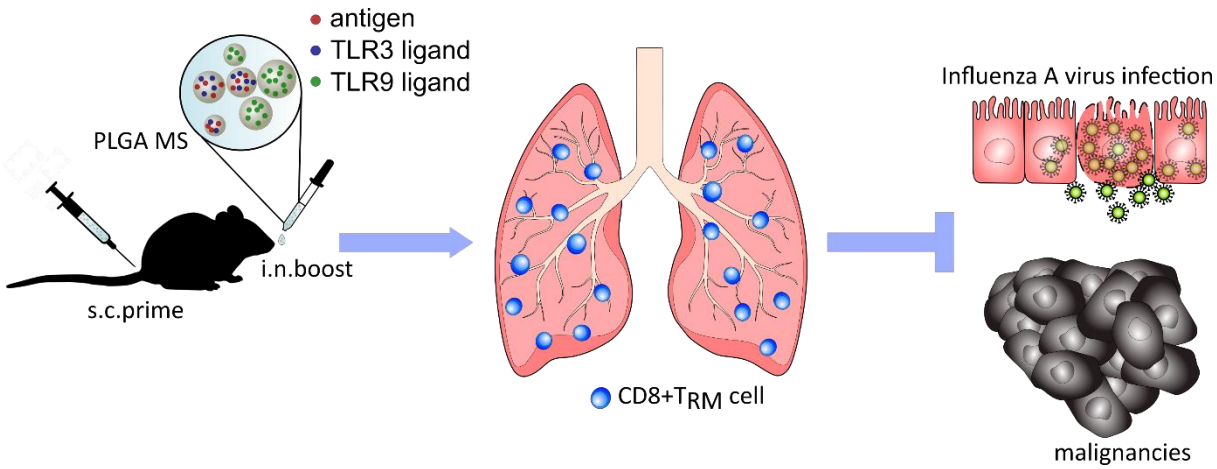

Figure 1: Graphical Abstract of the thesis

In a second project, we tried to encapsulate whole, inactivated IAV into PLGA MS. After comparing different methods of inactivation, we looked at the release characteristics of PLGA MS into which inactivated virus had been encapsulated. We found that these particles only released protein content during the first 24h, indicating that the virus had not been encapsulated but only bound to the surface. To verify this, we compared the morphology of these particles using scanning electron microscopy but were not able to detect any obvious differences. Moreover, we immunized mice with these PLGA MS to analyze the *in vivo* response but we were not able to observe a significant immune response induced by virus-containing PLGA MS compared to empty or adjuvant-only PLGA MS. Thus we concluded that it was not possible to encapsulate whole virus and that the virus bound to the surface was not sufficient to induce an antiviral immune response.

Zusammenfassung

Durch die COVID-19 Pandemie sind Impfstoffe, die einen breiten, langanhaltenden Impfschutz auslösen, besonders in den Fokus gerückt. Damit Impfungen lange Schutz bieten ist es wichtig, dass sie eine gute Gedächtnisantwort auslösen. Seit ihrer Entdeckung vor etwa 20 Jahren haben lokale, im Gewebe verbleibende Gedächtnis-T-Zellen (engl. tissue-resident memory T cells, T_{RM}) immer mehr an Bedeutung gewonnen. Durch ihre Lage im Gewebe sind diese Zellen direkt an vorderster Front, wenn Pathogene erneut auftreten. Eine Vielzahl an Studien hat gezeigt, dass diese T_{RM}-Zellen exzellenten Schutz vor vielen Infektionen und Tumorerkrankungen bieten. Daten von Krebspatienten zeigen außerdem, dass eine erhöhte Anzahl an T_{RM}-Zellen mit einer höheren Überlebensrate korreliert. Daher ist es nicht verwunderlich, dass die Entwicklung von Impfstrategien, welche zur Bildung dieser Zellen führen, von hoher Bedeutung ist.

In unserer Gruppe arbeiten wir an einer Impfstrategie, die auf Mikrosphären (MS) aus dem Polymer poly-(D,L-lactic-*co*-glycolic) acid (PLGA) beruht. Diese PLGA MS sind biologisch abbaubar und werden im Körper über einen Zeitraum von etwa 30 Tagen hydrolysiert. Mittels Sprühtrocknung ist es möglich verschiedene Antigene und Adjuvanzien in diese Partikel zu verpacken, die nach der Verabreichung langsam freigesetzt werden und zu dendritischen Zellen gelangen, welche die Antigene auf ihrer Oberfläche präsentieren. Frühere Projekte unserer Gruppe haben gezeigt, dass es möglich ist mit Hilfe dieser Immunisierungsmethode Mäuse sowohl vor verschiedenen Tumorerkrankungen als auch vor Influenza-Infektion zu schützen. Die $CD8^+$ T-Gedächtnisantwort und die Bildung der verschiedenen Gedächtniszellsubtypen haben wir bisher nicht erforscht.

Die vorliegende Arbeit zeigt, dass eine subkutane Impfung gefolgt von einer intranasalen Auffrischimpfung („boost“) 14 Tage später zur Bildung von $CD8^+$ T_{RM}-Zellen in der Lunge und den Atemwegen führt. Obwohl die Anzahl dieser Gedächtniszellen mit der Zeit schrumpfte, waren selbst 60 Tage nach dem boost noch spezifische Zellen auffindbar. Um zu untersuchen, ob diese T_{RM}-Zellen auch einen Schutz vor Tumorwachstum bieten, wurde eine Tumorzelllinie generiert, die sowohl das Modellantigen Ovalbumin (Ova) als auch das Enzym Luziferase exprimiert. Dadurch wurde es möglich Mäuse mittels Ova-haltigen PLGA MS gegen die Tumorzellen zu impfen, 6 Tage später die Tumorzellen zu injizieren und anschließend mit Hilfe der Luziferase das Tumorwachstum *in vivo* zu beobachten. Um zu erforschen, welchen Schutz die lokalen T_{RM}-Zellen ohne die Hilfe von rezirkulierenden Lymphozyten bieten, wurden einige Mäuse mit einem Inhibitor behandelt, der verhindert, dass Lymphozyten aus dem Lymphknoten aus- und in die Lunge einwandern. Wir konnten zeigen, dass Ova-geimpfte Mäuse vor Tumorwachstum geschützt waren und eine geringere Anzahl an Metastasen aufwiesen und dass dieser Schutz durch die lokale Gedächtnisantwort ausreichend gegeben

war. In weiteren Experimenten wurden die Tumorzellen zu späteren Zeitpunkten injiziert, um herauszufinden, wie lange der Schutz anhält. Obwohl der Schutz mit der Zeit geringer wurde, konnten wir dennoch beobachten, dass Ova-immunisierte Mäuse besser vor Tumorwachstum geschützt waren als die Kontrollgruppen.
Als nächstes wollten wir untersuchen, ob die T_{RM}-Zellen in unserem Modell auch vor Influenza-Infektionen schützen können. Bisherige Grippeimpfstoffe zielen vor allem auf die Bildung von Antikörpern gegen die Oberflächenproteine Hämagglutinin und Neuraminidase ab. Da diese beiden Proteine sehr anfällig für Mutationen sind, ist eine jährliche Reformulierung des Impfstoffes notwendig. Im Gegensatz zu Antikörpern zielen $CD8^+$ T Zellen vor allem auf interne, weniger mutationsanfällige Virusproteine ab. Daher könnte ein Impfstoff, der zur Bildung von $CD8^+$ T-Gedächtniszellen führt, den Impfschutz deutlich verbessern.
Um den Schutz vor Influenza nach PLGA MS Immunisierung zu untersuchen, wurden die Mäuse 6 Tage nach der Boosterimpfung mit einem rekombinanten Influenza A Virus (IAV) infiziert. Wir konnten zeigen, dass eine vorherige Impfung die Mäuse vor hohen Virustitern in der Lunge sowie starkem Gewichtsverlust und Tod schützt und dass die Anwesenheit der lokalen T_{RM} Zellen für diesen Schutz ausreichend war. Bei einer Infektion 30 Tage nach der Auffrischimpfung war dieser Schutz nicht mehr signifikant, allerdings immer noch in geringem Ausmaß vorhanden.

In einem zweiten Projekt ging es darum ganzen, inaktivierten IAV, anstatt kurzer viraler Peptide, in PLGA MS zu verpacken. Zuerst wurden verschiedene Inaktivierungsmethoden miteinander verglichen, bevor PLGA MS damit hergestellt wurden. Anschließend wurde die Freisetzung des Inhalts über die Zeit gemessen. Dabei stellten wir fest, dass die inaktivierten Viren nur innerhalb der ersten 24 Stunden freigesetzt wurden, was darauf hindeutet, dass diese nur an der Oberfläche der MS gebunden waren, anstatt verkapselt worden zu sein. Daher wurde anschließend die Morphologie der Partikel mittels Rasterelektronenmikroskopie untersucht, jedoch konnten wir hierbei keine offensichtlichen Unterschiede feststellen. Abschließend analysierten wir *in vivo*, ob die an der Oberfläche gebundenen Viren dennoch einen ausreichenden Immunschutz auslösen können. Im Vergleich zu den Kontrollgruppen konnte jedoch keine signifikante Immunantwort festgestellt werden. Daher schlussfolgerten wir, dass es nicht möglich war ganzen, inaktivierten IAV zu verkapseln und dass die an der Oberfläche der PLGA MS gebundenen Viren nicht ausreichten, um eine Immunantwort auszulösen.

1. Introduction

1.1. T cell immunity

1.1.1. Activation of T cells by DCs

Dendritic cells (DCs) are innate immune cells that are essential for regulating adaptive immune responses and therefore form a bridge between the innate and the adaptive immune system [5]. Based on their functions and transcriptional identities, DCs can be divided into two major subsets: conventional DCs (cDCs) and plasmacytoid DCs (pDCs). cDCs can be further divided into type 1 cDCs (cDC1s) and type 2 cDCs (cDC2s) [6]. cDC1 can be either resident in the lymph node (LN) (characterized by CD8α-expression in mice) or migratory (characterized by expression of CD103 in mice). In contrast, only one population is known in humans, which is characterized by the expression of CD141. cDC1s express Toll-like receptor 3 (TLR3), a transmembrane receptor found in the membrane of the endosome which can be stimulated by double-stranded RNA (dsRNA). These cells are very efficient at cross-presenting antigens and activating $CD8^+$ T cells. cDC2s, on the other hand, represent a very heterogeneous population but seem to share the expression of CD11b. Similar to cDC1s, they exist as a LN-resident as well as a migratory population, however, no marker has been found that can be used to distinguish these two subsets. $CD11b^+$ cDC2s correspond to $CD1c^+$ DCs in humans. cDC2s are involved in priming $CD4^+$ T cell responses [7]. Finally, plasmacytoid DCs, are found mostly in the blood and spleen. They express TLR7 and TLR9, both in the endosomal membrane, which recognize single-stranded RNA (ssRNA) and CpG dinucleotides, respectively. Upon stimulation of these receptors, pDCs are involved in antiviral immune responses by rapidly producing type I interferons (IFN) [8].

Migratory DCs constantly patrol the body for foreign antigens. In their immature state they express receptors that enable them to access peripheral and inflamed tissues and efficiently phagocytose different antigens [5]. When they take up an antigen that is associated with danger-associated molecular patterns (DAMPs) or pathogen-associated molecular patterns (PAMPs), they undergo maturation. These danger signals are bound by pathogen-recognition receptors (PRRs), such as TLRs [9]. In response to foreign antigen together with signaling via PRRs, DCs upregulate the CC-chemokine receptor CCR7 that enables migration of these cells to draining LNs. In addition, DCs upregulate the expression of molecules required for their function as professional antigen-presenting cells (APCs) such as major histocompatibility complex (MHC) class I and II as well as the costimulatory receptors of the B7 family (CD80, CD86). In turn, their phagocytic activities are downregulated [5]. Depending on the nature of the antigen, it can be presented on either MHC class I or MHC class II. Endogenous antigens

originate from endogenous proteins which have been degraded by the proteasome and are subsequently transported into the endoplasmic reticulum (ER) by transporter associated with antigen processing (TAP) where they are loaded onto MHC class I molecules before being transported to the cell surface for presentation to $CD8^+$ T cells. Exogenous antigen, on the other hand, are obtained from exogenous proteins which are degraded in lysosomes by proteases such as cathepsins before they are loaded onto MHC class II molecules and transported to the cell surface for presentation to $CD4^+$ T cells. In addition, exogenous antigens can be presented on MHC class I molecules in a process termed cross-presentation. This pathway is required to prime and activate naïve $CD8^+$ T cells to exogenous antigens such as those derived from tumor cells or viruses that do not infect DCs. Several types of APCs have been reported to cross-present antigens *in vitro*, however *in vivo* data has indicated that DCs are the most efficient cross-presenters. Although many details still remain unclear, two major pathways have been described for cross-presentation: a cytosolic pathway and a vacuolar pathway. Both pathways start with the uptake of exogenous antigen into a phagosome. In the cytosolic pathway the proteins are then released into the cytosol, where they are degraded into peptides by the proteasome. These peptides are loaded onto MHC class I molecules either in the ER or in the phagosomes after being transported to the respective location. In the vacuolar pathway, proteins are degraded by endosomal proteases such as cathepsin S before they are loaded onto MHC class II molecules in the phagosome [10, 11].

Upon arrival of mature DCs in the draining secondary lymphoid organ (SLO), they present their MHC-peptide complex to naïve T cells which are scanning the DCs for their cognate antigen. When a naïve T cell encounters a DC presenting its cognate antigen, it is activated by DCs via three signals. The first signal is comprised of the interaction of the MHC-peptide complex with the T cell receptor (TCR). This signal alone leads to anergy of the respective T cell and is a mechanism to enable tolerance. However, when T cells receive additional, costimulatory signaling via interaction of CD28 with members of the B7 family (CD80/CD86) on DCs they are activated. Finally, DCs produce cytokines (signal 3) that further influence T cell activation and differentiation into different subtypes [12].

1.1.2. T cell memory

Following their activation in SLOs, T cells undergo three phases of T cell development: First, the clonal expansion phase, during which activated specific T cells proliferate rapidly. Starting from as little as 100 to 200 naïve precursors T cells can expand 10^4 to 10^5 fold to yield sufficient numbers of effector T cells to combat the invading pathogen. Second, in the contraction phase, once the antigen has been cleared, most of the specific effector T cells die by apoptosis, leaving behind only a small pool of memory cells. In the third phase, the memory phase, this

population of memory T cells persists in an antigen-independent manner. However, memory T cells rely on the two cytokines, interleukin (IL)-7 and IL-15, for survival and homeostatic proliferation, respectively. Upon reinfection with the same pathogen, these memory T cells are able to rapidly produce effector molecules, expand drastically and differentiate into secondary effector T cells [13, 14]. A plethora of studies in the last two decades has illustrated that the memory T cell pool is very heterogeneous. Classically, memory $CD4^+$ and $CD8^+$ T cells in human blood were divided into two populations based on their expression of the LN homing receptor L-selectin (CD62L) and CC chemokine receptor 7 (CCR7) [15]. Subsequent studies in mice further characterized these cells [16-20]. $CD62L^+CCR7^+$ T cells could mostly be found in LNs, but also in spleen and blood. These cells were termed “central memory T cells” (T_{CM}). Upon restimulation these cells were able to produce the cytokines interferon (IFN)-γ and tumor necrosis factor (TNF) as well as IL-2. Moreover, T_{CM} cells were shown to possess a greater proliferative capacity. Therefore, their main function was believed to be proliferation and thus the generation of secondary memory T cells upon re-exposure to the same pathogen. $CD62L^-CCR7^-$ T cells were found mostly in non-lymphoid tissues (NLTs), at sites of pathogen entry, but also in the spleen and the blood. Due to the absence of LN homing receptors these cells were not detected in LNs. Upon restimulation these cells possessed immediate effector functions, rapidly producing the cytokines IFN-γ and TNF as well as the cytotoxic molecules perforin and granzyme B. Therefore, these cells were termed “effector memory T cells” (T_{EM}). As a result of their ideal location in NLTs, at sites of pathogen entry, these cells were believed to represent the first line of defense against invading pathogens [21]. Additional studies in mice revealed that T_{CM} cells provided better protection against systemic infection with lymphocytic choriomeningitis virus (LCMV) clone 13, whereas T_{EM} cells provided superior protection against peripheral infection with vaccinia virus [22-24]. These findings led to the hypothesis that due to their excellent ability to proliferate as well as their central location within SLOs, T_{CM} cells are specialized to fight systemic infections, whereas T_{EM} cells are designed to combat infections within peripheral organs due to their cytotoxic effector functions and their ability to migrate to tissues [24]. About a decade ago, parabiosis studies in mice led to the discovery of an additional set of memory T cells in NLTs: resident memory T cells (T_{RM}) [25-27]. As their name suggests these cells are resident in (peripheral) tissues and do not rejoin the circulation. Many studies in the past have often mistaken T_{RM} cells for T_{EM} cells, making interpretation of earlier data challenging. It is now clear that T_{EM} cells and T_{RM} cells represent two distinct subsets with different functions and characteristics [28]. More recently, further studies have suggested additional heterogeneity in the circulating memory T cell pool. Based on expression of the chemokine receptor CX3CR1, circulating memory T cells can be divided into three distinct subsets: $CX3CR1^{hi}$ cells, $CX3CR1^{int}$ cells and $CX3CR1^{lo}$ cells. $CX3CR1^{hi}$ cells show characteristics of “classical” T_{EM} cells, such as the absence from LNs, abundance in the

circulation and tissues, poor proliferative potential but efficient cytotoxic activities. Therefore, high CX3CR1 expression allows the identification of a more homogeneous subset of T_{EM} cells. $CX3CR1^{lo}$ and $CX3CR1^{int}$ cells can be detected in LNs and seem to represent two distinct populations among cells that typically were defined as T_{CM} cells. While $CX3CR1^{lo}$ cells seem to represent a more homogeneous population of T_{CM} cells, the $CX3CR1^{int}$ cells were termed peripheral memory T cells (T_{PM}). This new way of categorizing memory T cells also revealed that the newly defined T_{EM} cells, while absent from tissues, instead were very abundant in the circulation [29]. This led to the redefinition of the roles of the different subtypes of memory $CD8^+$ T cells: T_{EM} cells are thought to mediate immune-surveillance. Due to their presence in the circulation they can easily be recruited to sites of inflammation where they can exert their cytotoxic functions. T_{CM} cells are centrally localized in LNs and are able to proliferate extensively following antigen encounter. T_{PM} cells survey peripheral tissues and have been suggested to protect against chronic infection. Lastly, T_{RM} cells are thought to react to infections in peripheral tissues and, following infection, proliferate and recruit other immune cells [24].

Due to obvious difficulties in obtaining tissue samples from humans most of the studies on T_{RM} cells and memory T cell compartments in peripheral tissues have been performed in mice [30]. However, analysis of human tissues, such as organs for transplantation, also showed clear evidence of T_{RM} cells in humans [31]. Moreover, the circulating memory populations of T_{EM} and T_{CM} cells have been identified in human blood long ago [15]. Additionally, a terminally differentiated subset of cells that express CD45RA can be found in humans, but not in mice. CD45RA, one of the isoforms of CD45, is typically expressed on naïve cells, subsequently downregulated on memory T cells and considered as a marker of terminal differentiation when it is re-expressed on memory cells. Therefore, $CD45RA^+$ memory cells have been termed T_{EMRA} cells. The different populations of naïve T cells, T_{EM} cells, T_{CM} cells and T_{EMRA} cells found in the circulation in humans can be distinguished based on the expression of CD45RA, CD27 and CCR7 [24]. To further add to the complexity of the T cell memory pool, another population of memory T cells has been defined which has been termed stem cell-like memory T (T_{SCM}) cells. These cells, which can be found both in mice and humans, share characteristics with both naïve and memory T cells. Although they are antigen-experienced cells that are able to proliferate rapidly and secrete cytokines in response to antigen re-exposure, they maintain a stem cell-like ability to self-renew and the potential to reconstitute the entire spectrum of effector and memory T cells. Similar to naïve T cells, they are mostly found in LNs and are largely absent from peripheral mucosae [32]. In conclusion, these discoveries highlight the complexity of the T cell compartment and emphasize the necessity to further clarify the different roles and functions of the various T cell subsets. Furthermore, although some differences exist

between murine and human memory cells found in the circulation and periphery, they share many similarities.

1.1.3. T_{RM} cell phenotype & function

Since their discovery more than a decade ago, tissue-resident memory T cells have been a strong focus of research. T_{RM} cells have been identified in various tissues such as skin, lung, intestine, brain, liver as well as in SLOs, such as LNs and spleen, and even in the primary lymphoid organs thymus and bone marrow (BM) [26, 27, 33-39]. In addition to their residency, T_{RM} cells are identified based on typical markers such as the most widely used marker CD69 (see Figure 2). While this molecule is transiently expressed on recently activated T cells, T_{RM} cells show sustained cell surface expression of this molecule. CD69 can bind to and antagonize sphingosine-1-phophate receptor 1 (S1PR1), thereby interfering with sphingosine-1-phophate (S1P)-mediated tissue egress of lymphocytes [40]. In this way, CD69 promotes tissue residency of T_{RM} cells. A large fraction of T_{RM} cells, especially in mucosal tissues, also expresses the α_E subunit (CD103) of the integrin $\alpha_E\beta_7$ which interacts with E-cadherin on epithelial cells thereby further promoting tissue retention [41, 42]. The α_1 subunit CD49a (very late antigen-1, VLA-1) of integrin $\alpha_1\beta_1$, which further promotes tissue residency by binding to collagen type IV in basement membranes, is also expressed by a sizeable part of T_{RM} cells in different tissues [26, 43, 44]. Although not involved in tissue retention, T_{RM} cells have been shown to express fatty acid binding protein 4 (FABP4) and FABP5 which are involved in lipid uptake and intracellular transport of free fatty acids allowing them to use fatty acids as a source of energy which can improve their survival and long-term maintenance in the tissue [45].

A study in mice found a core “tissue residency” transcriptional signature for this resident T cell population, that is shared among T_{RM} cells across tissues and distinguishes them from their circulating T cell counterparts [42]. A similar core transcriptional profile for human T_{RM} cells has also been defined [43, 46]. Recent studies have identified that the major transcription factors involved in T_{RM} cell development, Blimp1 (B lymphocyte-induced maturation protein-1) and its homologue Hobit (homologue of Blimp1 in T cells), are required for T_{RM} formation in skin, liver, kidney and the small intestine [47]. Interestingly, in the lung T_{RM} formation seems to require only the action of Blimp1 [48]. In general, both of these transcription factors directly bind to the loci of Krüppel-like factor 2 (*Klf2*), *S1pr1* and *Ccr7*, which are all involved in tissue egress. In this way Blimp1 and Hobit regulate tissue residency [4].

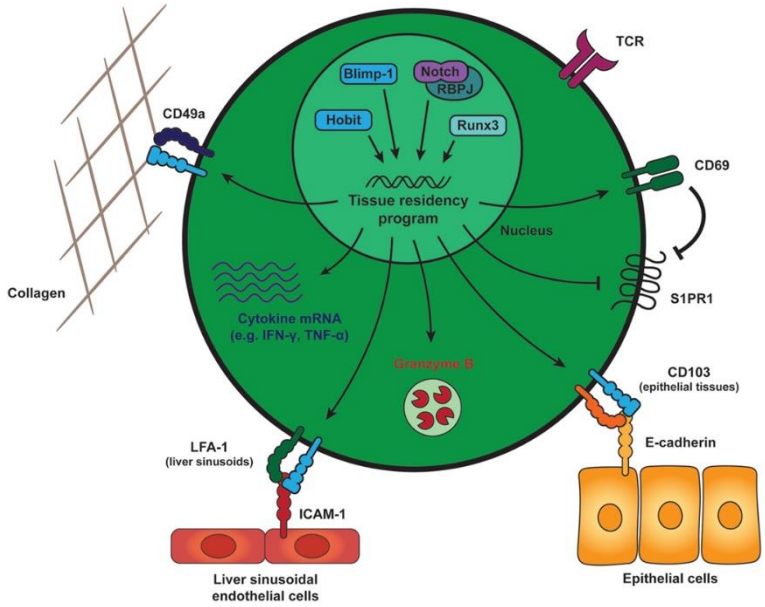

Figure 2: T_{RM} cell. These cells express a core "tissue residency" signature. Transcription factors such as Hobit, Blimp1, Notch and Runx3 promote the expression of genes that encourage tissue residency. These include the molecules CD69, which antagonizes S1PR1-mediated tissue egress and the integrins CD103 and CD49a, which bind to E-cadherin expressed on epithelial cells and collagen IV in the basement membrane, respectively. Moreover, the core T_{RM} signature induces the expression of genes that mediate the protective function of these memory cells. This is mediated either directly via granzyme B-mediated killing of target cells and indirectly via secretion of the cytokines IFN-γ and TNF that induce a state of alarm in the surrounding tissue thereby inducing further immune responses by other cells. Figure taken from [4]

Other transcription factors that seem to play a major role in T_{RM} cell development are Runx3 (Runt-related transcription factor 3) and Notch. Runx3 has been shown to suppress genes involved in tissue egress and circulation, such as *S1pr1* and *Klf2*, while promoting the expression of genes that enable tissue residency, such as *Cd69* and *Nr4a1*(Nuclear Receptor Subfamily 4 Group A Member 1) [49]. Notch has been reported to regulate the transcription of *Itgae* (encodes CD103) in T_{RM} cells in the lung [46]. The three transcription factors Eomes (Eomesodermin), T-bet and KLF2 which are critical in the formation of circulating memory T cells, negatively regulate T_{RM} cell development and therefore need to be shut down completely (in the case of Eomes) or expressed at low levels (in the case of T-bet and KLF2). In contrast to typical T_{RM} cell transcription factors such as Hobit and Blimp1, which drive tissue retention, KLF2 promotes expression of *S1pr1*, thereby allowing tissue egress of circulating memory T cells [50-53].

While a core signature of T_{RM} cells across different tissues has been identified, it is also evident that this population is very heterogeneous and very much influenced by the tissue of residency [54-57]. These differences affect phenotype, longevity, function, proliferation and maintenance requirements of T_{RM} cells among others [54]. In a study by Christo *et al.* the authors compared T_{RM} cells from different tissues. They found that certain characteristics, such as their functional or proliferative capacity, were mostly dependent on the tissue of residence rather than the

mode of infection or the presence of local antigen [58]. Recent analysis of $CD8^+$ T_{RM} cells in mice revealed the existence of two major subsets of T_{RM} cells in response to LCMV-Armstrong infection: effector-like $Id3^{lo}$ $Blimp1^{hi}$ T_{RM} cells, which dominated in the early phase of the immune response, and memory-like $Id3^{hi}$ $Blimp1^{lo}$ T_{RM} cells, which accumulated at a later time point [55]. The existence of two distinct subsets of resident memory T cells in the small intestine has also been observed in another study using single cell transcriptomics [59]. In addition to their distinct transcriptional programs these cells differed in cytokine production and the potential to form secondary memory, further highlighting the heterogeneity of the T_{RM} cell population. There seems to be a multitude of reasons for this heterogeneity, one being the presence of different cytokines and chemokines in the various tissues. For example, transforming growth factor β (TGF-β) has been shown to be a major player in the development and maintenance of $CD103^+CD8^+$ T_{RM} cells, but not $CD103^-CD8^+$ T_{RM} cells. Several reports have elucidated three main mechanisms by which TGF-β regulates the development of $CD103^+CD8^+$ T_{RM} cells. These include, skewing the $CD8^+$ T cell population towards a memory precursor phenotype, regulating the expression of CD103 and downregulating the expression of KLF2 which in turn leads to a downregulation of S1PR1 and thereby counteracts tissue egress [60]. Many other cytokines and chemokines have been described to have an impact on T_{RM} cell development in different tissues, including IFN-γ, IL-15 as well as the chemokines CXCL9 and CXCL10 which are ligands for the chemokine receptor CXCR3. Moreover, differences in the availability of antigen, niches for maintenance and nutrients also seem to shape the resident memory T cells compartment [2, 57].

Due to their location directly at sites of pathogen entry, T_{RM} cells are ideally placed to rapidly respond to re-encountered antigens. They possess two main mechanisms to exert their protective function: directly by killing antigen-presenting target cells via secretion of cytotoxic molecules such as granzyme B and perforin and indirectly, via secretion of cytokines such as IFN-γ, TNF and IL-2 that modify innate and adaptive immunity. The proinflammatory cytokine IFN-γ induces a state of alarm in the surrounding tissue and triggers the expression of antimicrobial genes. Moreover, it induces the expression of vascular cell adhesion molecule 1 (VCAM-1) on local endothelial cells and thereby leads to the recruitment of circulating memory T and B cells [61-63]. TNF promotes the maturation of DCs by stimulating the expression of the LN homing receptor CCR7 and the costimulatory molecule CD86. IL-2 stimulation induces the activation of natural killer (NK) cells by upregulating granzyme B expression [61].

Confocal microscopy images of T_{RM} cells in the skin have detected a dendritic morphology of these cells. It is believed that, at least for the populations in the skin, T_{RM} cells are able to migrate within the tissue and survey their surroundings, probably in order to detect cognate antigen [64]. Additionally, upon local antigen encounter T_{RM} cells are able to undergo

proliferation *in situ* to form secondary T_{RM} cells [65, 66]. Contrary to the former belief that T_{RM} cells do not rejoin the circulation, more recent studies have shown that upon secondary antigenic challenge a fraction of these cells is able to egress from the tissue and migrate to draining SLOs where they take up residence. In these positions they form populations of SLO T_{RM} cells that are believed to offer protection to SLOs as well as enable the repopulation of the downstream nonlymphoid tissue after reinfection [39]. Moreover, an elegant study recently showed that CD8 T_{RM} cells maintain migrational plasticity and are able to undergo retrograde migration after restimulation. Reactivated T_{RM} cells are capable of rejoining the circulation to give rise to circulating memory T_{EM} and T_{CM} cells which possess a strong tendency to home back to their original tissue of origin. It was proposed that this “outside-in” migration (i.e. from the periphery to the circulation instead of the traditional “inside-out” migration of T cells primed in the LN which then migrate to the periphery) of T_{RM} cells may be beneficial if the local frontline immunity decreases or is insufficient to combat the re-encountered pathogen. In this case the circulating memory T cell compartment already contains antigen-specific cells that have a heightened capacity to migrate back to the parent tissue to re-establish local resident immunity [67]. These findings highlight that the field of T_{RM} cell research is still in its infancy and will likely bring more fascinating discoveries to light.

1.1.4. The origin of T_{RM} cells

One of the major unknowns regarding T_{RM} cells is the origin of these cells. What are the precursors? When do T_{RM} cells commit to a resident memory phenotype? What are the signals they receive that make them commit to this fate? At what point in the immune response do they receive the decisive signals?

In general, multiple models have been suggested to explain the development of the different effector and memory T cell populations [14]. In one such model, the “fixed lineage model”, commitment to the effector or memory T cell lineage is believed to occur shortly after T cell stimulation and may be due to the asymmetric distribution of effector fate-associated factors. Another model, the “decreasing potential model”, assumes that all early effector cells have a potential to form memory cells. However, this potential is lost when cells receive prolonged stimulation with antigen or cytokines [57]. Studies that support this model have found that T_{EM} phenotypes are favored by higher affinity TCR interactions, whereas T_{CM} phenotypes are promoted by lower TCR interactions [68]. Rosato *et al.* recently proposed the “terrace model” which is an extended model of decreasing potential [69]. Similar to the decreasing potential model, this model believes in a stepwise loss of differentiation potential as memory T cells develop. In addition, the memory T cell pool is further split into a resident and a circulating pool

based on the migration status. However, in line with recent data, showing that T_{RM} cells have the potential to rejoin the circulation the migration status of T cells may not be permanent.

A lot of research has focused on memory T cell development and understanding what distinguishes cells that die during the contraction phase from cells that turn into memory cells already during the early phase of the immune response. The markers KLRG1 (Killer cell lectin-like receptor subfamily G member 1) and CD127 are often used to define the memory potential of T cells. KLRG1 is a marker of terminal differentiation and therefore used to identify senescent T cells, while CD127 (the α chain of the IL-7 receptor) enables T cells to respond to IL-7 signaling which promotes homeostatic T cell proliferation [24]. Based on these two markers, the $CD8^+$ T cell population during the effector phase can be divided into two groups: $KLRG1^+CD127^-$ short-lived effector cells (SLECs), which are highly cytotoxic and tend to undergo apoptosis after the antigen has been cleared, and $KLRG1^-CD127^+$ memory precursor effector cells (MPECs), which are more likely to survive and give rise to long-lived memory T cells [70, 71]. These studies identified that the circulating memory T cell populations T_{CM} and T_{EM} derive from MPECs. More recently, studies have found that T_{RM} cells also derive from MPECs, highlighting that T cells within NLTs follow a similar dichotomy [42, 72].

While it seems to be clear that T_{RM} cells derive from cells that already exhibit memory potential early on in the immune response, there remain a lot of questions about when the decision for the memory fate is made. Several studies have shown that distinct effector and memory $CD8^+$ T cells as well as resident and circulating memory T cells can arise from the same naïve precursor [73-75]. These findings suggest that an individual naïve T cell has the potential to give rise to all effector and memory T cells supporting the idea that the fate is not imprinted on naïve T cells [57]. Further studies have proposed that the commitment to a resident memory T cell fate is made only *after* the cells have entered the tissue when they receive the appropriate signals from the tissue microenvironment [76]. In contrast to this data, a more recent study by Kok *et al.* found that, while most of the cells in the naïve T cell pool are able to contribute to both the circulating and the resident memory $CD8^+$ T cell populations, this is not evenly distributed across the clones. Using genetic barcoding to track individual clones in combination with single cell transcriptomics, they were able to show that many clones displayed a preference in whether they formed the circulating or the resident memory compartment. Interestingly, this divergence was not due to stochastic reasons but rather due to cell intrinsic differences regarding the fitness to survive in different microenvironments, i.e. the circulation versus the skin. Moreover, they found that these intrinsic differences were already detectable in the circulating T cell population during the effector phase. Based on their data they proposed that the T_{RM} fate decision is imprinted on the cells already during the

effector phase *before* they have entered the tissue and that a T_{RM} cell precursor exists in the circulation [77].

Numerous studies have identified several factors in the tissue microenvironment that stimulate the differentiation of T_{RM} cells. These factors include the presence of antigen as well as the cytokines IL-7, IL-15 and TGF-β, among others [50, 72, 78-87]. As mentioned above, the cytokine TGF-β seems to play a major role in the differentiation of epithelial T_{RM} cells by regulating the expression of different core signature genes [60]. Due to these somewhat conflicting studies, two models have been proposed for T_{RM} cell lineage divergence [2]. The "tissue divergence model" postulates the existence of an uncommitted memory T cell precursor in the circulation which turns into resident or circulating memory T cells depending on the location and the signals received. Memory precursors that enter the tissue receive signals from the local microenvironment that skew the cells toward a T_{RM} phenotype, whereas memory T cells that remain in the circulation turn into circulating memory T cells. According to this model, the decisive signals for T_{RM} lineage commitment are given by the NLT. The "systemic divergence model" on the other hand proposes that a T_{RM} precursor is present in the circulating memory pool. This model believes that these T_{RM} precursors are primed in the circulation by various signals and are subsequently (more) poised to differentiate into T_{RM} cells [2]. In line with this model, different signals have been identified that may prime precursor cells to subsequently differentiate into T_{RM} cells. In mice basic leucine zipper ATF-like transcription factor 3 (Batf3)-dependent DCs (i.e. cDC1s), which are efficient at cross-presenting antigens and provide IL-15 and IL-12 signaling, have been shown to guide T cells towards a T_{RM} phenotype while $CD11b^+$ DCs (i.e. cDC2s) seem to induce T_{CM} cell differentiation [88, 89]. Moreover, recent work by Mani *et al.* found that migratory DCs expressing the α_V integrin are able to activate TGF-β signaling in naïve $CD8^+$ T cells in LNs and thereby precondition them to a T_{RM} cell phenotype [90]. While all of these results seem partially contradictory, it is possible that they may be integrated into one model: the presence of a T_{RM}-committed precursor in the circulation that has been equipped with a superior ability to form a resident memory T cell by showing an enhanced capacity for tissue accumulation as well as an increased responsiveness to T_{RM} cell-inducing signals. Ultimately however, whether these cells develop into T_{RM} cells is still somewhat dependent on local signals (see Figure 3) [2]. Additional research will certainly be necessary to fully understand the origin of T_{RM} cells and the signals driving their generation.

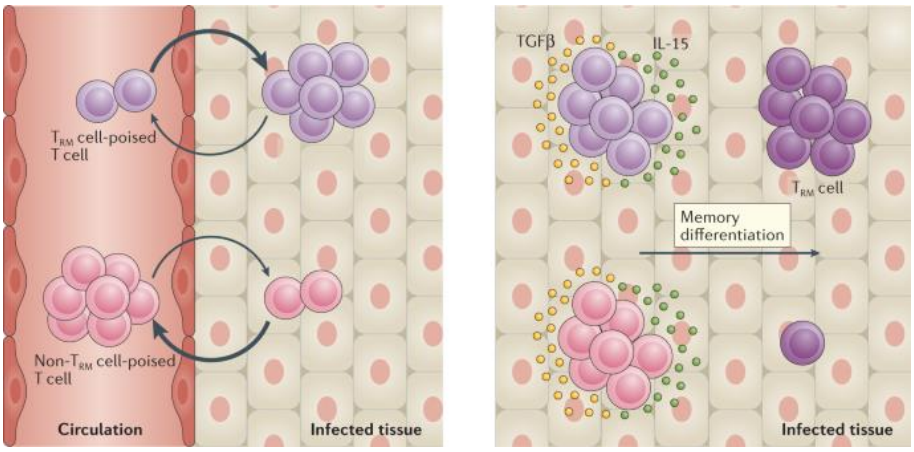

Figure 3: Model for T_{RM} cell development. The circulating memory T cell pool contains precursor cells that have received certain signals that preconditioned them to follow a T_{RM} cell fate (purple). In contrast to non-T_{RM} cell-poised T cells (pink), these cells have a higher capacity for tissue accumulation (left) as well as a higher responsiveness to T_{RM} cell-inducing signals such as signaling by TGF-β and IL-15 (right). Therefore, these cells are more likely to become resident than cells that have not received these signals. This model combines the importance of signals received in the circulation *prior* to tissue entry with signals received by the local microenvironment *after* entry into the tissue. Figure adapted from [2]

1.1.5. T_{RM} cells in the lung

Even though T_{RM} cells share a common core transcriptional signature and phenotype across tissues, they always adapt to their tissue of residence and the local conditions and thus differ between the various sites. However, T_{RM} cells in the lung seem to be exceptionally distinct from other T_{RM} cell populations. Lung $CD8^+$ T_{RM} cells can be divided into two populations based on their location. Airway-resident $CD8^+$ T_{RM} cells are localized in the epithelial layers of the upper respiratory tract and can be obtained by bronchoalveolar lavage (BAL), while interstitial $CD8^+$ T_{RM} cells are found in the interstitium and alveolar spaces and are obtained by digesting the lung tissue [91]. These two populations differ not only in their location, but also in their effector functions. Airway T_{RM} have been found to possess poor cytolytic functions compared to their interstitial counterparts. Yet, they are able to rapidly produce cytokines which enable protection against respiratory pathogens. These findings suggest that airway T_{RM} cells probably act mostly as sentinels by alarming the surrounding tissue and attracting further immune cells to the site [92-94]. Studies have confirmed that both of these lung T_{RM} cell populations are able to offer protection against secondary infection [92, 95, 96].

In certain tissues such as the skin and the female reproductive tract (FRT) a “prime-and-pull” strategy, i.e. a systemic antigen prime followed by a local inflammatory or chemotactic stimulus, can induce the forced recruitment of $CD8^+$ T cells to the site of inflammation and the subsequent establishment of $CD8^+$ T_{RM} cells [97, 98]. This inflammation-dependent, yet antigen-independent differentiation and maintenance of T_{RM} cells does not seem to occur in the lung. Several studies have confirmed that the presence of cognate antigen is required for

efficient long-term establishment of lung T_{RM} cell populations [83, 99]. Even though inflammation alone is sufficient to attract $CD8^+$ T cells to the lung, these cells are rapidly lost once the inflammation is resolved [99]. Interestingly, although skin T_{RM} cells can be induced in the absence of cognate antigen, their formation can be increased significantly when antigen is present [79, 81].

Another major difference between T_{RM} cell populations in the lung compared to their counterparts in the skin is their longevity. While T_{RM} populations in the murine skin can persist for up to 1 year, pulmonary $CD8^+$ T_{RM} populations disappear rapidly and are mostly gone after 7 months [96, 100]. Airway resident $CD8^+$ memory T cell populations have been shown to decline even more rapidly, with a half-life of only 14 days [92, 101]. This discrepancy is most likely due to the different niches and the environment these cells inhabit in the different tissues. For example, $CD8^+$ T_{RM} cell precursors recruited to the skin have been found to persist in the epidermal niche that was previously occupied by dendritic epidermal T cells (DETC). This preformed niche enables the durable persistence of skin $CD8^+$ T_{RM} cells [100]. In the healthy lung spaces that offer such ideal conditions for the establishment of T_{RM} cells do not exist and therefore need to be created first. Based on older findings it was previously believed that $CD8^+$ T_{RM} cells in the lung are present in inducible bronchus-associated lymphoid tissues (iBALT) [102]. These are ectopic lymphoid tissues which arise in response to respiratory viral infections [91, 102]. However, a more recent study by Takamura *et al.* found that only very few $CD8^+$ T_{RM} cells could be found in the iBALT. In contrast, these structures were mostly inhabited by $CD4^+$ T_{RM} cells as well as B lymphocytes [99]. Instead, interstitial $CD8^+$ T_{RM} cells were found to populate special structures in the interstitium that were created in response to tissue damage, which the authors named “repair-associated memory depots” (RAMDs) [99]. In these RAMDs, $CD8^+$ effector T cells that enter the lung to combat the viral intruder, receive environmental cues such as TGF-β, IL-7, IL-15 and cognate antigen that drive their differentiation into resident memory populations [103, 104]. In return, the $CD8^+$ T_{RM} cells can protect the already damaged lung tissue from a secondary infection [91, 99]. As the lung tissue is slowly regenerated, the RAMDs shrink and slowly disappear and with them the majority of the $CD8^+$ T_{RM} cell population is lost. A small fraction of the population may remain in the iBALT ready to respond to a re-encountered pathogen [91].

The niches in which airway $CD8^+$ T_{RM} cells persist have not yet been identified. The rapid loss of airway T_{RM} cell populations seems to be due to the harsh microenvironment in the airways. Epigenetic changes induced by environmental conditions, such as amino acid starvation, trigger the integrated stress response in airway T_{RM} cells subsequently inducing their death by apoptosis [105]. In addition to the loss of cells by apoptosis, the T_{RM} cell population in the airways does not undergo homeostatic proliferation highlighting that they must be replenished

from somewhere for a certain time following infection [106]. Many studies have tried to elucidate the source of these airway T_{RM} cells. In the past it was believed that these airway memory cells are constantly replenished by circulating T_{EM} cells [101, 107]. More recent data suggests that this population is continuously replenished from interstitial T_{RM} cells in the RAMDs by CXCR6-CXCL16-dependent migration into the airways. CXCL16 is expressed by the airway epithelium and attracts $CD11a^+CXCR6^+CD8^+$ T_{RM} cells into the airways where they subsequently downregulate the expression of CD11a and CXCR6 [101, 108-111]. T_{EM} cells on the other hand seem to access lung airways via CXCR3-dependent migration in response to basal levels of CXCR3 ligands [110]. Similar uncertainties exist regarding the source for replenishment of the interstitial population. Two mechanisms have been suggested to explain the means by which interstitial T_{RM} cell numbers are maintained at a reasonable level for some time. One study suggested that the interstitial T_{RM} cell population is replenished from the circulating T_{EM} cell population that is transformed to T_{RM} cells under the influence of different cytokines [112]. However, more recent findings have proposed that lung T_{RM} cell populations are maintained by homeostatic proliferation independent from the circulation [99, 110].

Irrespective of the source of the lung T_{RM} cell populations, the rather short-lived nature of these cells is something that can be agreed upon. As the number of T_{RM} cells in the lung has been found to correlate with the efficacy of protection against secondary infections, the rather rapid decline of lung T_{RM} cells seems to be somewhat counterintuitive [92, 95, 96]. It has been proposed that this ephemerality of resident memory populations in the lung may be necessary to ensure the lung's main function: gas exchange. The formation of niches for the maintenance of T_{RM} cell populations requires space and thereby reduces the efficacy of gas exchange. Clearly, future experiments will have to shed light on the requirements for maintaining a balance between long-lived protective immunity and immune pathology [91].

1.1.6. T_{RM} cells in infections

In 2009 Gebhardt *et al.* discovered a subset of memory T cells that were separated from the circulating lymphocyte pool and truly resident in the tissue [26]. The authors detected a $CD8^+$ resident population in the skin and sensory ganglia of mice which had been infected with herpes simplex virus (HSV). These cells exhibited a phenotype distinct from their circulating counterparts and were able to protect against new infection with the virus [26]. Since their discovery in this model of viral infection, T_{RM} cells have been identified in response to a myriad of viral, bacterial, fungal and parasitic diseases [113]. It appears that these resident memory cells are better suited to fight invading pathogens than their circulating counterparts [114-116]. For example, in respiratory infections with influenza virus, specific T_{RM} cells have been detected in the respiratory tract of infected patients [117]. Studies in mice have confirmed that

these cells play an essential role in the antiviral immune response [96]. Moreover, in contrast to humoral immunity which is very susceptible to antigenic changes of the virus, cellular T_{RM}-mediated immunity has the ability to provide heterosubtypic immunity [51]. Due to the short-lived nature of T_{RM} cells in the lung however, this protection wanes over time [88, 96, 118]. A number of studies has also found T_{RM} cells to be involved in the immune response to many other viruses, including respiratory syncytial virus (RSV), human immunodeficiency virus (HIV), cytomegalovirus (CMV), LCMV, vaccinia virus, varicella zoster virus (VZV), human papillomavirus (HPV), hepatitis B and C viruses (HBV and HCV) as well as HSV-1 and HSV-2 [113]. Interestingly, inoculation of skin tissue with vaccinia virus induced the formation of skin T_{RM} cells even at distinct sites in the skin as well as T_{RM} cell populations in non-related non-lymphoid organs, such as lungs and liver [37, 119]. Moreover, multiple exposures with the viral antigen expanded the T_{RM} cell population [75]. Typically, T_{RM} cells exert their protective "sense and alarm" function by directly killing infected target cells as well as secreting pro-inflammatory cytokines. These create a state of alarm in the surrounding tissue and induce the recruitment and activation of several innate and adaptive immune cells [61-63]. A study using LCMV and a recombinant vaccinia virus expressing Ova showed that this "state of alarm" induced by reactivated $CD8^+$ T_{RM} cells was able to stimulate nearly sterilizing immunity even to non-cognate viruses [61]. In HIV infection, "controllers", i.e. individuals who naturally control the infection, possess large amounts of polyfunctional $CD8^+$ T_{RM} cells highlighting the importance of these cells in combating HIV [120].

While T_{RM} cells have been studied most extensively in viral infections, they have also been found to play a vital role in fighting many bacterial pathogens such as *Bordetella pertussis*, *Streptococcus pneumonia*, *Mycobacterium tuberculosis*, *Listeria monocytogenes*, *Salmonella enterica* and *Chlamydia trachomatis* [113]. T_{RM} cells have been shown to keep respiratory infection with *B.pertussis* (whooping cough) in check even without the contribution of peripheral T cells [121]. Studies on tuberculosis (TB) established that $CD4^+$ and $CD8^+$ T_{RM} cell responses were important for controlling infection. Both populations could best be induced via a mucosal vaccination strategy highlighting the importance of developing new vaccines to control TB infection [122-128]. Unfortunately, the currently employed vaccine Bacillus Calmette–Guérin (BCG) is not very efficient in adults at inducing strong immunity against pulmonary TB [129].

More recently, T_{RM} cell populations have also been discovered in infections with parasites such as *Toxoplasma gondii*, *Plasmodium spp.* and *Leishmania spp.* as well as fungal agents such as *Candida albicans* [113]. Malaria, caused by five different species of *Plasmodium*, causes a major public health burden. In recent years, liver T_{RM} cells have been discovered as ideal candidates for efficient protection against *Plasmodium* infection due to their ability to slowly

patrol the liver for cognate antigen [130]. Also in *Leishmania* as well as *T.gondii* infections, T_{RM} cells have been shown to offer superior protection to circulating T cells [131-135].

In summary, T_{RM} cells have been found to provide immune protection against a variety of pathogens in a multitude of tissues highlighting their central role in immune protection of different pathogen entry sites. Ongoing research will surely contribute to a deeper understanding of the roles and mechanisms of T_{RM} cells in immune protection

1.1.7. T_{RM} cells in tumors

Originally, T_{RM} cells were identified in antiviral immunity [26, 27]. However, an accumulating amount of data now also supports their role in malignancies. Resident tumor-infiltrating lymphocytes (TILs), which are often termed T_{RM}-like TILs, have been found in many human solid tumors [136-149]. Moreover, in human patients a correlation between the presence of T_{RM} cells in clinical tumor samples and an improved outcome has been observed in a variety of cancers such as melanoma, non-small cell lung carcinoma (NSCLC), breast cancer, cervical cancer and ovarian cancer [150]. It has been suggested that the presence of these T_{RM}-like TILs may be a better predictor of survival than the presence of total $CD8^+$ TILs [137, 148, 151]. Also in mice, several studies have proven that T_{RM} cells play a critical role in antitumor immunity. Melanoma challenge experiments using mice in which essential T_{RM} molecules, such as CD69, CD49a and CD103, were knocked-out or blocked with antibodies showed that these mice were more susceptible to tumor growth than their WT or untreated counterparts [151-154]. Moreover, when T_{RM} cells were induced by prophylactic vaccination, mice were protected from tumor growth in transplantable melanoma as well as head and neck tumor [155, 156].

Similar to T_{RM} cells in non-malignant tissues, T_{RM}-like TILs are characterized by the expression of the tissue retention molecules CD69 and CD103. However, using only these surface markers to identify resident memory T cells in tumors may be problematic. CD69 is commonly transiently expressed on recently activated cells and due to the presence of antigen and/or inflammation in the tumor microenvironment (TME) this molecule may also be expressed in peripheral T cells which are simply in transit, but not resident [116, 157]. Moreover, it may be induced due to the oxygen deprivation in the microenvironment of solid tumors [158]. CD103 expression can be induced by TGF-β signaling, which is often required for T_{RM} cell differentiation [159]. However, TGF-β is also frequently secreted by tumor cells to suppress the immune response [159, 160]. Therefore, analysis of T_{RM}-like TILs based solely on these two markers may be less reliable. One marker which is not expressed by T_{RM} cells in healthy tissue, but frequently found in tumor neoantigen-specific $CD103^+$ T_{RM}-like TILs is the cell surface ectonuclease CD39. This enzyme dephosphorylates ATP to AMP and is frequently

found in exhausted T cells [140, 161]. In addition, it is expressed on regulatory T cells (Tregs) and seems to be implicated in their inhibitory function [162]. It has been suggested that in the TME it may protect T_{RM}-like TILs from ATP-induced cell death [111]. Notably, this molecule could be used to distinguish tumor-specific T_{RM}-like TILs from bystander TILs that are specific for non-tumor antigens [161]. Despite their lack of tumor specificity these bystander TILs might nevertheless contribute to antitumor immunity by producing cytokines that support tumor-specific T_{RM}-like TILs and by recruiting circulating effector T cells [111].

As mentioned above, T_{RM} cells typically express proteins of the fatty acid metabolism that enable these cells to metabolize free fatty acids. This ability could provide an advantage for T_{RM} cells because rapidly growing tumor cells typically rely on glucose as a source of energy and subsequently induce a state of glucose deprivation in the TME [45]. Other advantages of T_{RM} cells in antitumor immunity include their residence within the tissue, their close contacts with epithelial cells at risk of malignant transformation via CD103 – E-cadherin interactions and their ability to rapidly respond to persistent antigens due to high amounts of mRNA encoding for pro-inflammatory cytokines and cytotoxic mediators [111]. In addition to these inherent benefits, increasing evidence suggests that T_{RM} cells may also be ideal targets of cancer immunotherapy [111, 163]. Typically, immune checkpoint molecules such as programmed cell death protein 1 (PD-1) and cytotoxic T-lymphocyte-associated protein 4 (CTLA-4) are expressed by exhausted T cells to counteract activation molecules and thereby enable immune tolerance and prevent immunopathology [164]. In the immunosuppressive TME these molecules are often upregulated thereby preventing the T cells from exerting their antitumor functions. While these inhibitory molecules are commonly expressed by T_{RM} cells in healthy tissues, they seem to be expressed at even higher levels on $CD103^+$ T_{RM}-like TILs compared to their $CD8^+CD103^-$ TIL counterparts. This suggests that $CD103^+$ T_{RM}-like TILs may be the main targets of immune checkpoint blockade (ICB) therapy, an immunotherapy approach that aims to counteract tumor-induced immunosuppression of T cells by blocking checkpoint inhibitor molecules [136, 139, 140, 161, 165]. Indeed, several studies have indicated that T_{RM} cell effector functions can be boosted by ICB [163]. For example, a preclinical murine model showed that the combination of adoptive T_{RM} cell transfer together with anti-PD-1 therapy was more efficient at preventing the growth of B16-Ova tumors than the adoptively transferred T_{RM} cells alone [166]. Therefore, it has been suggested that the presence of T_{RM} cells in tumor lesions could be used to predict whether patients will respond to ICB therapy [137, 148]. Additional data has shown that T_{RM} cells are also ideal candidates for adoptive T cell therapy. In a study using a murine model of melanoma Milner *et al.* showed that transferred *Runx3* $^{-/-}$ $CD8^+$ T cells (non-resident phenotype) failed to accumulate in the tumors which therefore led to increased mortality. In contrast, the adoptive transfer of Runx3-overexpressing $CD8^+$ T cells (tissue-resident phenotype) into mice enabled the accumulation of $CD8^+$ T cells in the tumor

and thus prolonged survival [49]. In summary, these studies show that the presence of T_{RM} cells in tumors is highly beneficial and underscore the benefits of inducing resident memory T cells by vaccination.

1.1.8. T_{RM} cell-mediated immunopathology

An extensive body of research has uncovered the beneficial role of T_{RM} cells in a myriad of infectious and malignant settings. Not entirely unexpectedly, more recent studies have found T_{RM} cells to also play a role in unwanted immune reactions, such as allergies, autoimmunity and transplant rejection. To date, the most studied tissue for T_{RM}-related immunopathology is the skin [167-169]. Several studies have found skin T_{RM} cells to be involved in autoimmune disorders such as psoriasis, vitiligo as well as cutaneous lupus erythematosus [78, 170-173]. In accordance with the current knowledge about the heterogeneity of T_{RM} cells in different sites and settings, diverse subsets of T_{RM} cells have been identified in pathological disorders in the skin: in psoriasis $CD8^+CD49a^+CD103^+$ T_{RM} cells have been shown to mediate disease outbreaks through the production of the pro-inflammatory cytokine IL-17, whereas $CD8^+CD49a^-CD103^+$ T_{RM} cells were found to produce IFN-γ and thereby drive vitiligo [170, 171]. Interestingly, vitiligo, an autoimmune disorder in which melanocytes are targeted by autoreactive CTLs, often appears as an immune-related adverse event in melanoma patients receiving anti-PD-1 antibodies as ICB therapy. In addition to activating cytotoxic memory T cells that target transformed melanoma cells, this antibody therapy seems to activate CTLs targeting normal melanocytes [174]. However, since the presence of T_{RM} cells has been shown to correlate with improved survival in melanoma patients, these skin-related immune adverse events of ICB are an excellent prognostic value [175]. In addition to these autoimmune disorders of the skin, the involvement of T_{RM} cells has also been documented in atopic dermatitis, acute skin graft-versus-host-disease (GvHD) as well as cutaneous T cell lymphoma [84, 176-180]. These findings highlight the heterogeneity of aberrant T_{RM} cell responses similar to their diversity in protective immune responses.

Although less well studied, T_{RM} cell involvement in immunopathological responses in other organs and tissues has also been described. Studies based on murine asthma models of house dust mite (HDM) exposure described the presence of Th2-type $CD4^+$ T_{RM} cells in the lung which contributed to airway resistance [181-183]. Furthermore, a possible role of T_{RM} cells has been implicated in several immune disorders across the body such as inflammatory bowel disease, rheumatoid arthritis, type 1 diabetes and multiple sclerosis [184-188]. Moreover, T_{RM} cells seem to play a role in transplant rejection. Studies of lung transplants showed that increased proportions of recipient-derived T_{RM} cells in the lung were associated with increased acute cellular rejection of the transplant [189].

Together, these studies emphasize the need for a deeper understanding of T_{RM} cell biology. When T_{RM} cells induce unwanted immune reactions in the body, interfering with their generation or maintenance may provide a new therapeutic option for these disorders. For example, $CD8^+$ T_{RM} cells in vitiligo-affected skin are known to express the α-chain of the IL-15 receptor (CD122) indicating their dependence on this cytokine for survival and maintenance. Treating mice with anti-CD122 monoclonal antibodies (mAb) led to re-pigmentation of affected skin areas confirming that targeting T_{RM} cell development or maintenance may open up new treatment options for autoimmune disorders [78].

1.1.9. $CD4^+$ T_{RM} cells

Most of the research on resident memory T cells has focused on $CD8^+$ T_{RM} cells. Due to several reasons the study of memory $CD4^+$ T cells has proven to be more challenging than that of memory $CD8^+$ T cells. Firstly, $CD4^+$ T cells are less proliferative and while memory $CD8^+$ T cells are relatively stable, once established, memory $CD4^+$ T cells seem to diminish after antigen removal. This means fewer cells are available to be studied. Secondly, the effector $CD4^+$ T compartment is highly diverse, consisting of different T helper cell populations, such as T_H1, T_H2, T_H9, T_H17, T_H22 and follicular T helper (T_{FH}) cells, making the analysis of memory $CD4^+$ T_{RM} cells more complex [190]. Additionally, the development of memory $CD4^+$ T cells in general, circulating and resident, is not as well understood. For example, no clear markers exist to distinguish $CD4^+$ memory precursor cells in the circulation from $CD4^+$ terminal effector cells, as is the case for $CD8^+$ T cells [190]. Nevertheless, the characteristics of CD4+ T_{RM} cells are gradually being uncovered. $CD4^+$ T_{RM} cells have been identified in numerous NLTs such as the lung, FRT, skin, small intestine and liver as well as the bone marrow [121, 183, 191-201]. In these tissues mucosal $CD4^+$ T cells have been found to offer protection from different viral and bacterial pathogens, such as influenza virus, HSV-2, *M.tuberculosis*, *N.gonorrhoeae*, *C.muridarum* and others [195, 202-205]. Similar to $CD8^+$ T_{RM} cells, their $CD4^+$ counterparts have been shown to exert their protective functions by secreting cytokines and thereby activating the surrounding immune cells as well as recruiting help from circulating cells [206]. In general, $CD4^+$ T cells interact with other immune cells of the innate and adaptive immune system and in doing so help these cells to perform (better). In line with this, in a model of viral infection in the lung, $CD4^+$ T_{RM} cells have been shown to interact with B cells as well as $CD8^+$ T cells to promote humoral and cellular immune responses [207, 208]. As described above for the lung, $CD4^+$ T_{RM} cells in multiple tissues have been shown to form clusters with other resident immune subsets such as $CD8^+$ T cells, B cells, but also innate immune cells such as macrophages. This close proximity to other immune cells may improve the “sense-and-alarm” function of helper T_{RM} cells [62, 190, 191, 209]. A recent study by Beura *et al.* found that, as with $CD8^+$ T_{RM} cells, immune surveillance of NLTs by memory $CD4^+$ T cells is achieved mostly

by resident rather than circulating cells. Moreover, similar to their $CD8^+$ counterparts, $CD4^+$ T_{RM} cells were found to take up residence in draining LNs. However, in contrast to $CD8^+$ T_{RM} cells, resident memory T cells made up 30% of the $CD4^+$ T cells present in the LNs, which is much more than what has been observed for $CD8^+$ T_{RM} cells. Furthermore, the authors found that $CD4^+$ T_{RM} cells shared a core phenotypic and transcriptional signature across several tissues which was similar to that of $CD8^+$ T_{RM} cells [210]. The C-type lectin CD69, which is involved in tissue retention of $CD8^+$ T_{RM} cells seems to be expressed by most $CD4^+$ T_{RM} cells too. Another molecule expressed by resident $CD4^+$ T cells which is likely involved in tissue retention is the integrin CD11a (integrin α_L which combines with β_2 to form lymphocyte function-associated antigen-1, LFA-1) [195, 211]. In contrast, the molecule CD103, which is often expressed by $CD8^+$ T_{RM} cells in epithelial sites and is likewise involved in tissue retention, does not seem to play a role in $CD4^+$ T_{RM} cells [195, 212, 213]. As with $CD8^+$ T_{RM} cells different cytokines have been reported to play an important role in the recruitment, formation and maintenance of resident helper T cells. While IL-2 signaling appears to be important for the generation of some, but not all, $CD4^+$ T_{RM}, it is still largely unknown which cytokines are critical in which tissues [190, 214].

During the early phase of a primary immune response naïve $CD4^+$ T cells are primed by DCs which provide the necessary stimulation via the TCR as well as the costimulatory molecules and the third signal via cytokines. Depending on the type of pathogen (viral, bacterial, helminth, intracellular, extracellular) a different cytokine milieu directs the differentiation of the naïve $CD4^+$ T cells to acquire distinct helper T cell functions. This ensures that the immune response is appropriate for each type of pathogen. In the simpler models, effector $CD4^+$ T cells can be divided into 5 different subtypes. T_H1 cells are promoted by IL-12 signaling and the transcription factor T-bet. They are characterized by production of the proinflammatory cytokine IFN-γ and are optimal for fighting intracellular viral and bacterial pathogens. T_H2 cell differentiation is induced by signaling via IL-4 and the typical transcription factor GATA3. By producing the cytokines IL-4 and IL-5 T_H2 cells are ideal to fight helminth infections, but may also induce allergic immune responses. T_H17 cells are promoted by IL-6 and TGF-β signaling and the transcription factor RORγT. They are characterized by production of the proinflammatory cytokines IL-17 as well as IL-22 and are optimal for fighting fungal and extracellular bacterial pathogens. Moreover, $CD4^+$ T cells can also form follicular T helper (T_{FH}) cells, which are involved in B cell responses, and Tregs, which regulate the immune response in a suppressive way thereby promoting immune tolerance and preventing exacerbated immune reactions that can lead to autoimmune disorders [215]. Based on this division of the $CD4^+$ T cell effector phase compartment, one of the most interesting questions regarding $CD4^+$ T_{RM} cells is whether they can also be divided into these different subtypes. Indeed, several studies have identified $CD4^+$ T_{RM} with different functions. A model studying the immune response in the skin following

infection with *Candida albicans* found IL-17-producing $CD4^+$ T_{RM} cells [193]. Infection with *L.monocytogenes*, on the other hand, led to the generation of resident $CD4^+$ memory T cells with a T_H1 profile which secreted IFN-γ, TNF and IL-2 [199]. Moreover, $CD4^+$ T_{RM} cells with a T_H2 profile were detected in the lung in an asthma model involving HDM extract [182, 183]. These findings suggest that the $CD4^+$ T_{RM} pool is also very heterogeneous and can be divided into different subtypes.

Several models of viral and bacterial infection have identified a major role for $CD4^+$ T_{RM} cells in offering protection from recurrent pathogens. However, $CD4^+$ T_{RM} also seem to be involved in chronic inflammatory diseases and immunopathology, such as inflammatory bowel disease (IBD), asthma as well as psoriasis [182, 183, 216-218]. In summary, early evidence points to a critical role for $CD4^+$ T_{RM} cells in many different immune settings but also emphasizes that further research is necessary to fully understand this subset and prevent $CD4^+$ T_{RM}-induced aberrant immune reactions.

1.2. Cancer immunotherapy

Cancer is the second leading cause of death worldwide, highlighting the need for effective treatments and therapies. Treatment options in the past have consisted mainly of surgical removal, chemotherapy and radiotherapy. However, in addition to the strong side effects of chemo- and radiotherapy, these therapies often only prolong the life of cancer patients but do not lead to complete remission. This is especially pronounced when tumors are detected at later stages. Therefore, an extensive body of research has focused on improving the treatment options after a cancer diagnosis mostly by enhancing the patient's own immune response to the tumor. This fourth option, collectively termed cancer immunotherapy, has brought great advances to the field [219-221].

Some of the major challenges in fighting tumors are the induction of a highly immunosuppressive TME as well as the changes tumor cells acquire over time, enabling them to escape the immune response. During the process of tumor development, tumor cells are shaped by the immune response in a process called "immunoediting". Because the immune system attacks tumor cells that express the most immunogenic epitopes, cells that have lost or "edited" these epitopes have a greater chance of surviving and proportionally increase in the lesion. Eventually the tumor manages to escape immune recognition and is able to persist despite the presence of immune cells [222-224]. This is also achieved due to the changing TME which evolves from an antitumor to a pro-tumor environment. Whereas pre-malignant lesions are infiltrated by active innate and adaptive immune cells, such as NK cells and

macrophages or T and B cells, respectively, malignant tumors contain mainly immunosuppressive cells such as myeloid-derived suppressor cells (MDSCs), Tregs and immunosuppressive tumor-associated macrophages (TAMs) [225-228]. Together with the cancer cells, these immune cells create a strong immunosuppressive environment that prevents TILs from exerting their antitumor effector functions [229]. Despite the high presence of TILs in many tumors, these are often not functional and express an exhausted phenotype [230, 231]. Therefore, cancer immunotherapies are aimed at inducing and boosting the immune response to tumor cells. Currently used therapeutic approaches can be grouped into 4 different categories: cytokine therapy, immune checkpoint blockade (ICB), adoptive cell transfer and cancer vaccines [232].

Administration of the cytokine IL-2, an important factor for T cell growth and expansion, has been approved for the treatment of renal cell carcinoma and melanoma and has been described to induce antitumor responses in some patients [233, 234]. Unfortunately, in addition to inducing antitumor responses it leads to significant toxicity in multiple organs and tissues [235].

ICB therapy has made great advances since the discovery of the function of the immune checkpoint molecules PD-1 and CTLA-4 and their potential use in cancer immunotherapy less than 3 decades ago [236-240]. For this work James P. Allison and Tasuko Honjo were awarded with the Nobel Prize in Physiology or Medicine in 2018 [241]. In the past decade, several antibodies have been approved for the blockade of CTLA-4, PD-1 and its ligand PD-L1 in multiple solid tumors with different response rates depending on the cancer type [219, 232]. Therapeutic immune checkpoint modulators targeting further molecules, such as TIM-3 (T-cell immunoglobulin and mucin-domain containing-3) and LAG-3 (Lymphocyte-activation gene 3) are currently under investigation [220]. The approved monoclonal antibodies bind to the respective immune checkpoint molecules expressed on T cells or cancer cells and thereby prevent the inhibition induced by the immunosuppressive TME. Unfortunately, while the responses are very promising in some patients, overall response rates can be very low. Evidence has shown that T cells which have spent a substantial amount of time in the immunosuppressive TME may not be able to fully regain their functions, even when they are treated with ICB [242].

Adoptive cell transfer (ACT) therapy involves the transfer of tumor-reactive immune cells to cancer patients. TILs isolated from the patient's tumor are expanded *ex vivo* and then reinfused into the patient [243]. In CAR-T cell therapy, a special form of ACT therapy, isolated T cells derived from the patient are transduced with a retrovirus encoding chimeric antigen receptors (CARs). The extracellular domain of the CAR consists of an antigen-specific single-chain variable fragment (scFv), which is a fusion protein of the variable regions of a heavy and a light

chain of an immunoglobulin, as well as intracellular domains of the TCR signaling pathway [244-246]. Therefore, CAR-T cells can recognize MHC-non-restricted tumor antigens on the surface of tumor cells [247]. The use of $CD19^+$ CAR-T cell therapy has been approved for acute lymphoblastic leukemia and large B cell lymphoma [232]. Due to the high diversity of tumor antigens on solid tumors as well as the inability of the transferred cells to enter a solid tumor, developing a CAR-T cell therapy for non-hematological malignancies is challenging [248].

As a fourth cancer immunotherapy strategy, cancer vaccines have also been extensively studied [225]. The goal of vaccines is to reactivate the adaptive immune response to recognize and fight the tumor [249]. This can be achieved in several ways: by administering peptide/protein-based or DNA/RNA-based vaccines that represent or code for tumor-associated antigens (TAAs), respectively, or alternatively, by administering vaccines based on tumor cells or dendritic cells [250-254]. The administration of irradiated tumor cells or tumor cell lysates aims to induce immune responses against known TAAs, as well as potentially unidentified antigens [255]. DC-based vaccines are built on *in vitro* generated and activated DCs that have been loaded with tumor antigens [256]. Despite the large number of clinical trials of DC-based vaccines which have been tested in various cancer types, only one therapeutic cancer vaccine has been approved so far: sipuleucel-T [225]. It is generated by isolating peripheral blood mononuclear cells (PBMCs), mainly DCs, from the blood of a cancer patient and subsequently activating these autologous DCs by culturing them with a specific tumor antigen (in this case: prostatic acid phosphatase, PAP) and the growth factor GM-CSF (granulocyte-macrophage colony-stimulating factor) [232, 257]. These DCs are then reinfused into the patient where they display the PAP antigen and induce antigen-specific T cell responses that hopefully combat the tumor. This vaccine was approved by the FDA (U.S. Food and Drug administration) in 2010 for the treatment of castration-resistant prostate cancer due to a 4.1-month increase in median survival [258]. Overall, the success of therapeutic cancer vaccines has been very moderate with only a minimal impact on disease-free survival, overall survival and cancer recurrence [259]. Despite their easy use and low toxicities in preclinical and clinical trials, they have only been able to induce tumor regression in a very small fraction of patients and most trials have been stopped in phase II due to limited supportive data [260, 261].

It has been suggested that the limited efficacies of the different approaches of cancer immunotherapy are, at least in part, due to the complex immunosuppressive environment and response induced by the tumor. Employing only one of the above mentioned approaches, such as cancer vaccines or immune checkpoint blockade, may not be sufficient to overcome the strong immunosuppression. However, the combination of several therapies might enhance

their ability to withstand the pro-tumorigenic environment [225]. In line with this approach, several studies have shown that combination therapy, including cancer vaccines administered together with immune checkpoint blockade, induced superior antitumor responses [262-264]. In this case, the cancer vaccine may induce tumor-specific T cells that can infiltrate the tumor, where they avoid suppression by the TME due to the administration of immune checkpoint inhibitors. Recently, we have demonstrated the synergistic antitumor effect of a therapeutic PLGA MS vaccination in combination with anti-CTLA-4 immune checkpoint therapy in a preclinical tumor model [265]. Collectively, these findings indicate that there is still much potential for innovative advances in the field of cancer immunotherapy.

1.3. Influenza

Influenza viruses are enveloped, negative-sense, single-stranded RNA viruses that belong to the family *Orthomyxoviridae*. They can be divided into 4 different genera: Influenza A, B, C and D viruses. Human disease is mainly caused by influenza A and B viruses, although influenza C viruses are known to cause influenza-like disease in some cases, especially in children [266]. Influenza A and B viruses possess a segmented genome consisting of 8 RNA segments, which encode the different viral proteins such as the RNA polymerase subunits polymerase basic protein 1 and 2 (PB1 and PB2) and polymerase acidic protein (PA). Other viral glycoproteins are hemagglutinin (HA) and neuraminidase (NA), nucleoprotein (NP), matrix protein (M1), membrane protein (M2), nonstructural protein NS1 and nuclear export protein (NEP) (see Figure 4) [1].

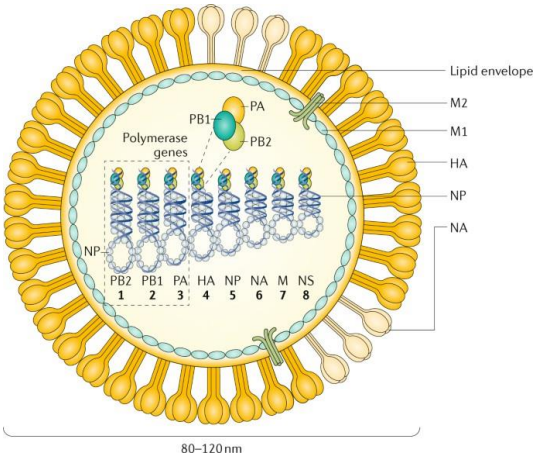

Figure 4: Structure of the influenza A virus. Both influenza A and B viruses are enveloped, negative-sense single-stranded RNA viruses. Their segmented genome consists of 8 segments which encode the different viral proteins. The three viral RNA polymerase subunits PB2, PB1 and PA are encoded by the three largest segments. The other segments encode the viral transmembrane proteins hemagglutinin (HA) and neuraminidase (NA), as well as nucleoprotein (NP), matrix protein M1, membrane protein M2, the nonstructural protein NS1 and nuclear export protein (NEP). Figure taken from [1]

Influenza A viruses can further be subdivided based on antigenically different HA and NA subtypes. 16 different HA and 9 different NA serotypes of avian influenza A viruses are known to date [1, 267]. Additionally, two HA and two NA serotypes have been identified in bat influenza-like viruses [268, 269]. Most of these strains circulate in birds, with only three combinations known to have circulated in humans: A/H1N1, A/H2N2 and A/H3N2 [270]. Infections in humans with the avian influenza viruses H5N1 and H7N9 have been reported, although so far human-to-human transmission was very rare with these strains [1]. Influenza A viruses (IAVs) cause seasonal epidemic outbreaks and have been responsible for 5 documented pandemics: 1918 (H1N1), 1957 (H2N2), 1968 (H3N2), 1977 (H1N1) and 2009 (H1N1) [1]. In contrast, influenza B viruses (IBV) cannot be divided into different serotypes based on HA and NA, but diverged into two distinct lineages in the 1970s: B/Victoria/2/1987 and B/Yamagata/16/1988 [271, 272]. Unlike IAV, the B viruses do not cause pandemics, but play an important role in seasonal epidemics.

Unlike IBV, for which no animal reservoirs are known, IAV also circulates in domestic animals, pigs, horses, poultry and in wild migratory birds [1, 273, 274]. This poses a great threat as new strains can spill over from animals to humans, such as the 2009 pandemic strain H1N1 which was caused by a new virus that was previously circulating in pigs [275, 276]. In addition to new strains from zoonotic origin other mechanisms exist that greatly enhance the genetic diversity (see Figure 5). First, the viral RNA-dependent RNA polymerases are very error prone and lack proof-reading mechanisms. This leads to higher mutation rates than with cellular DNA polymerases. The gradual accumulation of mutations is known as “antigenic drift” [273, 277, 278]. Second, the segmented RNA genome of IAV allows for genetic reassortment. This process, known as “antigenic shift”, happens when one cell is infected with two different viral strains. In this case viral segments can be exchanged between the two viruses resulting in the generation of a new strain that carries some segments from either strain. Due to the lack of pre-existing immunity in the human population, this new strain is rapidly transmissible between humans and often leads to the pandemics [279]. Usually, genetic change happens in the surface proteins hemagglutinin and neuraminidase rendering the neutralizing antibodies to these proteins generated through previous infection or vaccination, less functional [1, 270]. Antigenic drift of T cell epitopes has also been reported although it seems to be less frequent and seems to be associated with a loss in fitness of the virus [280, 281].

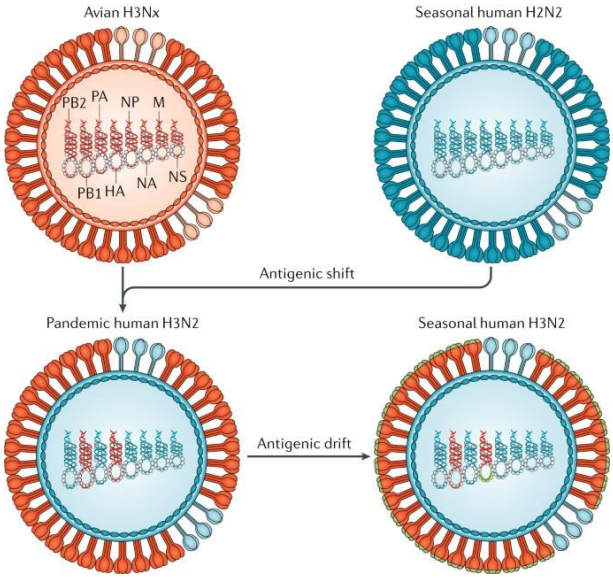

Figure 5: Acquisition of genetic variety in IAV. "Antigenic shift" occurs when two different strains superinfect the same host cell. Due to the segmented nature of the RNA genome segments can be exchanged between the different strains resulting in the generation of a new strain. Depicted here is the 1968 pandemic strain H3N2 which received the PB1 and HA segments from the avian strain and the other six segments from the previously circulating human H2N2 strain. Due to the lack of pre-existing immunity in the human population this strain was easily transmissible between humans and caused the 1968 pandemic. Following the pandemic, the new H3N2 strain slowly acquired mutations in the genome due to the high mutation rate of the RNA polymerase. This process, known as "antigenic drift", leads to the emergence of new seasonal strains. This figure is taken from [1].

Following the emergence of a new pandemic strain the previous circulating strain typically goes extinct. However, during the 1977 pandemic the newly emerged H1N1 strain started to co-circulate with the previous H3N2 strain [282]. The 2009 pandemic resulted in the extinction of the former H1N1 strain, which was replaced by the 2009 H1N1 strain. Thus, currently 4 strains of influenza viruses are co-circulating in humans: A/H1N1, A/H3N2, B/Victoria and B/Yamagata. Interestingly, recent data suggests that due to the COVID-19 pandemic and the concomitant measures to reduce viral spread (masks, contact and travel restrictions, isolation of symptomatic individuals) the B/Yamagata lineage may have gone or may be going extinct [283].

In humans influenza viruses are transmitted through the respiratory route and subsequently infect epithelial cells in the respiratory tract. Mild respiratory disease is usually characterized by infection of the upper respiratory tract with typical symptoms such as fever, cough, headache and sore throat. Severe respiratory disease is often associated with infection of the lower respiratory tract. Patients with severe infection often develop pneumonia which can either be primary virus-induced pneumonia or secondary bacterial pneumonia and can be lethal [1]. Every year IAV and IBV cause seasonal epidemics with 3-5 million cases of severe illness and approximately 290,000-650,000 deaths, with the highest mortality rates in sub-

Saharan Africa and southeast Asia [284, 285]. The constant threat of newly emerging pandemic strains poses a huge threat to human health and societies. Even though the current COVID-19 pandemic was not caused by IAV but by severe acute respiratory syndrome coronavirus type 2 (SARS-CoV-2), it nevertheless highlights the potential consequences of a further pandemic involving influenza viruses and the need for vaccines that efficiently protect against (severe) influenza infection.

1.3.1. Influenza vaccines

The first influenza vaccine was developed shortly after the isolation of the influenza virus in 1933 and was available to the civilian population in the United States in 1945. This vaccine was based on an inactivated virus that had been grown in embryonated chicken eggs. Despite the known difficulties regarding the mutation of the targeted viral proteins, the production method has not markedly changed. The virus is still amplified in embryonated chicken eggs and subsequently harvested and inactivated. However, some changes have been made to this method to improve the vaccine: First, the circulating strain is reassorted with the high-yielding influenza A/Puerto Rico/8/1934 (PR8) strain to improve the growth conditions of the virus. Second, the whole virus is treated with ether or detergent to obtain subvirion or split virus preparations making the vaccine much less immunogenic, but more tolerable for the patient [1]. The inactivated influenza vaccines (IIV) currently used are either trivalent or quadrivalent. The trivalent vaccine contains one H1N1 strain, one H3N2 strain and one of the two B virus strains. The quadrivalent strain contains both A and both B strains [286-288]. The protection offered by these vaccines largely relies on the induction of a specific antibody-response to the surface proteins HA and NA [289]. However, as these proteins are very prone to mutation the efficacy of the vaccine is highly variable. Moreover, due to antigenic changes of the virus the vaccine requires an update every year. Additionally, as the manufacturing process in embryonated eggs is very slow, the decision for which strains to include has to be made months in advance. For the northern hemisphere the decision is typically made in February allowing enough time for new strains to emerge by the start of the influenza season [290-293]. In the case of a new pandemic strain, there is generally insufficient time to produce a new vaccine. Further changes to the vaccine strain can arise due to egg-adapted modifications, such as in the 2016-2017 seasonal influenza vaccine [294]. These issues have led to the development of new techniques. To circumvent the problems caused by growing the virus in embryonated eggs, new methods include the amplification of the virus in cell culture, such as Madin-Darby canine kidney (MDCK) cells [295, 296]. Additionally, the vaccine “Flublok” is based on baculoviruses, which express the HA molecules of the predicted circulating influenza virus strains. These baculoviruses are used to infect continuous insect cell lines and subsequently the HA proteins are extracted and purified from the infected cells. In contrast to

the previously described methods, this type of production does not require the use of active influenza viruses or embryonated eggs. Moreover, the vaccine strains do not require any modifications to improve their amplification in embryonated eggs or tissue culture cells. Both of these improvements greatly reduce the time of production [1, 295, 297]. Furthermore, in 2003, a live-attenuated influenza virus (LAIV) was approved for use. This vaccine is produced by using an attenuated, cold-adapted virus backbone which is modified with the HA and NA genes from the circulating strains. The cold-adapted virus can replicate modestly in the cooler upper respiratory tract, but is prevented from replicating in the warmer lower respiratory tract [298, 299]. Because this vaccine is administered intranasally, it mimics a natural infection more closely and seems to be better suited to induce mucosal and more broadly protective immune responses [300, 301]. However, recent data demonstrated low effectiveness against the A/H1N1 strain [302, 303]. Moreover, this LAIV also requires seasonal adaptations and due to its production in chicken eggs the problems of adaptations and the long production time remain. Most importantly, this vaccine cannot be used in the risk groups of elderly patients, pregnant women and patients with comorbidities [304].

One of the largest problems associated with the current vaccines is that their protection largely relies on the induction of neutralizing antibodies specific for HA and NA. While neutralizing antibodies are essential for sterilizing immunity, they are not able to offer heterosubtypic protection against constantly changing strains [304]. This heterosubtypic protection seems to be given by the cellular arm of the adaptive immune response. Mouse models have demonstrated that $CD8^+$ T cells are the main mediators of heterosubtypic protection. To do so, they make use of the perforin/granzyme-dependent cytotoxic pathways as well as production of inflammatory cytokines such as IFN-γ and TNF [92, 305-307]. More recently, studies have recognized that lung $CD8^+$ T_{RM} cells play a major role in protection against subsequent IAV infections. However, these influenza-induced respiratory T_{RM} cells seem to wane within 7 months [96]. Data from humans has confirmed the importance of T cells for cross-protective immunity. One study found an inverse correlation of illness severity in H1N1 infections with pre-existing, cross-reactive T cells specific for PB1, M1 and NP [308].

As the importance of the cellular immune response for heterosubtypic protection has been proven multiple times and the emergence of new pandemic strains remains a big threat, the goal to produce a “universal” vaccine is highly desirable. Ideally this vaccine would protect against different influenza virus strains and be effective for all age groups.

1.4. PLGA MS

Poly-(D,L-lactic-*co*-glycolic acid) (PLGA)-based delivery systems have been studied extensively in the past for the controlled delivery of drugs, proteins and various other molecules [309, 310]. PLGA is a polymer made up of lactic acid and glycolic acid, which are connected via ester bonds (see Figure 6). In aqueous solutions PLGA is degraded by hydrolysis into its nontoxic monomers which are metabolized in the citric acid cycle [311].

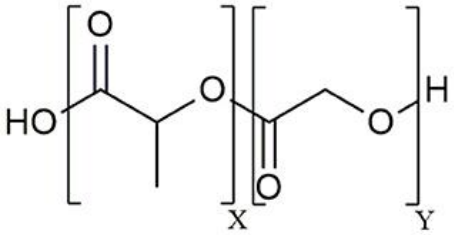

Figure 6: Chemical structure of the poly(D,L-lactide co-glycolide) (PLGA) co-polymer. The polymer consists of lactic acid (X) and glycolic acid (Y) which are linked via ester bonds. Figure taken from [3]

The great advantage of PLGA-based delivery systems is the versatility of the polymer: PLGA particles can be produced in many different shapes and sizes and are thus able to encapsulate a wide range of molecules [3, 310, 312]. Depending on the ratio of lactic acid (LA) to glycolic acid (GA) (LA/GA), the molecular weight, the end group (acid or ester), the molecular shape (linear or branched) and the method and conditions of production, the properties of PLGA particles can be tailored to specific needs [309, 313]. For example, as polylactic acid (PLA) is hydrophobic in nature, a higher amount of PLA leads to a slower degradation rate, whereas in turn a higher amount of the more hydrophilic polyglycolic acid (PGA) leads to a faster degradation rate [314]. In this way, the rate of release of the contents can be adjusted.

Due to these excellent properties of biodegradability and biocompatibility, various pharmaceutical PLGA and PLA products have been approved by the FDA [315]. They are used for the controlled delivery of various molecules, such as drugs and antibiotics. Moreover, PLGA-based particles have efficiently been shown to be efficient vaccine delivery systems [265, 316-327]. Due to the controlled release of antigens over an extended period of time, PLGA particles lead to prolonged antigen presentation and can be used for single-dose vaccines that mimic repeated administrations of conventional prime-boost vaccination schedules [328-333]. Remarkably, PLGA-based systems can be used for two types of vaccine antigen release: a sustained, continuous release of antigen which mimics the administration of several small boosters, as well as a pulsatile release scheme with distinct releases at different time points [334]. This is achieved by combining PLGA microsphere (MS) types with

different release patterns (e.g. PLGA MS with a 50:50 LA/GA ratio together with PLGA MS with a 75:25 ratio and PLA MS). This has been shown to yield a pulsed release pattern with second and third releases, 3 to 5 and 8 to 12 weeks after the initial release, respectively [335].

PLGA particles can be produced by different methods such as the single and double emulsion technique, coacervation or spray-drying. Due to the improved encapsulation efficiency as well as the ability to scale-up the production, we have focused on the spray drying technique. An aqueous solution containing the antigenic proteins or peptides together with the adjuvants is dispersed in the organic phase containing the PLGA polymer (in our case the organic solvent dichloromethane, DCM). This emulsion is nebulized by heated air into a gas stream of compressed air. Subsequently, the solvent evaporates rapidly from the droplets formed yielding microspheres with different particle sizes, depending on the conditions. The microspheres are collected from the airstream using a cyclone separator which makes use of the tangential air stream in the cyclone. The centrifugal force creates a downward spiral movement that causes the particles to be deposited in the collection vessel. Further vacuum drying of the obtained particles can remove solvent residues [309, 336-338].

In our lab we have used the resomer RG502H which consists of 50% glycolate and 50% lactate and has a molecular mass of 14 kDa. This creates amorphous, spherical particles of different sizes from the nanometer range up to 10 µm [265]. After spray-drying the particles are washed out of the collection vessel using a surfactant (Poloxamer188) which binds to the surface of the particles and thereby improves the solubility of these particles in biofluids. PLGA particles show a typical burst release within the first 24h followed by a continuous release over time. Complete degradation occurs within 30 to 60 days [265, 327]. The burst release within the first 24h is due to antigen adsorbed on the surface of the particle and is a common effect observed with PLGA-based particles [339].

PLGA MS-based vaccination strategies have been shown to offer many great advantages compared to the administration of soluble antigen. Most importantly, encapsulated proteins are protected from degradation by proteolytic enzymes. Moreover, encapsulation of antigens has been shown to enhance their antigen presentation by human DCs and to induce a more efficient recognition of the presented epitopes by the immune system [326, 340]. When PLGA MS are administered, they are taken up by immature APCs, mainly DCs, via unspecific phagocytosis since they resemble pathogens due to their sizes [3, 327]. Previous work has established that the uptake of PLGA MS does not negatively affect the function of the DCs [341]. Subsequently, the content is internalized into endosomes and prepared for the classical pathway of presentation via MHC class II molecules to $CD4^+$ T cells. However, the antigens may also escape the endosomes and enter the cytoplasm where they are processed by the proteasome and subsequently loaded onto MHC class I molecules to be presented to $CD8^+$ T

cells via cross-presentation [342, 343]. Previous work from our lab and others has established that coencapsulation of antigens and adjuvants into the same microparticle greatly improves the activation of DCs and the subsequent induction of antigen-specific CTL responses [325, 342]. Moreover, we have shown that co-administration of a second adjuvant, encapsulated into a separate particle, further enhanced the immune response [325]. Immunization using these PLGA MS was able to induce a strong CTL response and protect mice from tumor growth in several tumor models [265, 322, 324, 325]. Furthermore, immunizing mice with PLGA MS containing the highly conserved IAV antigen $M1_{58-66}$ as well as the TLR9 ligand CpG ODN (CpG oligodesoxynucleotide) which were co-administered together with PLGA MS bearing the TLR3 ligand polyinosinic-polycytidilic acid (polyI:C), was able to induce a strong and sustained CTL response and protect mice from IAV infection [321]. Importantly, we have recently shown that the GMP (good manufacturing practice)-grade TLR3/RIG-I (retinoic acid-inducible gene I) ligand Riboxxim can be used to achieve antitumor responses *in vivo*, thereby enabling this vaccine delivery system to be used in a clinical setting.

2. Aim of the thesis

An extensive body of work in the past decade has demonstrated the outstanding potential of tissue-resident memory T (T_{RM}) cells in a wide array of disease settings. These findings have encouraged the development of vaccination strategies capable of inducing local memory T cells responses.

Previous work from our lab has shown that immunization using PLGA MS as an efficient vaccine delivery system is able to induce immune protection from tumors as well as IAV infection in murine models. However, so far we have not yet analyzed the phenotype of the memory T cells generated in response to immunization with PLGA MS. Therefore, this study sought to determine the different $CD8^+$ T cell memory subtypes generated in response to PLGA MS vaccination and assess whether PLGA MS are capable of inducing long-lasting $CD8^+$ T_{RM} cell responses in peripheral organs, sufficient to protect mice in different disease settings.

In a second project, we attempted to generate PLGA MS that can be used for vaccinating against IAV. While our previous work in this setting relied on the encapsulation of short peptides derived from internal viral proteins, the aim of this work was to encapsulate whole, inactivated virus into PLGA MS which would expand the repertoire of epitopes to which an immune response is developed. Thereby this strategy could reduce the risk of immune escape.

3. Material and Methods

3.1. Cell culture

The human embryonic kidney cell line HEK293T (ATCC, USA), was cultured in complete Dulbecco's modified Eagle medium (DMEM, +10% FCS, 1% penicillin/streptomycin, 0.1% β-mercaptoethanol) and used for production of lentiviral particles. BWZ.36 cells were cultured in complete Iscove's modified Dulbecco's medium (IMDM) supplemented with 500 µg/mL hygromycin B and used for the LacZ assay to determine expression of Ovalbumin. Madin-Darby canine kidney (MDCK II)-cells were grown in complete IMDM (+10% FCS, 1% penicillin/streptamycin, 0.1% β-mercaptoethanol) unless otherwise stated and used for IAV amplification and titration. $Ova^{+}Luc^{+}$B16BL6 cells were grown in DMEM (+10% FCS, 1% G418 and 0.1% β-mercaptoethanol) and used for *in vivo* tumor experiments. All cell lines were cultured at 37°C and 5% CO2. Aliquots of $2x10^{6}$ cells of each cell line were frozen gradually in 90% FCS with 10% dimethyl sulfoxide (DMSO) (Sigma-Aldrich) in freezing containers at -80°C overnight (o/n) and finally transferred to a -150°C deep-freezer for long-term storage. Culture media and supplements were obtained from Gibco, Thermo Fisher Scientific.

3.2. Preparation of PLGA MS

PLGA MS were prepared using 14 kDa PLGA 50:50 carrying hydroxyl- and carboxyl-end groups (Resomer ® RG502H, Evonik Röhm GmbH). The antigens Ovalbumin (Sigma-Aldrich, 50 mg) or $M1_{58-66}$ peptide from influenza A Virus (Peptides & Elephants, sequence GILGFVFTL, 10 mg) or $8x10^{6}$ PFU of inactivated IAV and the TLR ligands CpG oligodeoxynucleotides with a phosphothioate backbone (CpG-ODN 1826, Microsynth, 5 mg) as well as polyI:C (Sigma-Aldrich, 0.5 mg) were dissolved in 0.5 ml 0.1 M $NaHCO_3$ (aqueous phase). For coencapsulation of antigens, such as Ova + CpG or $M1_{58-66}$ + CpG both antigens were dissolved together in $NaHCO_3$. 1 g of PLGA was dissolved in 20 ml dichloromethane (organic phase). The aqueous and the organic phase were mixed by ultrasonication and immediately spray dried using the Mini Spray drier 191 (Büchi) at a flow rate of 2 ml/min at a room temperature of 25°C. The obtained PLGA MS were washed out using 0.05% poloxamer 188 (Sigma) and subsequently collected on a cellulose acetate membrane. The PLGA MS were dried for 48h in a vacuum drying cabinet at room temperature (RT) and stored at 4°C until further use. Immediately before use they were dispersed in PBS by ultrasonication (amplitude:40; 10s).

3.2.1. Release of protein from PLGA MS

For quantification of the release 10 mg of PLGA MS were dispersed in 400 µl PBS + protease inhibitor (cOmplete Roche) via ultrasonication and incubated for 6 days at 37°C and 800 rpm in a thermomixer (Eppendorf). At different time points (24h, 48h and 96h) the samples were centrifuged (2000 rpm, 2.5min) and the resulting supernatants transferred to 1.5 ml tubes for further analysis. The remaining MS pellet was resuspended in 400 µl of fresh PBS with protease inhibitor and incubated at 37°C and 800 rpm in a thermomixer for release measurements at later time points. Released protein was either analyzed by using a micro BCA™ protein assay kit (ThermoFisher Scientific), according to the manufacturer's instructions, or via SDS-PAGE with subsequent silver staining

3.2.2. SDS PAGE

In order to separate proteins according to their size, sodium dodecyl sulfate - polyacrylamide gel electrophoresis (SDS-PAGE) was performed under denaturing conditions using the Mini-PROTEAN 3 or Tetra cell system (both Bio-Rad).10% SDS separating gels were prepared and after polymerization topped with 5% stacking gels as listed below. PageRuler Prestained Protein Ladder (10-180 kDa) (ThermoFisher Scientific) was used as molecular weight marker. SDS PAGE was performed in 1x SDS running buffer (10% (v/v) of Laemmli running buffer (pH 8.3, 250mM Trizma (SigmaAldrich), 1.92M glycine (Roth) in dd$H_2$0), 0.1% (w/v) SDS (Serva) in dd$H_2$0) for 45min at an initial voltage of 50V to allow the samples to align at the running front. Then voltages were increased to 110V until the protein loading front had completely passed the separation gel.

Table 1: Protocol for SDS-PAGE gels

5% stacking gel (6ml)	**10% separation gel (15ml)**
4.1 ml MilliQ-H_2O	5.9 ml MilliQ-H_2O
1.0 ml acrylamide mix	5.0 ml acrylamide mix
0.75 ml 1.0 M Tris (pH 6.8)	3.8 ml 1.5 M Tris (pH 8.8)
0.03 ml 20% SDS	0.075 ml 20% SDS
0.06 ml APS (ammonium persulfate)	0.15 ml APS
0.006 ml TEMED (tetramethylethylenediamine)	0.009 ml TEMED

3.2.3. Silver staining

Following separation of the proteins by SDS-PAGE, a silver staining was performed for sensitive protein detection on polyacrylamide gels according to the manufacturer's instructions (Pierce™ Silver Staining Kit, Fisher Scientific). SDS gels were incubated for 1h in fixing solution at RT and afterwards washed in ddH_2O for 1h. The ddH_2O was exchanged several times. Subsequently, the gel was incubated for 1min in sensitizing solution and washed 3 times in ddH_2O for 20s. Next, the gel was stained in cold silver nitrate solution (Silver Stain Solution) for 20min. After washing the gel 3 times in ddH_2O for 20s, 3% sodium carbonate (Developing Solution) was added. As soon as bands occurred, the gel was washed one last time for 20s seconds in ddH_2O before the staining was stopped with 5% acetic acid.

3.2.4. Scanning electron microscopy

To characterize surface morphology using scanning electron microscopy (SEM) particles were mounted on aluminum stubs and sputter-coated with a 6 nm thick layer of platinum by an argon beam sputter coater (Quorum Q150R, Quorum Technologies, Lewes, UK). Micrographs were produced on a Zeiss Auriga 40 at 1, 3, or 5 kV and the sample observed with SmartSEM v6.0 (Zeiss, Germany).

3.3. Mice

C57BL/6 mice and HLA-A*0201 transgenic mice (AAD mice) were originally obtained from Charles River Laboratories. AAD mice (HLA-A*0201 transgenic mice) express a recombinant MHC class I molecule consisting of the peptide binding region of the human HLA-A*0201 and the CD8 binding domain of the murine H2-D^d. Male and female mice were used at 8 - 12 weeks of age. All mice were kept in a specific pathogen-free environment on a 12/12h light/dark cycle with *ad libitum* access to food and water. The experiments were approved by the review board of the Regierungspräsidium Freiburg (G-17/132, G-18/47, G-19/129, G-20/79, G-20/153, G-21/017, G-21/104).

3.3.1. Genotyping of AAD mice

For genotyping of AAD mice ear biopsies were incubated in 500 µl of Lysis buffer (10 mM Tris pH 8.0, 150 mM NaCl, 10 mM EDTA, 0.1% SDS, 0.2 mg/ml proteinase K) at 56°C and 500 rpm for 2h or o/n. Subsequently 350 µl of isopropanol were added and each sample was mixed by inversion. Following 5min of centrifugation at 12500 rpm at RT, the supernatant was discarded and 350 µl of 70% ethanol were added to each sample. This time samples were not inverted.

Following another 5min of centrifugation at 12500 rpm at RT, the supernatant was discarded and the pellet was left to dry to remove all traces of ethanol. Then, the pellet was dissolved in 50 µl of nuclease-free H_2O. These DNA samples were used for PCR using the GoTaq polymerase kit (Promega) according to the manufacturer's instruction and the Biometra Trio Thermocycler (Analytic Jena). PCR products were analyzed on 1.5% agarose gels.

Table 2: PCR mix

Kit reagent	**Volume per sample in µl**
5x Buffer	2.5
$MgCl_2$	1
dNTPs (2 mM)	0.2
H2D forward/reverse primer	0.25
internal control forward/reverse primer	0.125
Taq polymerase	0.125
template DNA	2
nuclease-free H_2O	5.925

Table 3: Primer sequences

Primer	**Forward (5' → 3')**	**Reverse (5' → 3')**
H2D	ACG GAA AGT GAA GGC CCA CTC	GCA GCC ATA CAT CCT CTG GAC G
internal control	CAA ATG TTG CTT GTC TGG TG	GTC AGT CGA GTG CAC AGT TT

Table 4: PCR program for genotyping

Cycles	**Temperature**	**Time**	**Step**
1	94 °C	3min	Initialization
35	94 °C	30s	Denaturation
	67 °C	1min	Annealing
	72 °C	1min	Elongation
1	72 °C	2min	Final elongation

3.3.2. Agarose gel electrophoresis

Agarose gels were prepared with 1.5% (w/v) agarose (Serva) in TAE buffer (2M Trizma, 1M acetic acid, 50mM EDTA, pH 8.0). Per gel (50 ml) 4 µl of Midori Green (NIPPON Genetics) were added during gel casting. 9 µl of PCR products were loaded into gel cavities and run for 25min at 100V. SmartLadder small fragments (eurogentec) was used as a molecular weight marker.

3.3.3. Immunization

For subcutaneous prime immunization mice received a mixture of 5 mg PLGA MS containing CpG with or without the antigen (Ova or $M1_{58-66}$ peptide) together with 5 mg PLGA MS containing polyI:C dissolved in 200 µl PBS injected into the base of the tail. 14 days later mice received an intranasal boost vaccination. For intranasal immunization mice received a mixture of 2.5 mg PLGA MS containing CpG with or without the antigen (Ova or $M1_{58-66}$ peptide) together with 2.5 mg PLGA MS containing polyI:C. To ensure proper intranasal application of the vaccine and reduce stress levels mice were anesthetized with isoflurane (5% in oxygen; CP Pharma). PLGA MS were dispersed in 50 µl PBS and slowly pipetted onto the nostrils (25 µl/nostril). The concentrations of the encapsulated antigens and TLR ligands per mouse was as follows. Subcutaneous immunization: Ova (250 µg), $M1_{58-66}$ (50 µg), inactivated IAV ($5x10^4$ PFU before inactivation) CpG (25 µg) and polyI:C (2.5 µg). Intranasal immunization: Ova (125 µg), $M1_{58-66}$ (25 µg), inactivated IAV ($2.5x10^4$ PFU before inactivation) CpG (12.5 µg) and polyI:C (1.25 µg).

3.3.4. Treatment with FTY720

S1PR1 inhibitor FTY720 (Sigma-Aldrich) was added to the drinking water of mice 2 days before the infection with IAV or the injection of Ova^+Luc^+B16BL6 tumor cells or two days before flow cytometry analysis of the immune response. Every 3 days the drinking water was exchanged with fresh water containing a new aliquot of the inhibitor. The concentration of the inhibitor was 7 µg/ml, leading to an approximate uptake of 1 mg/kg per day. To confirm the absence of circulating lymphocytes blood was collected from the mice after they had been sacrificed, stained for CD3, CD4 and CD8 and subsequently analyzed by flow cytometry. The mean value of $CD3^+$ T cells of mice not treated with the inhibitor was set to 100% and the values of all mice normalized to this value.

3.4. Flow cytometry analysis

3.4.1. Isolation of murine cells for flow cytometry

Mice were sacrificed by administration of carbon dioxide. Immediately thereafter, blood was collected by heart puncture and directly added to FACS buffer (PBS, 2% FCS, 2 mM EDTA) to prevent clotting. Subsequently, a bronchoalveolar lavage was performed by flushing the airways twice with 800 µl of cold PBS. Next, spleens were collected. After collection of the spleen, mice were perfused using cold PBS to ensure removal of blood from the lungs. Spleens were gently mashed through a 40 µm strainer. Lungs were digested using the Lung Dissociation Kit, mouse (Miltenyi, Germany) and the gentleMACS Octo Dissociator with Heaters (Miltenyi, Germany) according to the manufacturer's protocol. Briefly, lungs were transferred to a gentleMACS C tube containing the enzyme mix (2.4 ml 1x Buffer S, 100 µl enzyme D, 15 µl enzyme A) and digested using the program "37C_m_LDK_1". Next, samples were filtered through a 70 µm MACS SmartStrainer and the C tubes were washed with 2.5 ml of Buffer S to minimize cell loss. After a 10-minute centrifugation step at 300 g, the supernatant was removed and the pellet was resuspended in FACS buffer for further use. All obtained single cell suspensions were incubated with erythrocyte lysis buffer (155mM NH_4Cl, 10 mM $KHCO_3$, 0.1 mM EDTA) for 5min at RT before they were washed and subsequently used for staining.

3.4.2. Flow cytometry

First, F_c receptors of single cell suspensions were blocked by incubating samples with 2.4G2 antibody (obtained from the supernatant of 2.4G2 hybridoma cells) for 15min at 4°C. For tetramer analysis samples were incubated with HLA-Ax0201 Influenza-M1 (GILGFVFTL) tetramer or H-2 K^b Ovalbumin (SIINFEKL) coupled to BV421 (MBL International Corporation, USA) in FACS buffer (1x PBS, 2% FCS, 2mM EDTA) for 30min at RT protected from light (1:100 in 50 µl PBS). After washing the samples with PBS they were incubated with the extracellular staining mix (old mix: Alexa Fluor 488-conjugated anti-CD8, APC-conjugated anti-CD62L, PE/Cy7-conjugated anti-CD69, BV605-conjugated anti-CD127 and fixable viability stain (FVS) 700; new mix: Alexa Fluor 488-conjugated anti-CD8, BV711-conjugated anti-CD44, APC-conjugated anti-CD62L, PE/Cy7-conjugated anti-CD69, PE-conjugated anti-CD103 and FVS620) in PBS for another 30min at 4°C, before they were washed twice and subsequently analyzed on a BD LSR Fortessa™.

For intracellular cytokine staining (ICS) analysis samples were also incubated with 2.4G2 antibody following the stimulation period. After washing the samples with PBS, they were incubated with the extracellular staining mix (Alexa Fluor 488-conjugated anti-CD8, APC-conjugated anti-CD62L, PE/Cy7-conjugated anti-CD69, BV605-conjugated anti-CD127 and FVS700) for 30min at 4°C before they were washed and incubated for 30min at 4°C with Foxp3 Transcription Factor Staining Buffer Set (Invitrogen/eBioscience). After washing with the permeabilization buffer of the same kit they were incubated o/n with the intracellular staining mix (BV421-conjugated anti-IFN-γ). Samples were then washed twice with permeabilization buffer (eBioscience) before they were resuspended in FACS buffer for analysis on a BD LSR Fortessa™.

For determination of the T-lymphocyte reduction in the blood of FTY720-treated mice, samples were stained with FVS780, FITC-conjugated anti-CD3, APC-conjugated anti-CD4 and V450-conjugated CD8 in PBS for 30min at 4°C and subsequently washed with FACS buffer. Next, cells were fixed with 4% paraformaldehyde (PFA) in PBS for 5min at RT, before they were washed with FACS buffer once again. Then samples were measured on a BD FACSVerse™.

Table 5: Antibodies used for flow cytometry

Epitope	Clone	Fluorochrome	Supplier	Dilution
Protein (living cells)		FVS620	BD Biosciences	1600x
Protein (living cells)		FVS700	BD Biosciences	1000x
Protein (living cells)		FVS780	BD Biosciences	1000x
CD3	145-2C11	FITC	Biolegend	800x
CD4	GK1.5	APC	Biolegend	800x
CD8α	53-6.7	V450	eBioscience	800x
CD8α	53-6.7	Alexa Fluor 488	Biolegend	1000x
CD44	IM7	Brilliant Violet 711	BD Biosciences	600x
CD62L	MEL-14	APC	Biolegend	800x
CD69	H1.2F3	PE/Cy7	Biolegend	200x
CD103	2E7	PE	BD Biosciences	400x
CD127	A7R34	Brilliant Violet 605	Biolegend	200x
IFN-γ	XMG1.2	Brilliant Violet 421	Biolegend	800x

3.4.3. Restimulation

To measure activation of CTLs an ICS was performed. Splenocytes or lung cells were incubated with or without 10 µM of peptide ($M1_{58-66}$ peptide for AAD mice; $PA_{224-233}$, $NP_{366-374}$, $PB1_{703-711}$, $M1_{128-135}$, $NS2_{114-121}$, $PB1F2_{62-70}$, $PB2_{198-206}$ for C57BL/6 mice, peptides & elephants) in the presence of 10 mg/ml brefeldin A (BFA) (Sigma-Aldrich; dissolved in DMSO) for 5h at 37°C Subsequently, samples were stained as described in the section “flow cytometry”. Background values of each sample (“unstimulated”) were subtracted from each sample (for spleen samples the mean of each duplicate was used). As a positive control samples were stimulated with phorbol 12-myristate 13-acetate (PMA) (0.5 µg/ml) and ionomycin (5 µg/ml), (both Sigma, pre-solved in DMSO). For ICS analysis of mice immunized with inactivated virus-bearing PLGA MS DC2.4 cells which had been infected with IAV (MOI = 1.75) 4h previously were used as an additional positive control.

Table 6: Peptide sequences

Peptide	sequence	restriction element
$M1_{58-66}$	GILGFVFTL	HLA-A*0201
$PA_{224-233}$	SSLENFRAYV	H-2D^b
$NP_{366-374}$	ASNENMETM	H-2D^b
$PB1_{703-711}$	SSYRRPVGI	H-2K^b
$M1_{128-135}$	MGLIYNRM	H-2K^b
$NS2_{114-121}$	RTFSFQLI	H-2K^b
$PB1F2_{62-70}$	LSLRNPILV	H-2D^b
$PB2_{198-206}$	ISPLMVAYM	H-2K^b

3.5. Generation of Ova$^+$Luc$^+$B16BL6 cells

3.5.1. Generation of competent bacteria

The generation of chemically competent bacteria was performed as follows: an aliquot of 5 ml of lysogeny broth (LB) medium (1% (w/w) tryptone, 1% (w/w) NaCl, 0.5% yeast extract) was inoculated with the desired *E. coli* strain and grown o/n at 37°C and 250 rpm. A 100-fold dilution of this pre-culture was used to inoculate fresh LB that was further grown at 37°C and 250 rpm. The OD_{600nm} was determined using a SmartSpec Plus spectrophotometer (Bio-Rad). Once an OD_{600nm} of 0.5 was reached, the bacterial culture was placed on ice for 15min and was kept on

ice during the following procedures. After the 15-minute incubation period, the culture was centrifuged at 4000xg and 4°C for 10min before the bacteria were resuspended carefully in 50 ml of 0.1 M ice-cold sterile $MgCl_2$ (Acros Organics). The bacteria were centrifuged once more at 4000 g and 4°C for 10min and subsequently were resuspended carefully in 50 ml of 0.1 M ice-cold sterile $CaCl_2$ (Roth), in which they were incubated on ice for 20min. Following a final 10-minute centrifugation step at 4000xg the bacteria were resuspended in a total volume of 5 ml of sterile $CaCl_2$/glycerol. Aliquots of 200 µl were prepared and stored at -80°C for further use.

3.5.2. Cloning

DNA fragments encoding full-length ("Ova full") or cytosolic ("Ova cyto", missing the first 150 bp, [344]) Ovalbumin were amplified from pre-existing vectors using oligonucleotides including Not-I or Nhe-I restriction sites (5'-GTA CTA GCT AGC ATG GGG CTC ATC GGT GCA G-3' and 5'-GTA CTA GCG GCC GCT GAA GGG GAA ACA CAT CTG CCA AAG-3' for "Ova full" and 5'-GTA CTA GCT AGC ATG ACC AGG ACA CAG ATA-3' and 5'-GTA CTA GCG GCC GCT TAA GGG GAA ACA CAT CTG-3' for "Ova cyto") and the Q5 High-Fidelity DNA Polymerase (NEB) according to the manufacturer's instruction. The amplified fragment was purified via agarose gel electrophoresis and using the NucleoSpin Gel and PCR Clean-up Kit (Macherey-Nagel). The purified "Ova full" and "Ova Cyto" DNA fragments and the target vector pCDH-EF1a-MCS-IRES-copGFP (System Biosciences/BioCat) were both digested with NotI-HF and NheI-HF (NEB) according to the manufacturer's instruction. Digested plasmid DNA was dephosphorylated using Shrimp Alkaline Phosphatase (NEB). Both insert and plasmid were purified via agarose gel electrophoresis. Ligation was performed at a molar ratio of 1:5 of plasmid vector to insert using the Quick DNA ligase (NEB) according to the manufacturer's instruction. The ligation reaction was carefully mixed with 50 µl of chemically competent *E.coli* TOP10F' and incubated on ice for 30 min. Bacteria were then heat shocked for 30s at 42°C, cooled on ice for several minutes, and mixed with 950 µl LB medium. Transformed bacteria were incubated for 1h at 37°C while shaking to allow for antibiotic resistance to develop. Bacteria were plated on LB agar plates (2% (w/w) agar in LB medium) containing 100 µg/ml ampicillin and incubated o/n at 37°C. For sequence analysis, 5 ml LB medium containing ampicillin were inoculated with a single bacterial colony picked from LB-agar plates. Cultures were grown o/n at 37°C and 150 rpm and plasmid DNA was extracted using the NucleoSpin Plasmid kit (Macherey-Nagel). DNA sequences of pCDH-EF1a-Ova_full-IRES-copGFP and pCDH-EF1a-Ova_Cyto-IRES-copGFP were verified by Sanger sequencing at Eurofins Genomics (Germany).

3.5.3. Generation and purification of lentiviral particles

Production of lentiviral particles was done by transiently co-transfecting a lentiviral expression vector (either pCDH-EF1a-Ova_full-IRES-copGFP or pCDH-EF1a-Ova_cyto-IRES-copGFP), the lentiviral envelope vector pMD2.G (Addgene plasmid #12259) and the lentiviral packaging vector psPAX2 (Addgene plasmid #12260) into HEK293T cells using the TransIT-LT1 transfection reagent (Mirus, Madison, WI, USA). For this purpose lentiviral vector DNA was mixed at a ratio of 1 µg pMD2.G: 1.84 µg psPAX2 : 2.1 µg lentiviral expression vector in serum-free IMDM. This mix was incubated at room temperature for 30-60min before it was added dropwise to different areas of the well containing hthe HEK293T cells. After 8–16h of incubation the medium was removed and replaced with lentiviral harvest medium (complete IMDM). 48 to 72h post transfection the supernatant which contained the lentiviral particles was harvested. Contaminating plasmid vector DNA was digested by adding 1 µg/mL DNase I (Roche) and 1 mM $MgCl_2$ (Acros Organics) and incubating at 37°C for 20min. Next, samples were centrifuged to remove cell debris and the remaining supernatants containing lentiviral particles were stored at -80°C until further use.

3.5.4. Transduction of Luc$^+$B16BL6 cells

To generate B16BL6 cells which stably express ovalbumin we lentivirally transduced the target cell line Luc$^+$B16BL6. Luciferase-expressing B16BL6 (Luc$^+$B16BL6) cells were obtained from Olaf van Tellingen (Netherlands), who introduced a bAct-Luc-IRES-GFP construct by transfection. These cells were infected with the supernatant containing the lentivirus (either “Ova full” or “Ova cyto”) which was mixed 1:1 with DMEM (+ 10% FCS, 1% G-418, 0.1% β-mercaptoethanol). Following an incubation period of 48h the medium was replaced with DMEM which contained no lentiviral particles. After 3 passages the cells were not considered infectious any longer. To obtain a single clone, cells were single cell-sorted for high GFP expression by FACS (this was performed by the Flow Cytometry Core Facility at the University of Konstanz). These single cell clones were left to grow for 3-4 weeks until sufficient cell numbers were obtained for further testing. Over the following 6 weeks cells were kept in culture and the expression of Ova and luciferase were tested regularly by LacZ Assay or Luciferase activity assay respectively. Finally, the clone with the best expression of both Ova and luciferase was chosen for *in vivo* experiments, in this case one of the “Ova cyto” clones.

3.5.5. LacZ Assay

LacZ assays were performed to check for Ova expression of the generated Ova$^+$Luc$^+$B16BL6 clones. Therefore, triplicates of $1x10^4$ Ova$^+$Luc$^+$B16BL6 cells were seeded into a round bottom

96-well-plate. After a brief centrifugation step of 1min at 1200 rpm the supernatant was discarded and $5x10^4$ B3Z Ova Hybridoma cells were added to each well. This mixed culture of cells was incubated o/n at 37°C. The following day the plate was washed with PBS before cells were resuspended in 100 µl of LacZ buffer (1x PBS, 6.5 mM $MgCl_2$, 0.13% NP40, a pinch of chlorophenolred β-D-galactopyranoside) and incubated at 37°C for another 3h. To analyze the change of color in this chromogenic assay samples were measured at 570 nm wavelength and 620 nm reference wavelength using a TECAN plate reader (TECAN group Ltd.). Hybridoma cells stimulated with 50 ng/ml PMA and 500 ng/ml Ionomycin (both Sigma-Aldrich, dissolved in DMSO) were used as positive control. Hybridoma cells that had not been incubated with either Ova^+Luc^+B16BL6 cells or PMA/ionomycin were used as a negative control.

3.5.6. Luciferase assay

To measure luciferase activity luciferase-expressing B16BL6 cells were seeded into a black 96-well-plate at a density of $1x10^5$ cells per well. Cells were left to settle in the incubator at 37°C and 5% CO_2 for 1h. Then DMEM (+ 10% FCS, + 0.1% β-Mercaptoethanol) containing 300 µg/ml of D-Luciferin*K (#bc219, Synchem) was added to the cells at a ratio of 1:1 to give a final concentration of D-Luciferin of 150 µg/ml. Cells were incubated for 10min at 37°C before bioluminescence was measured using a TECAN plate reader (TECAN group Ltd.). Cells with no luciferase construct and wells containing only the substrate D-luciferin were used as negative controls.

3.6. Tumor experiments

3.6.1. Injection of tumor cells

Ova^+Luc^+B16BL6 tumor cells were injected 6, 18, 30 or 60 days after the intranasal boost immunization. The first *in vivo* experiment performed using this cell line was to determine the optimal number of cells to be injected for optimal tumor growth. The following cell numbers were tested: $1x10^5$, $3x10^5$, $6x10^5$ and $1x10^6$ cells. $1x10^6$ tumor cells were found to yield optimal tumor growth in all of the groups analyzed. Therefore, for all future experiments $1x10^6$ tumor cells were injected intravenously into the tail vein in a volume of 100 µl PBS (+ 1mM EDTA). Immediately after the injection of tumor cells and every 2-3 days up to 24 days after the injection of tumor cells, growth of metastases was monitored using the IVIS200 System (Perkin-Elmer). B16BL6 melanoma cells are derived from B16 melanoma cells, which were originally isolated from a spontaneously formed tumor in a C57BL/6 mouse. Through 10

subsequent selective procedures according to Fidler's method, the cell line B16F10 was obtained. This method involves the injection of melanoma cells into a mouse and isolation of the cells from the formed pulmonary metastases. The cells obtained from these metastases are then injected into a new C57BL/6 mouse. This step was repeated 10 times to obtain the B16F10 cell line. B16BL6 cells were generated by injecting B16F10 cells into the urinary bladder of male C57BL/6 mice and subsequent removal and maintenance of the bladder on semi-solid agar. Tumor cells that migrated through the wall of the bladder were recovered from the agar, cultured and repassaged. This step was repeated 6 times to obtain the B16BL6 cell line. Intravenous injection of these B16BL6 melanoma cells leads to the formation of metastases in the lung and is a commonly used murine tumor model [345].

3.6.2. IVIS measurements

To monitor tumor growth in C57BL/6 mice *in vivo* measurements were performed using the IVIS200® System (Perkin Elmer). Immediately following the injection of tumor cells and every 2-3 days thereafter measurements were done to follow the growth of lung metastases. Mice were anaesthetized by inhalation of 2.5% Isoflurane in the XGI-8 chamber of the IVIS200. Under anesthesia each mouse received 3mg of luciferin in a volume of 200 µl PBS intraperitoneally. Next, mice were transferred to the measurement chamber of the IVIS System and placed on the heating pad (37°C) to prevent them from cooling down. After an incubation period of 10min, the generated bioluminescence was measured using the CCD camera and the following settings: Em Filter=Open, Ex Filter=Block, Bin:(M)8, FOV:22.2, f1, 180s. During the entire time mice were kept anaesthetized. Once the measurement was completed mice were carefully placed back into their home cage and watched until they had woken up. Before each measurement mice were weighed to monitor their health status. The data was analyzed using Living Image Software (Perkin Elmer).

3.7. Influenza A Virus experiments

3.7.1. Influenza A Viruses

For experiments with AAD mice the IAV strain A/Regensburg/D6/09 (H1N1pdm09, RB1) was used. For experiments with C57BL/6 mice the recombinant A/Puerto Rico/8/1934 (rPR8) strain was used. This recombinant IAV strain expresses the SIINFEKL peptide in the stalk of NA ("insOva IAV"). It was kindly provided by Jonathan Yewdell (NIH, Bethesda, MD) [346].

3.7.2. Virus amplification

Amplification of both IAV strains was done in Madin-Darby canine kidney (MDCK II) cells. On day 0 cells were seeded at 1.2x 10^7 in a 175 cm^2 flask. The following day cells were washed with Infection-PBS (PBS, 0.21% bovine albumin solution, 884 nM CaCl2, 492 nM MgCl2, 1% PenStrep) before they were infected with IAV at a multiplicity of infection (MOI) of 0.001 for 60min at 37°C. Subsequently, the supernatant was removed and 20 ml of BA medium (IMDM, 1% glutamine, 1% PenStrep, 0.21% BA solution, 20 µg trypsin) were added to the cells before they were incubated at 37°C for 72h. Following this incubation period, the supernatant was harvested and stored at – 80°C until further processing. To concentrate the virus, the supernatants of several flasks were thawed, centrifuged at 4000 rpm for 10min to remove cells and cell debris and were subsequently transferred to ultracentrifuge tubes. Next, the supernatants were centrifuged at 28.000 to 41.000 rpm for 16h at 4°C. Following this step, the virus was concentrated in the pellet. Therefore, the supernatant was discarded and the pellet was dissolved in Infection-PBS by incubating the samples at 4°C for 15min. Now, all the pellets were pooled, thoroughly vortexed, aliquoted and stored at -80°C until further use. For each experiment a new aliquot was used to prevent loss due to freeze-thawing.

3.7.3. Influenza A Virus infection

Infection of mice with IAV occurred at indicated time points after their boost immunization (6, 18, 30 or 60 days after the boost). Mice were anesthetized by inhalation of 5% isoflurane in a XGI-8 chamber before they were i.n. inoculated with IAV using 25 µl per nostril. A 10 x 50% mouse lethal dose (MLD_{50}) was used (10 x MLD_{50} = 5 × 10^4 PFU in C57BL/6 mice) for infection of AAD mice with RB1. C57BL/6 mice were infected with 1000 PFU of insOva rPR8. For determination of the viral titer in the lungs mice were sacrificed 48h after infection. Lungs were removed, weighed and 10 ml PBS added per 1 g of lung. Subsequently, lungs were smashed through a 40 µm mesh. Cell suspensions were frozen and thawed three times to ensure lung cells released the virus. After the last freeze/thaw cycle, samples were centrifuged for 10s at 1200 rpm to remove cell debris. The supernatant of each sample was aliquoted and stored at -80°C until a plaque assay was performed. For observation of bodyweight, mice were weighed daily from the day of infection. When mice were euthanized at the clinical endpoint of 80% of the initial bodyweight at the time of infection, the last recorded bodyweight (at the endpoint) was used throughout the observation period.

3.7.4. Plaque Assay

To determine the number of infectious particles in the lungs or in a fresh batch of IAV, a plaque assay was performed in 96-well plates as previously described [321, 347]. Briefly, MDCK II cells were grown to confluence in 96-well plates before they were washed with PBS and infected with serial dilutions of the virus-containing samples (lung supernatants or aliquot of a new stock) in PBS for 60min at 37°C. Next, the supernatant was discarded and cells were overlaid with overlay-medium [1:1, MEM-medium:2.5% AVICEL® -Medium (FMC BioPolymer)] for 24h. The next day, virus-infected cells were washed and fixed with 4% Roti-Histofix (in PBS) for 30min at 4°C. Thereafter, cells were stained with a monoclonal antibody specific for the IAV nucleoprotein (Serotec, Puchheim, Germany) for 1h at RT, followed by a 1h with peroxidase-labeled anti-mouse antibody (DIANOVA, Hamburg, Germany) and lastly incubation with True BlueTM peroxidase substrate (KPL, sera care) for 10min. Stained plates were scanned on an Immunospot plate scanner (C.T.L. Europe). Viral titers are shown as the logarithm to the base 10 of the mean values.

3.7.5. Virus inactivation

To inactivate IAV, we tested 4 different methods: heat inactivation, UV irradiation, β-propiolactone (BPL) and formaldehyde (FA). For heat inactivation an aliquot of virus was incubated at 56°C for 30min and subsequently frozen at -80°C until further analysis. For inactivation using UV irradiation an aliquot of virus was placed under UV light (wavelength of 312 nm) at a distance of 15 cm for 30min before sample were frozen at -80°C. Inactivation using BPL was done by incubating virus samples in 0.1% BPL at 4°C o/n. Inactivation using FA was done by incubating virus in 0.02% FA at 37°C o/n. The following day samples inactivated with BPL or FA were centrifuged at 14,000g for 30min using an Amicon 3K (Merck) to remove the remaining BPL or FA respectively. The obtained concentrate (approximately 50 µl) was washed out with 450 µl of PBS, making sure that the filter was flushed properly to minimize sample loss. Subsequently, these samples were stored at -80°C. To confirm inactivation of the virus a plaque assay was performed.

3.8. Statistics

Data are given as mean ± SD. Statistical significance for comparison of multiple groups was determined by applying a one-way or two-way ANOVA followed by Tukey's post-hoc tests. The Kaplan–Meier survival analysis was used to estimate statistical significance in overall survival distribution between the groups. Log-rank (Mantel–Cox) tests were applied to compare survival rates. All statistical analyses were performed using GraphPad.

4. Results

4.1. Generation of local CD8$^+$ memory T cells using PLGA MS

4.1.1. Identification of an effective immunization strategy

The aim of this project was to identify whether immunization with PLGA MS could induce the highly desirable tissue-resident memory T cell population and if so, to analyze how long this population lasts and whether it is capable of protecting individuals from tumor growth and infections.

While many studies in the past years have investigated the generation of T_{RM} cells following different immunization or infection protocols none of these studies have used PLGA MS. Therefore, we set out to find the most efficient immunization protocol to generate a high number of T_{RM} cells in the lung. Since prior work has demonstrated that a mucosal route of vaccination is more efficient at inducing T_{RM} cells at mucosal sites than a systemic one, we decided to compare three vaccination strategies: in the first strategy mice received only one i.n. immunization with PLGA MS (referred to as “i.n. prime only”), while in the second one this i.n. prime immunization was followed up by an i.n. boost vaccination 14 days after the prime (referred to as “i.n. prime-boost”). As a third strategy we decided to analyze the response after a s.c. prime vaccination followed by an i.n. boost 14 days later (referred to as “s.c. prime – i.n. boost”) [156, 348-350]. This third strategy has previously been shown by our group to induce strong and sustained CD8$^+$ T cell responses, however no T_{RM} cells were analyzed in this study [321]. To investigate T cell responses induced by the different vaccination regimens lung and splenic lymphocytes were collected and analyzed for vaccine-specific CD8$^+$ responses 6 days after the last vaccination. The flow cytometry gating strategy we used to distinguish the different memory CD8$^+$ T cell subtypes was based on the expression of CD62L, CD69 and CD127 (Figure 7). CD62L (L-selectin) is a cell adhesion molecule that facilitates homing of lymphocytes into SLOs [351]. CD69 counteracts S1P-mediated egress of lymphocytes via the cognate receptor S1PR1 and thereby promotes tissue retention [352]. CD127 is the α-chain of the IL-7 receptor and typically expressed on MPECs [24]. SIINFEKL-specific CD8$^+$ T cells were broken down into the previously described subtypes: effector T cells (T_{EFF}: CD62L$^-$CD69$^-$ CD127$^-$), central memory T cells (T_{CM}: CD62L$^+$CD69$^-$CD127$^+$), effector memory T cells (T_{EM}: CD62L$^-$CD69$^-$ CD127$^+$) and resident memory T cells (T_{RM}: CD62L$^-$CD69$^+$CD127$^-$).

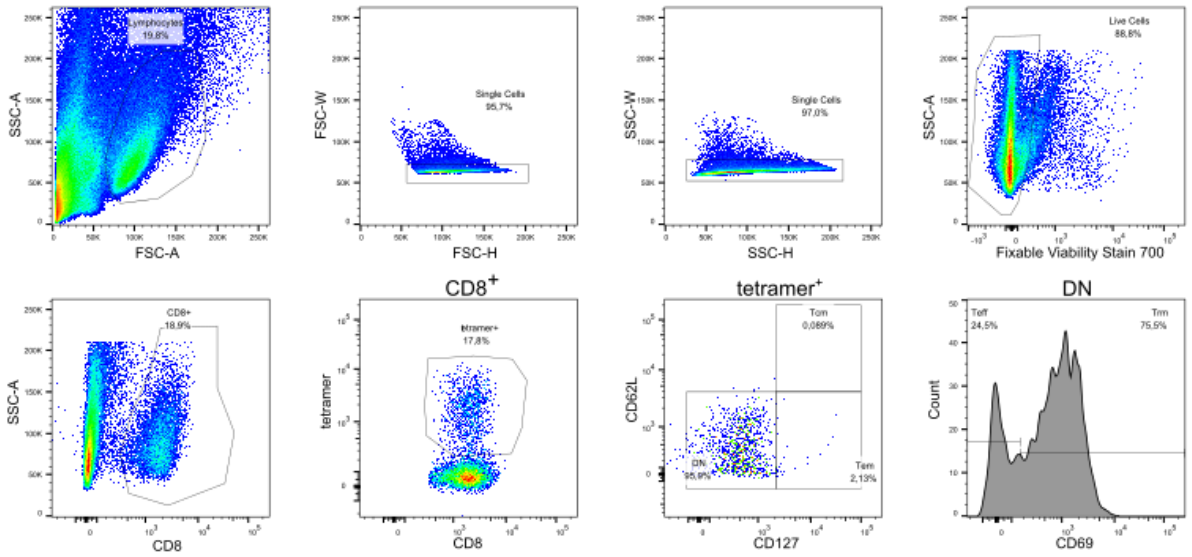

Figure 7: Flow cytometry gating strategy to identify the different specific CD8⁺ T cell populations. After gating on lymphocytes, singlets and live cells, the remaining cells were gated on CD8⁺ SIINFEKL-tetramer⁺ cells. These SIINFEKL-specific cells were further divided into three different populations based on the expression of CD62L and CD127: CD62L⁺CD127⁺ cells were classified as T_{CM} cells, CD62L⁻CD127⁺ cells as T_{EM} cells and double-negative cells were further divided into T_{EFF} (CD69⁻) and T_{RM} cells (CD69⁺) based on the expression of CD69.

Our results showed that both prime-boost immunization regimens were able to induce vaccine-specific CD8⁺ T cells in the lung (Figure 8A). However, the heterologous "s.c. prime – i.n. boost" immunization scheme resulted in the highest percentage of SIINFEKL-specific CD8⁺ T cells in the lung as well as the spleen (Figure 8A; lung: 47.1% ± 18.7, spleen: 3.1% ± 2.4; compared to "i.n. prime only" lung: 1.4% ± 1.5, spleen: 0.2% ± 0.09; "i.n. prime – boost" lung: 13.7% ± 12.3, spleen: 0.2% ± 0.1). Similarly, the percentage of T_{RM} cells among SIINFEKL-specific CD8⁺ T cells induced was also strongest in the "s.c. prime – i.n. boost" vaccination group (Figure 8B: "i.n. prime only": 8.2% ± 8.3; "i.n. prime – boost": 70.4% ± 14.8; "s.c. prime – i.n. boost": 84.2% ± 5.3). Taken together, our data showed that a s.c. prime – i.n. boost immunization using PLGA MS was highly efficient at inducing T_{RM} cells in the lung. We therefore decided to continue all future experiments using this vaccination strategy.

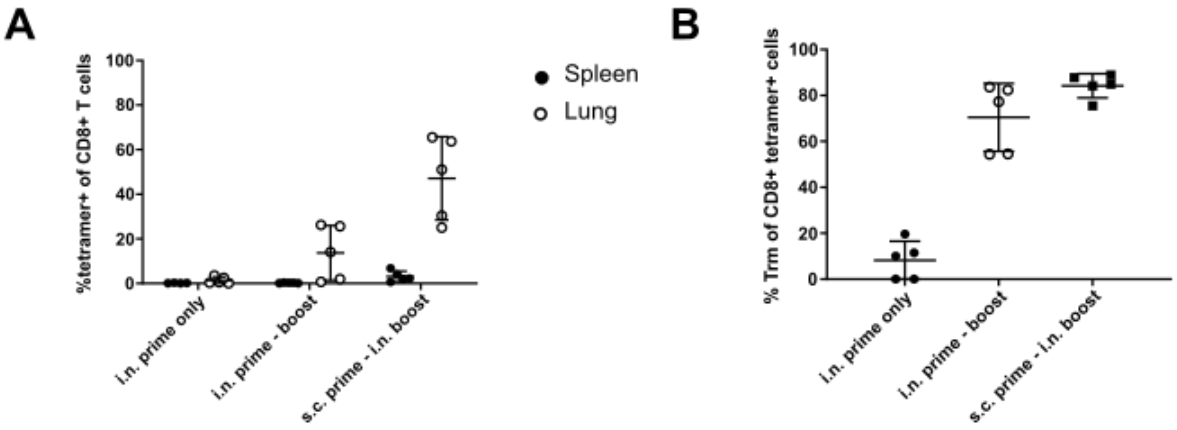

Figure 8: S.c. prime – i.n. boost vaccination generates highest percentage of vaccine-specific CD8$^+$ T_{RM} cells. C57BL/6 mice (n=5) received a prime immunization on day 0. Depending on the protocol this was either an i.n. or a s.c. immunization using a mixture of PLGA MS containing Ova/CpG and PLGA MS containing polyI:C. For the prime – boost vaccination protocols mice received an i.n. boost vaccination on day 14. Lungs and spleens were removed 6 days after the last vaccination and analyzed for the presence of vaccine-specific CD8$^+$ T cells by flow cytometry. (A) The percentage of SIINFEKL-specific CD8$^+$ T cells (tetramer$^+$) of all CD8$^+$ T cells is shown for spleen and lung for the different immunization protocols. (B) Percentage of CD8$^+$ tetramer$^+$ T_{RM} cells of all CD8$^+$ tetramer$^+$ T cells in the lung. Results are shown as mean ± SD.

4.1.2. Subtypes of memory CD8$^+$ T cells induced by PLGA MS immunization

Having established an ideal immunization scheme, we next analyzed the generation of the different CD8$^+$ T cell subtypes in the lung and spleen 6 days after boost immunization. Because the previously used flow cytometry gating strategy was not ideal to distinguish the different subtypes, we optimized it by including CD44 instead of CD127. CD44 is a marker of previous T cell activation and displays an expression gradient in T cells (naïve < effector < memory) and can be used to identify memory cells in mice [353]. CD127 can be expressed on some T_{RM} cell populations [4]. The revised flow cytometry gating strategy is shown in Figure 9 (from here on referred to as “new”).

SIINFEKL-specific CD8$^+$ T cells were divided into the previously described subtypes: effector T cells (T_{EFF}: CD44$^-$), central memory T cells (T_{CM}: CD44$^+$CD62L$^+$CD69$^-$), effector memory T cells (T_{EM}: CD44$^+$CD62L$^-$CD69$^-$) and resident memory T cells (T_{RM}: CD44$^+$CD62L$^-$CD69$^+$). Since T_{RM} cells, especially in mucosal tissues, often express CD103 we further looked at CD103$^+$ T_{RM} cells [354]. Lung T_{RM} cells consist of two distinct populations: airway T_{RM}, which can be obtained by BAL and interstitial T_{RM} cells, which are obtained by digestion of lung tissue [91]. In contrast to interstitial T_{RM} cells, airway T_{RM} cells are reported to be poorly cytolytic but able to produce antiviral cytokines rapidly after encountering their cognate antigen in a model of influenza infection [92]. Moreover, the number of airway T_{RM} cells has been shown to correlate with the efficacy of cellular immune protection in pulmonary infection [96]. Therefore, we decided to analyze both populations of T_{RM} cells.

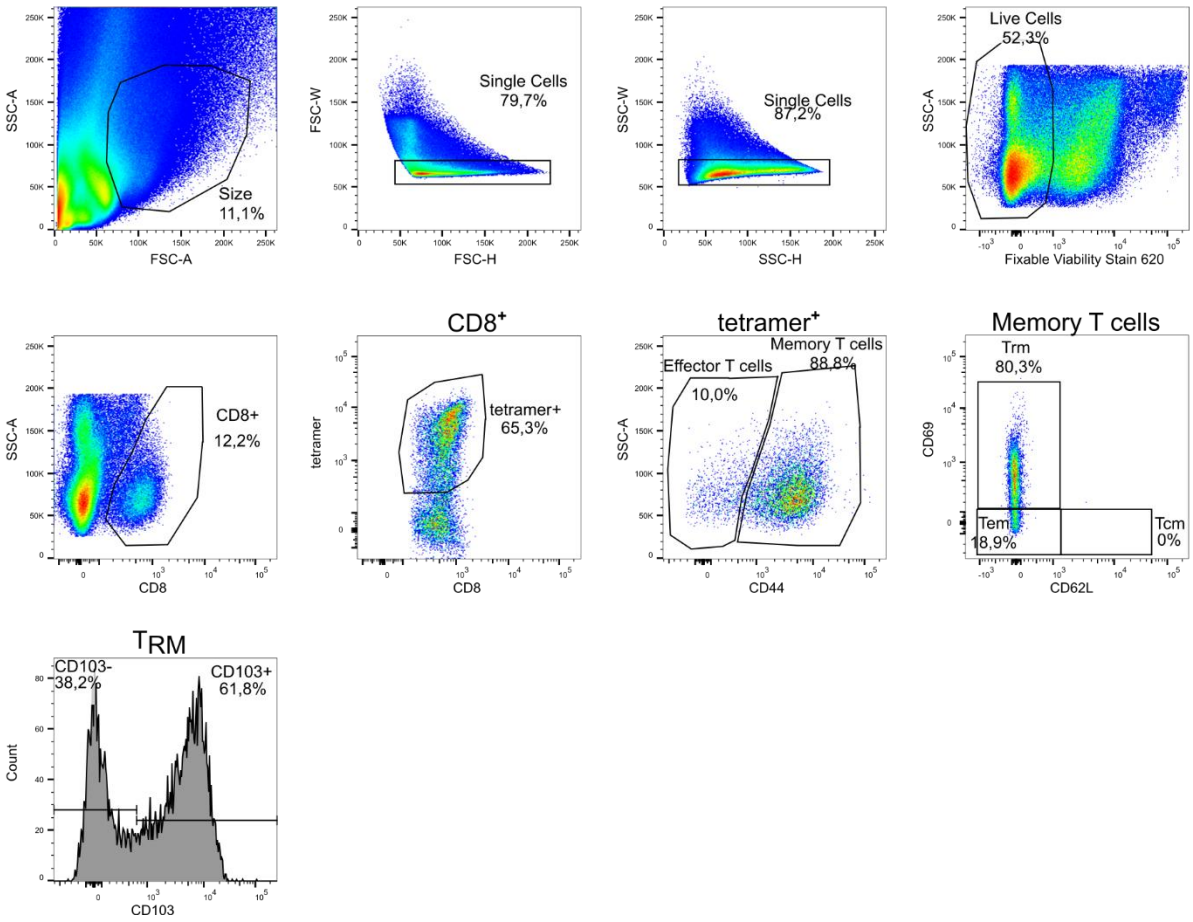

Figure 9: New flow cytometry gating strategy to identify the different specific CD8⁺ T cell populations. After gating on size, singlets and live cells, the remaining cells were gated on CD8⁺ SIINFEKL-tetramer⁺ cells. These SIINFEKL-specific cells were further divided into effector (CD44⁻) and memory T cells (CD44⁺). To distinguish the different CD8⁺ memory T cell subtypes, these cells were further divided based on the expression of CD62L and CD69. Double-negative cells were classified as T_{EM} cells, CD62L⁺CD69⁻ cells as T_{CM} cells and CD62L⁻CD69⁺ cells as T_{RM} cells. T_{RM} cells were further analyzed for expression of CD103.

Our data revealed that the pool of CD8⁺ T cells in the lung airways predominantly consists of T_{RM} (CD103⁺ and CD103⁻) and T_{EM} cells (Figure 10). As expected, a similar distribution was found in lung tissue, although the percentage of T_{RM} cells among tetramer-positive CD8⁺ T cells was even higher compared to the airways. In both lung airways and tissue about half of the CD62L⁻CD69⁺ T_{RM} cells also expressed CD103. Interestingly, while we were not able to detect any effector T cells in the airways, there were some present in the lung tissue. As expected, we were not able to detect T_{CM} cells in either lung airways or tissue. In the spleen most of the vaccine-specific CD8⁺ T cells represented an effector memory phenotype, although some T_{CM} cells as well as effector T cells were also detectable. Even though the CD8⁺ T cells response was analyzed only 6 days after the boost vaccination, which represents the peak of the T cell response, most of the specific CD8⁺ T cells in either of the tissues analyzed already displayed a memory phenotype. This is likely due to the fact that the systemic prime

immunization 20 days before already led to the induction of an effector response. Moreover, it has been shown that T_{RM} cells (or their precursors) are present in the lung at very early time points after mucosal cancer vaccine administration [156]. In conclusion, these experiments established that PLGA MS immunization led to a strong induction of T_{RM} and T_{EM} cells in the lung airways and interstitium.

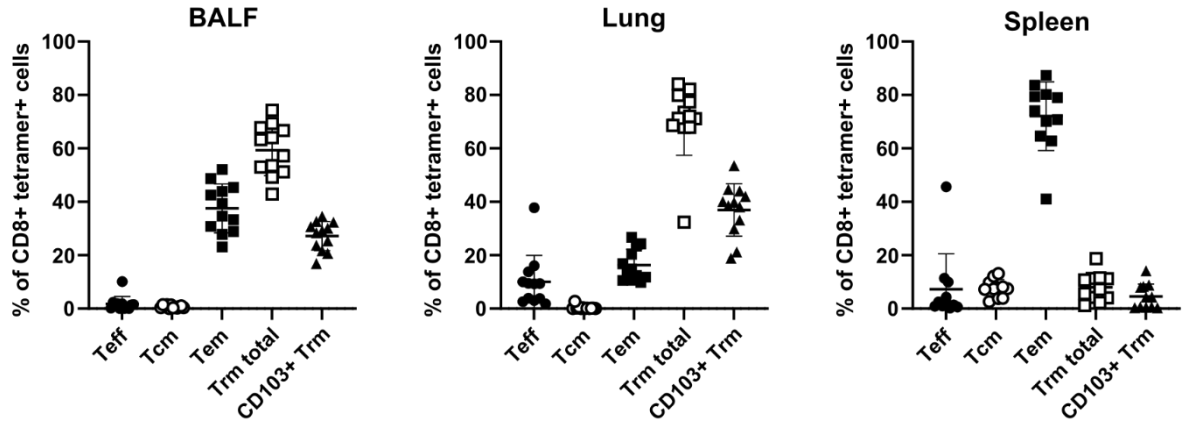

Figure 10: PLGA MS vaccination induces CD8⁺ T_{RM} cells in lung airway and interstitium. C57BL/6 mice (n=12) were immunized with the s.c. prime – i.n. boost immunization protocol using PLGA MS containing Ova/CpG which were co-administered together with PLGA MS containing polyI:C. 6 days after the boost vaccination the bronchoalveolar lavage fluid (BALF), lung tissue and spleen were collected and analyzed by flow cytometry for the presence of SIINFEKL-specific CD8⁺ T cells. Graphs show the percentage of the different T cell subtypes of total CD8⁺ SIINFEKL-tetramer⁺ cells. Results are shown as mean ± SD.

4.1.3. Necessity of local antigen for T_{RM} cell generation

Next, we wanted to analyze how long the different memory T cell populations persist. After activation of lymphocytes in the LN, they are dependent on sphingosine-1-phosphate-(S1P)-dependent migration to exit the LN to traffic to the inflamed tissue [355, 356]. Treating mice with the sphingosine 1-phosphate receptor-1 (S1PR1) inhibitor FTY720 (Fingolimod) sequesters circulating T cells within secondary lymphoid tissues and thus prevents the migration of circulating lymphocytes into peripheral tissues [356]. Adding FTY720 to the drinking water of mice 2 days before analysis of the cell populations by flow cytometry enabled us to study the generation of local T_{RM} cells in the lung independently of circulating T cells. To confirm the impaired emigration of lymphocytes from SLOs in FTY720-treated mice, we first analyzed the frequency of CD3⁺ T cells in the blood. As expected, we observed a 70% reduction of circulating CD3⁺ T lymphocytes in the blood of FTY720-treated mice (Figure 11; w/o FTY720: 100% ± 11.27; +FTY720: 29.64% ± 11.73), confirming that emigration of these cells from lymphoid organs into the periphery was inhibited.

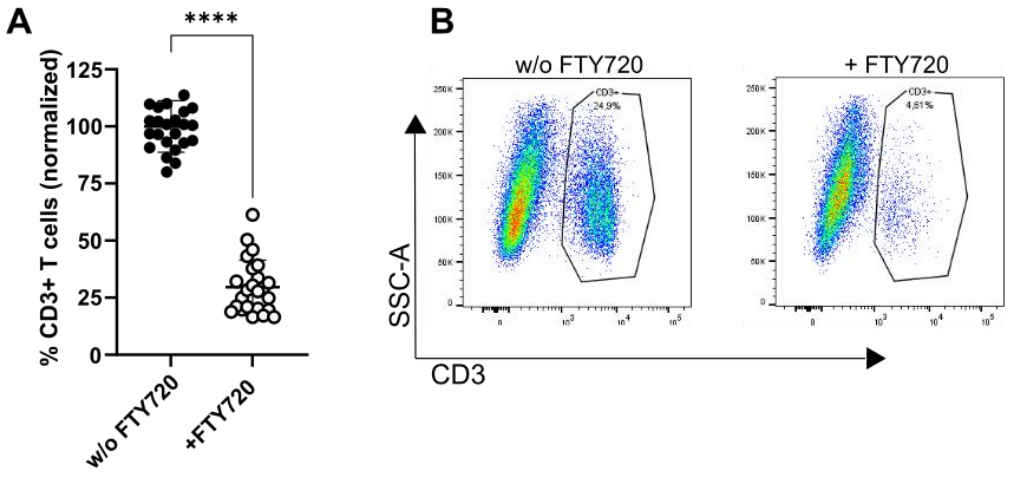

Figure 11: FTY720 induces a sustained depletion of circulating T cells in mice. The S1PR1-inhibitor FTY720 was added to the drinking water (7 µg/ml) of the indicated group two days before analysis. Blood samples were collected and the frequency of $CD3^+$ T cells was quantified by flow cytometry. (A) $CD3^+$ T cells in FTY720-treated mice are reported as a percent relative to 100% $CD3^+$ T cells in non-treated WT mice. Results are shown as mean ± SD. Statistics: unpaired t-Test; ****P < 0.0001. (B) Representative flow cytometry images of blood samples. Pre-gated on size, single cells and live cells.

More importantly, there was no significant difference in the formation of $CD69^+CD103^+$ T_{RM} cell numbers in mice treated with the inhibitor (Ova/CpG/polyI:C + FTY720) compared to mice which did not receive the inhibitor (Ova/CpG/polyI:C), indicating that these cells were seeded in the lung already during the early phase of the vaccination response without further input from circulating $CD3^+$ T lymphocytes from the blood (Figure 12A+B).

Another important aspect in the generation of T_{RM} cells is the requirement of antigen presence. In this context, it has been shown for several tissues, including the skin and the FRT, that local inflammation, but not local antigen, is required to induce T_{RM} cells [97, 98, 357]. In the lung the situation seems to be different: without local antigen, T_{RM} cells that had been formed, did not persist after resolution of the inflammation [83, 99].

Thus, we aimed to determine if local antigen presentation is a prerequisite for the establishment of a robust lung T_{RM} formation in the context of PLGA MS immunization. To this end, we used a prime-boost regimen in which mice were subcutaneously primed with PLGA MS containing Ova and the adjuvants (Ova/CpG/polyI:C) followed by the intranasal boost immunization without the antigen (CpG/polyI:C) on day 14 ("boost without antigen ± FTY720") and compared this group to mice receiving intranasal boost immunization containing the antigen ("Ova/CpG/polyI:C ± FTY720"). 6 days after the boost immunization we analyzed the formation of vaccine-specific memory $CD8^+$ T cells in the lung airways, lung interstitium and the spleen (Figure 12). In line with the previously mentioned work, our results confirmed that while a local boost vaccination without antigen clearly induced an infiltration of $CD8^+$ T cells

into the airways (Figure 12A, left graph), it did not induce the generation of vaccine-specific tetramer-positive CD8$^+$ T cells, especially that of T_{RM} cells, in either of the sites analyzed. In contrast, a strong induction of vaccine-specific CD8$^+$ T cells was observed in the lung airways (Figure 12A, middle + right graph) and tissue (Figure 12B) as well as the spleen (Figure 12C) of mice that received antigen-bearing PLGA microspheres both times. In summary, our results confirmed that local antigen is required to induce efficient vaccine-specific T_{RM} cells in the lung also in a vaccination approach using PLGA MS. However, when local antigen is present even mice that are no longer able to recruit lymphocytes from the circulation possess a significant number of T_{RM} cells in the lung.

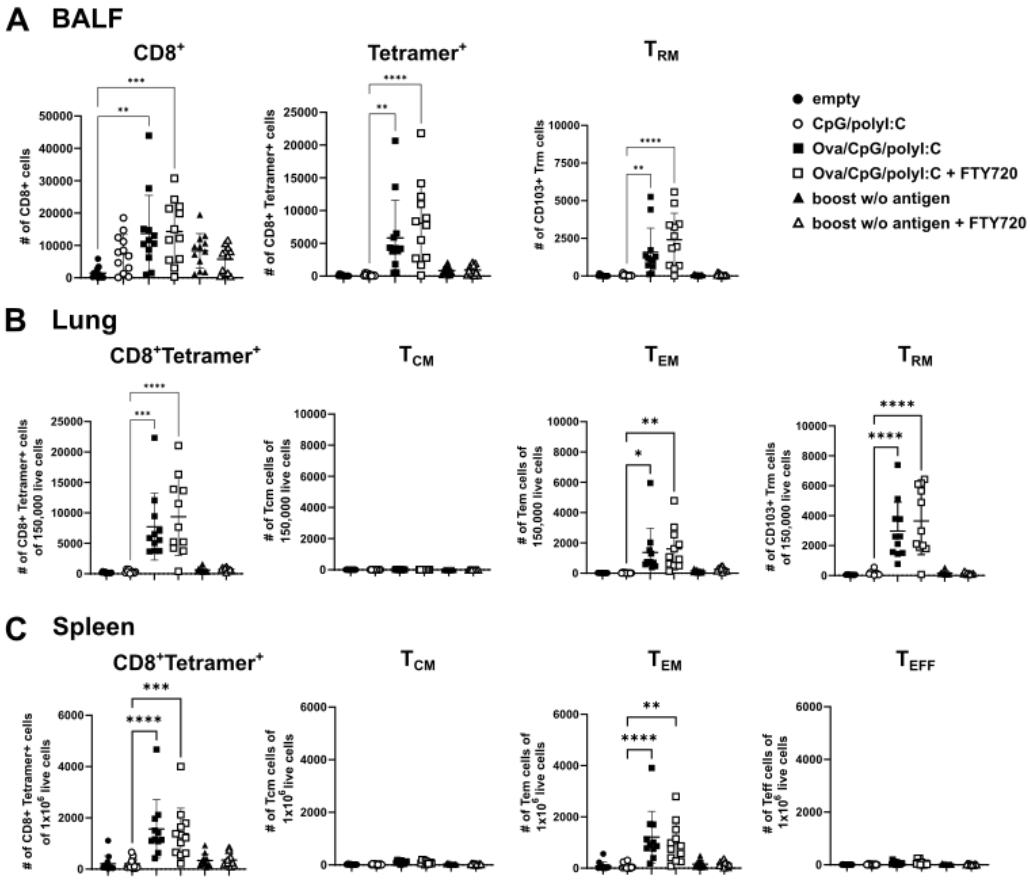

Figure 12: Local antigen is required for induction of SIINFEKL-specific CD8$^+$ T_{RM} cells in the lung. C57BL/6 mice (n=12) were immunized with the s.c. prime – i.n. boost immunization protocol using PLGA MS containing Ova/CpG which were co-administered together with PLGA MS containing polyI:C. The "boost w/o antigen" groups received antigen-bearing PLGA MS (Ova/CpG/polyI:C) for their s.c. prime immunization, but were intranasally boosted with adjuvant-only PLGA MS (CpG/polyI:C). The S1PR1-inhibitor FTY720 was added to the drinking water (7 µg/ml) of the indicated groups two days before analysis. Control groups were immunized with either empty PLGA MS or adjuvant-only PLGA MS (CpG/polyI:C) for prime and boost vaccination. (A) Absolute cell count of CD8$^+$ cells, CD8$^+$ SIINFEKL-tetramer$^+$ cells or CD103$^+$ T_{RM} cells in the BALF. (B) Numbers of CD8$^+$ SIINFEKL-tetramer$^+$ cells, T_{CM} cells, T_{EM} cells and CD103$^+$ T_{RM} cells in the lung. Cell numbers were normalized to 150,000 live cells. (C) Numbers of CD8$^+$ SIINFEKL-tetramer$^+$ cells T_{CM} cells, T_{EM} cells and T_{EFF} cells in the spleen. Cell numbers were normalized to 1x10^6 live cells. Results are shown as mean ± SD. Statistics: one-way ANOVA with a Tukey's multiple comparisons test. *p < 0.05; **p < 0.01; ***p < 0.001; ****p < 0.0001.

4.1.4. Kinetic of T_{RM} cell generation

Since the main goal of a vaccine is to induce a long-lasting memory response, we next longitudinally monitored the magnitude of the vaccine-induced memory $CD8^+$ T cell cells in the lung and spleen at different time points. Mice that had been immunized with PLGA MS according to the "s.c. prime – i.n. boost" vaccination approach were sacrificed 6, 18, 30 or 60 days after the boost vaccination and examined for the presence of $CD8^+$ memory T cells in the lung. While the numbers of all SIINFEKL-specific $CD8^+$ T cells and T_{RM} cells declined in the airways (Figure 13A) and the interstitium (Figure 13B) over time, there were still specific memory $CD8^+$ T cells detectable even 60 days after the boost vaccination indicating that T cell memory did indeed persist. Also in the spleen we were able to find specific $CD8^+$ T cells, mainly T_{EM} cells, at this late time point, however the overall response was lower than in the lung (Figure 13C). Confirming our previous results, no differences were observable between mice treated with FTY720 for two days prior to analysis compared to mice that did not receive the inhibitor, highlighting that the induced memory response in these mice could be maintained locally. It is interesting to note that the percentage of tetramer-positive cells of all $CD8^+$ T cells strongly declined in the BALF and lung between day 30 and day 60 post boost in mice immunized with antigen-bearing PLGA MS treated with or without FTY720 (Figure 13D). On the other hand, in the spleen the decline in SIINFEKL-specific $CD8^+$ T cells was gradual. This indicates that most of the specific $CD8^+$ T cells in the lung are lost approximately 1-2 months after boost immunization raising the potential need for a further boost immunization at a later time point. Taken together, we showed that the vaccine-specific $CD8^+$ T cell memory response in the lung following immunization with PLGA MS is maintained over a period of 2 months.

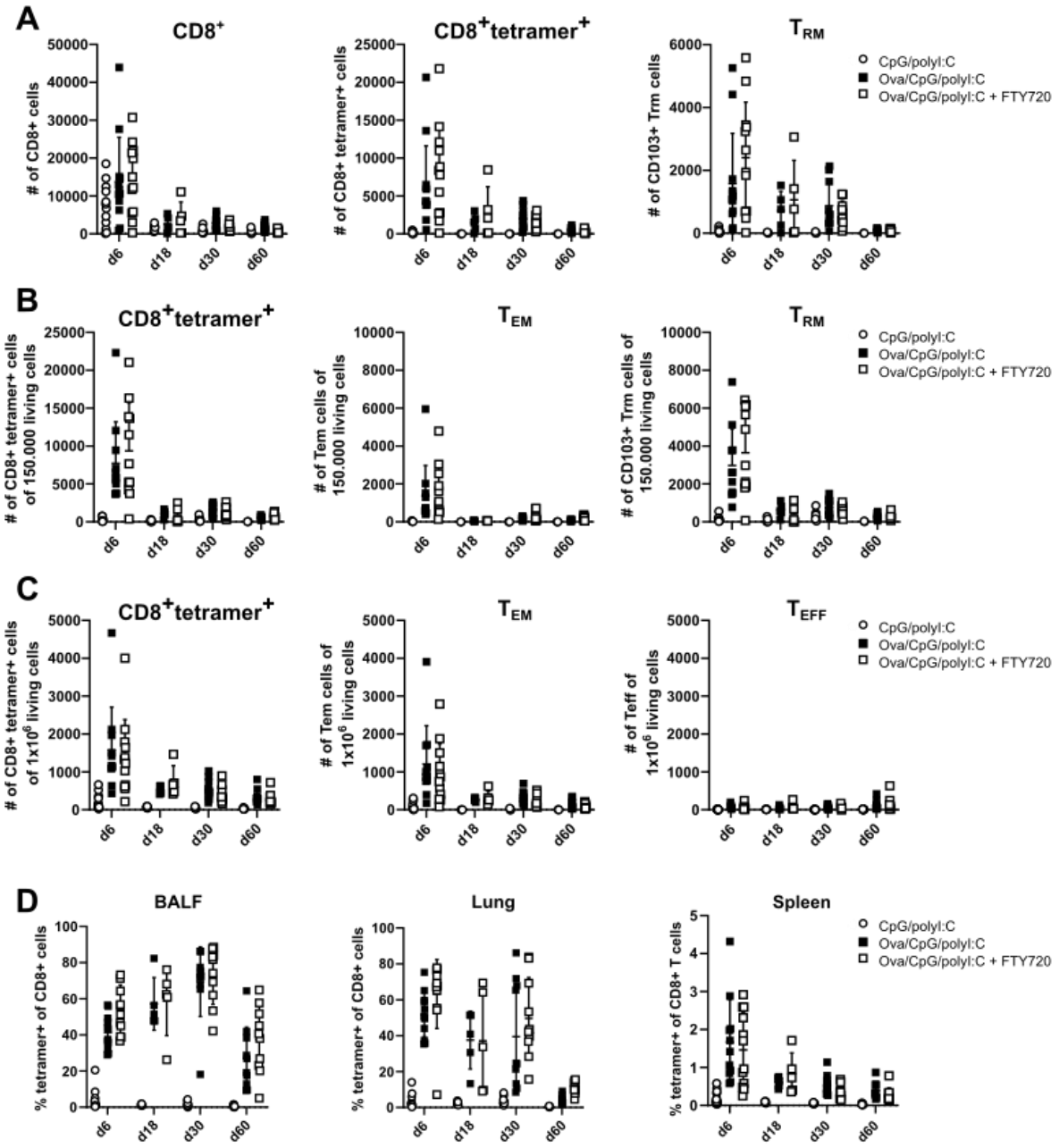

Figure 13: The vaccine-specific memory CD8$^+$ T cell response in the lung persists for up to 60 days. C57BL/6 mice (n=12) were immunized with the s.c. prime – i.n. boost immunization protocol using PLGA MS containing Ova/CpG which were co-administered together with PLGA MS containing polyI:C. The S1PR1-inhibitor FTY720 was added to the drinking water (7 µg/ml) of the "Ova/CpG/polyI:C + FTY720" group two days before analysis. The control group was immunized with adjuvant-only PLGA MS (CpG/polyI:C). Mice were sacrificed 6, 18, 30 or 60 days after the boost immunization. (A) Cell count of CD8$^+$, CD8$^+$ SIINFEKL-tetramer$^+$ or CD103$^+$ T_{RM} cells in the BALF. (B) Numbers of CD8$^+$ SIINFEKL-tetramer$^+$, T_{EM} cells and CD103$^+$ T_{RM} cells in the lung. Cell numbers were normalized to 150,000 live cells. (C) Numbers of CD8$^+$ SIINFEKL-tetramer$^+$, T_{EM} cells and T_{EFF} cells in the spleen. Cell numbers were normalized to 1x10^6 live cells. (D) % tetramer$^+$ cells of all CD8$^+$ T cells in BALF, lung and spleen. Results are shown as mean ± SD.

A similar kinetic was observed in AAD mice which had been immunized with the same immunization protocol, but with PLGA MS containing the $M1_{58-66}$ peptide as an antigen. AAD mice (HLA-A*0201 transgenic mice) express a recombinant MHC class I molecule consisting of the peptide binding region of the human HLA-A*0201 and the CD8 binding domain of the murine H2-D^d. Therefore, these mice can be used to study the immune response to HLA-A*0201-restricted peptide epitopes. Because these experiments were performed with the "old" flow cytometry gating strategy they cannot be compared exactly to the kinetic of SIINFEKL-specific $CD8^+$ T cells in C57BL/6 mice. However, the obtained results were similar. Strong numbers of $M1_{58-66}$-specific $CD8^+$ T cells were induced in the lungs of AAD mice 6 days after the boost immunization. While these numbers continuously declined over time, tetramer-positive cells were still detectable even 60 days after the boost immunization (Figure 14A). The majority of specific cells in the lung exhibited a T_{RM} cell phenotype. As expected, the overall response in the spleen was lower, but also in this organ, specific $CD8^+$ T cells could be detected at the latest time point analyzed (Figure 14B). In addition to staining for $M1_{58-66}$-specific cells with a tetramer, we also performed an ICS for IFN-γ. Similar to the results obtained with our tetramer staining, PLGA MS immunization induced IFN-γ producing cells in the lung that persisted for up to 60 days (Figure 15A). Again, most of the IFN-γ^+ cells in the lung displayed a T_{RM} cell phenotype. Interestingly, the number of IFN-γ^+ cells was lower than the number of tetramer-positive cells indicating that not all of the specific cells identified with the tetramer staining were capable of producing IFN- γ when stimulated with their cognate antigen *in vitro*. Taken together, these results highlight that the induction of T_{RM} cells by PLGA MS can be achieved with different antigens.

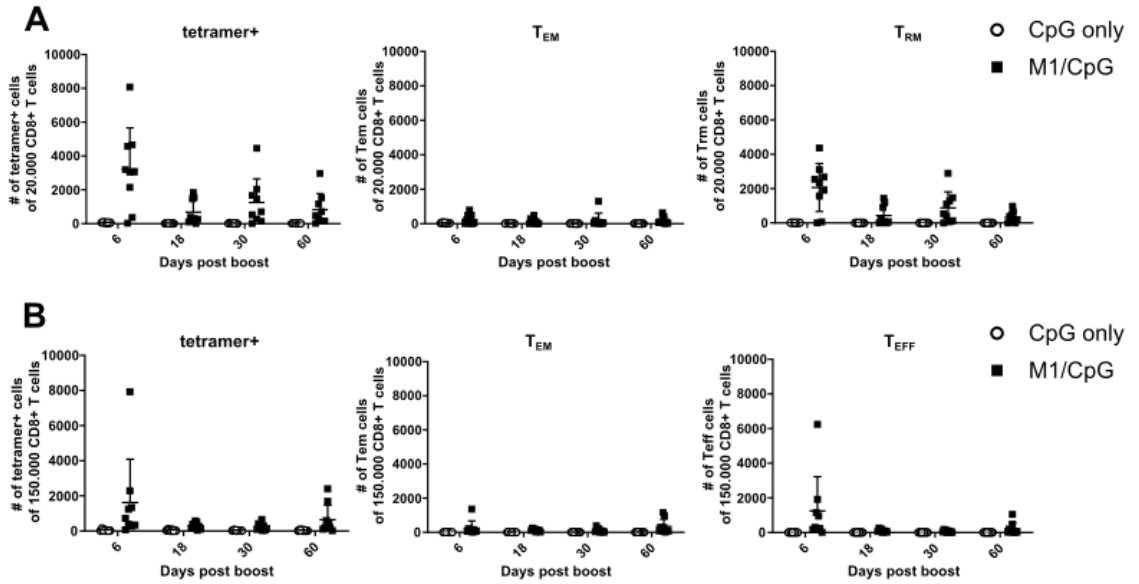

Figure 14: Kinetic of $M1_{58-66}$-tetramer-specific $CD8^+$ T cells in AAD mice. AAD mice (n=8-10) were immunized with the s.c. prime – i.n. boost immunization protocol using PLGA MS containing $M1_{58-66}$/CpG which were co-administered together with PLGA MS containing polyI:C. The control group was immunized with adjuvant-only PLGA MS (CpG/polyI:C). Mice were sacrificed 6, 18, 30 or 60 days after the boost immunization and the lung and spleen analyzed by flow cytometry. (A) Numbers of $CD8^+$ $M1_{58-66}$-tetramer$^+$, $CD8^+$ $M1_{58-66}$-tetramer$^+$ T_{EM} cells and $CD8^+$ $M1_{58-66}$-tetramer$^+$ T_{RM} cells in the lung. Cell numbers were normalized to 20,000 $CD8^+$ T cells. (B) Numbers of $CD8^+$ $M1_{58-66}$-tetramer$^+$, $CD8^+$ $M1_{58-66}$-tetramer$^+$ T_{EM} cells and $CD8^+$ $M1_{58-66}$-tetramer$^+$ T_{EFF} cells in the spleen. Cell numbers were normalized to 150,000 $CD8^+$ T cells. Results are shown as mean ± SD.

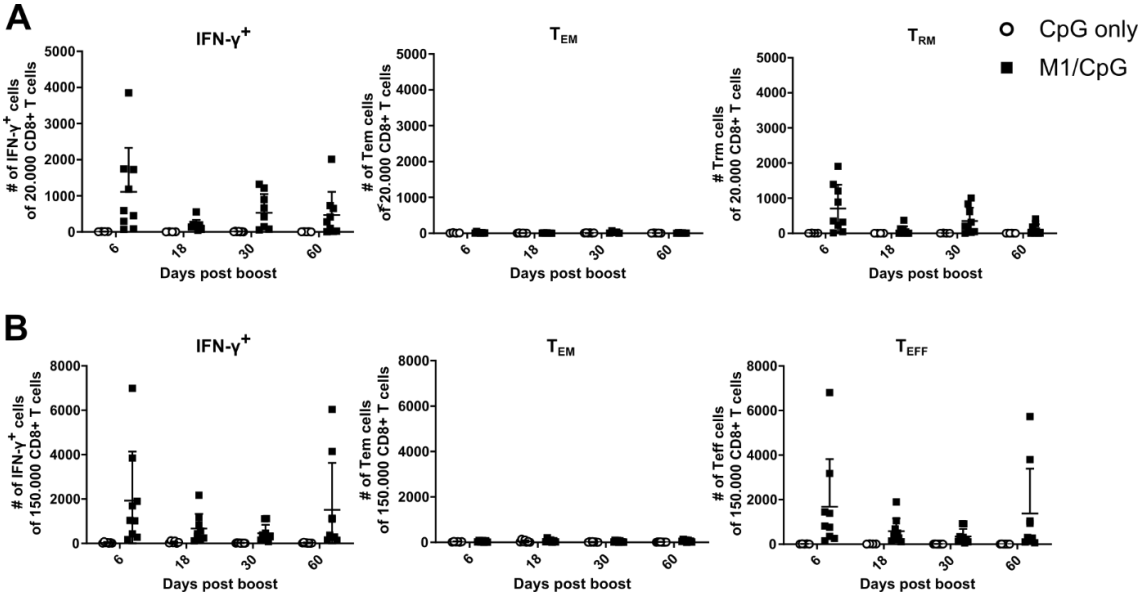

Figure 15: Kinetic of $M1_{58-66}$-stimulated IFN-γ^+ $CD8^+$ T cells in AAD mice. AAD mice (n=8-10) were immunized with the s.c. prime – i.n. boost immunization protocol using PLGA MS containing $M1_{58-66}$/CpG which were co-administered together with PLGA MS containing polyI:C. The control group was immunized with adjuvant-only PLGA MS (CpG/polyI:C). Mice were sacrificed 6, 18, 30 or 60 days after the boost immunization, lungs and spleen removed and digested and the obtained single cell suspensions restimulated with $M1_{58-66}$ peptide. Next, the IFN-γ response of $CD8^+$ T cells analyzed by intracellular cytokine staining. (A) Numbers of $CD8^+$ IFN-γ^+, $CD8^+$ IFN- γ^+ T_{EM} cells and $CD8^+$ IFN- γ^+ T_{RM} cells in the lung. Cell numbers were normalized to 20,000 $CD8^+$ T cells (B) Numbers of $CD8^+$ IFN- γ^+, $CD8^+$ IFN- γ^+ T_{EM} cells and $CD8^+$ IFN- γ^+ T_{EFF} cells in the spleen. Cell numbers were normalized to 150,000 $CD8^+$ T cells Results are shown as mean ± SD.

4.1.5. Protection from tumor growth

4.1.5.1. Generation of Ova+Luc+B16BL6 melanoma cells

Having established that vaccination with PLGA MS induces persistent $CD8^+$ T_{RM} cell populations in the lung, we next wanted to analyze whether these cells are capable of protecting mice from tumor growth. To be able to monitor tumor growth *in vivo* over time, we decided to create a cell line stably expressing the model antigen ovalbumin as well as the enzyme luciferase. In this way we would be able to immunize mice with Ova-bearing PLGA MS to induce an antitumor immune response and monitor the growth of the tumor cells *in vivo* using the in vivo imaging system (IVIS) that detects the bioluminescence signal emitted from luciferase-expressing cells after intraperitoneal injection of the substrate luciferin. Injecting B16BL6 melanoma cells intravenously into the bloodstream of mice, is known to lead to the formation of metastases in the lung. Therefore, this model was ideal to study the antitumor protection offered by the T_{RM} cells in the lung.

Luciferase-expressing B16BL6 melanoma cells (Luc^+B16BL6) were obtained from Olaf van Tellingen who introduced a bAct-Luc-IRES-GFP construct by transfection. When we analyzed GFP expression of these cells by flow cytometry, we found that the expression of GFP, and thus luciferase, in the bulk population of Luc^+B16BL6 cells had decreased considerably indicating that some cell clones had lost the expression of luciferase (Figure 16A). Therefore, we decided to bulk sort this cell line to obtain Luc^+B16BL6 cells with a high expression of GFP (Figure 16B). By performing a luciferase activity assay we were able to confirm that GFP expression correlated with luciferase activity (Figure 16C). The "GFP^+" Luc^+B16BL6 cells were used to generate a cell line stably expressing Ova. For this purpose, the genes of full length or cytosolic Ova were inserted into the multiple cloning site of the pCDH-EF1α-MCS-IRES-copGFP plasmid to obtain the pCDH-EF1α-Ova_cyto-IRES-copGFP and pCDH-EF1α-Ova_full-IRES-copGFP plasmids. Using these two plasmids, lentiviral particles were produced in Hek293T cells. The "Ova cytosolic" (Ova cyto) or "Ova full-length" (Ova full) lentiviral particles were used to transduce Luc^+B16BL6 cells. Flow cytometry analysis showed that these cells displayed a similar GFP expression level as the "GFP^+"Luc^+B16BL6 cell line (Figure 16B). Moreover, the luciferase activity of the generated Ova-expressing cell lines (Ova cyto and Ova full) was lower than that of the freshly thawed "GFP^+"Luc^+B16BL6 cells indicating that luciferase-expression was lost in culture (Figure 16C).

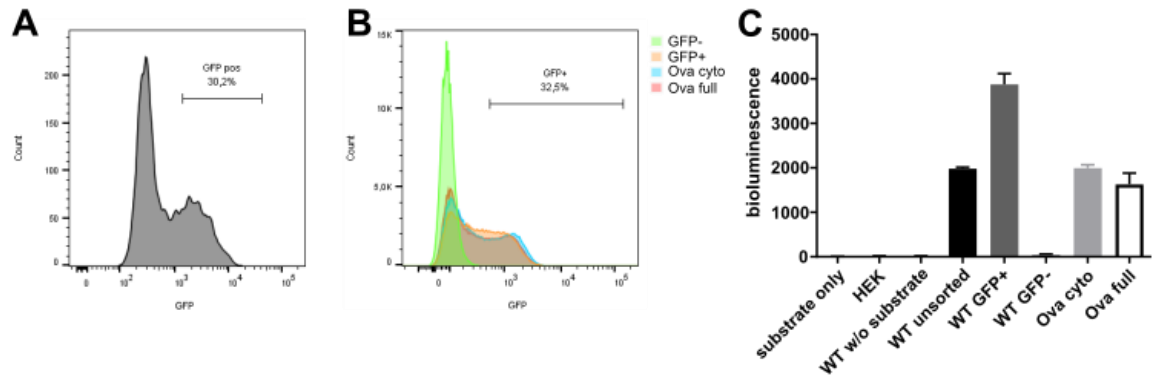

Figure 16: Generation of the Ova$^+$Luc$^+$B16BL6 cell line. (A) Histogram of GFP expression of the unsorted Luc$^+$B16BL6 cells. (B) Histogram of the GFP expression of Luc$^+$B16BL6 cells that had been bulk sorted based on their GFP expression into GFP-negative (green) and GFP-positive (orange) cells. GFP expression of GFP$^+$Luc$^+$ B16BL6 cells that were lentivirally transduced with lentiviral particles containing cytosolic (blue) or full-length (red) Ova. (C) Analysis of luciferase expression by luciferase activity assay. WT corresponds to Luc$^+$B16BL6 cells.

Next, the “Ova cyto” and “Ova full” cell lines were single cell sorted and the individual clones grown in culture. Once sufficient numbers of cells had been obtained, a LacZ assay was performed with several clones of each line to analyze expression of Ova (Figure 17, left graphs). Since we had previously observed that expression of luciferase was lost in the majority of Luc$^+$B16BL6 cells when they were kept in culture, we also performed a luciferase activity assay to ensure that our cell line maintained expression of luciferase (Figure 17, right graphs). Based on the obtained results, we chose 4 “Ova cyto” clones and 2 “Ova full” clones to be kept in culture. These clones were expanded until sufficient cell numbers were obtained to freeze aliquots of these clones. However, some cells of each clone were kept in culture to continuously monitor the expression of luciferase and Ova. After 6 weeks in culture, the clone with the best expression of both luciferase as well as Ova was chosen for further experiments. This was clone 7 of the “Ova cyto” line, which is referred to as “Ova$^+$Luc$^+$B16BL6” from here on (Figure 18). Therefore, previously frozen aliquots of this clone were thawed, expanded and subsequently frozen again so that an aliquot could be thawed shortly before the *in vivo* experiments. We assumed that this way the chosen clone would maintain expression of both luciferase and Ova for the duration of the *in vivo* analysis.

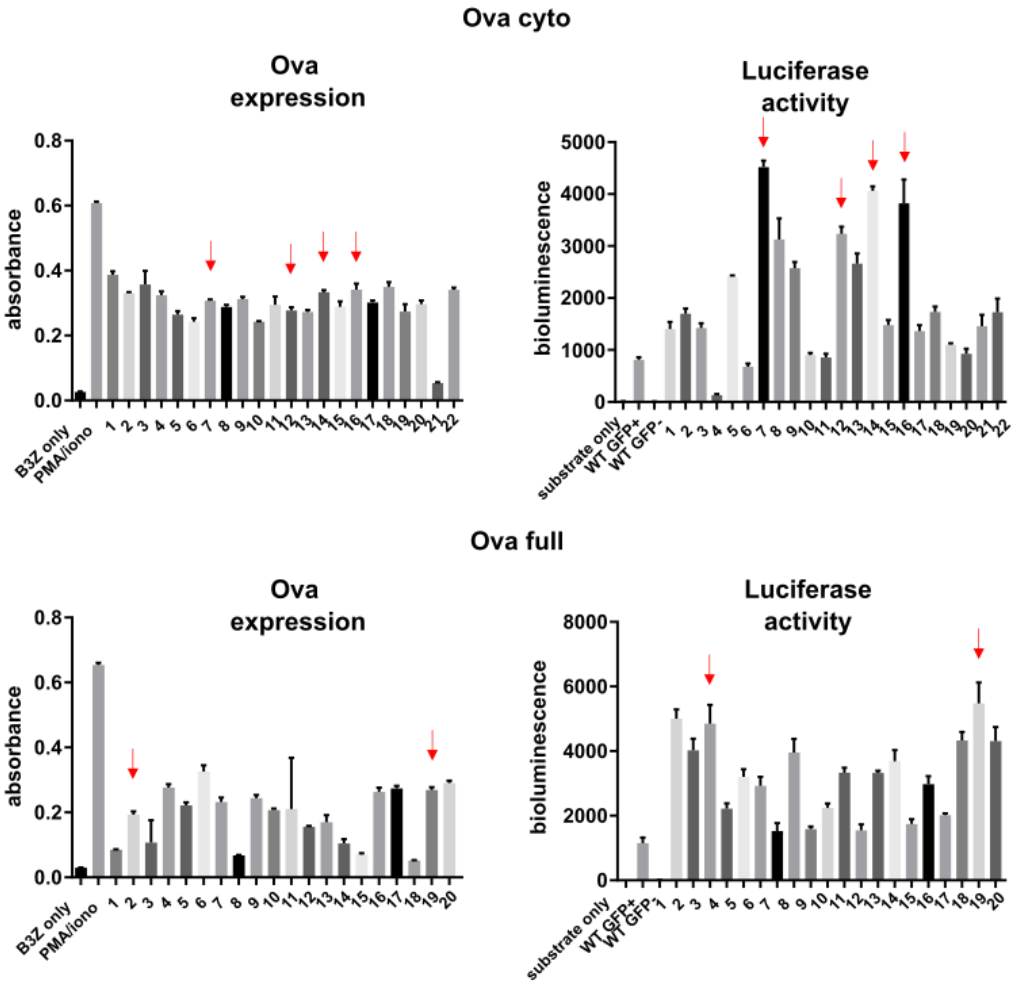

Figure 17: (left graphs) Analysis of Ova expression by lacZ assay. B3Z Hybridoma cells were stimulated with cell clones transduced with cytosolic or full-length Ova. Hybridoma cells stimulated with PMA/ionomycin were used as a positive control, hybridoma cells without any stimulation were used as a negative control. (right graphs) Analysis of luciferase expression by luciferase activity assay of single cell sorted cell clones lentivirally transduced with cytosolic or full-length Ova. GFP^+Luc^+B16BL6 cells were used as a positive control, GFP^-Luc^+B16BL6 cells and one sample with substrate only were used as negative controls. Results are shown as mean ± SD. Arrows indicate cell clones that were kept for further expansion and analysis.

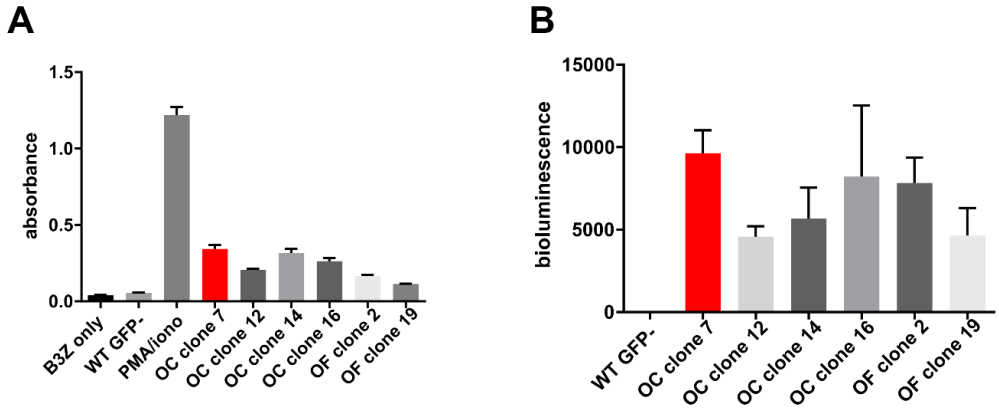

Figure 18: Selection of clones. (A) Analysis of Ova expression by lacZ assay. B3Z Hybridoma cells were stimulated with cell clones transduced with cytosolic (OC) or full-length (OF) Ova to analyze expression of Ova. Hybridoma cells stimulated with PMA/ionomycin were used as a positive control. Hybridoma cells alone or "GFP^-" Luc^+B16BL6 cells were used as negative controls. (B) Analysis of luciferase expression by luciferase activity assay. GFP^-Luc^+B16BL6 cells were used as a negative control.

Having successfully generated a mouse melanoma cell line that expressed both luciferase and Ova *in vitro*, we proceeded to determine whether the expression of these proteins could also be maintained *in vivo*. Moreover, we wanted to titrate the required amount of cells to be injected to ensure that the cells would not be rejected in non-Ova-immunized mice, but would not overwhelm the immune response of Ova-immunized mice to fight the tumor cells. Therefore, we immunized mice with Ova/CpG/polyI:C PLGA MS according to our established s.c. prime – i.n. boost strategy. As a control, a group of mice was immunized with only adjuvant-bearing PLGA MS (CpG/polyI:C). On day 20, 6 days after the boost immunization, we injected different numbers of Ova$^+$Luc$^+$B16BL6 cell i.v. into the tail vein.

Over the next 24 days we monitored tumor growth *in vivo* using the IVIS system, before we sacrificed mice to count the number of metastases in the lung (Figure 19A). We found that only the highest cell number tested (1x10^6 cells) led to a consistent formation of metastases in the lungs of adjuvant only-immunized mice, but not antigen-immunized mice, confirming that the generated cell line was recognized by the antitumor response of Ova-immunized mice. Moreover, the expression of luciferase and thus the ability to monitor *in vivo* growth of this cell line was stable *in vivo* over the period of 24 days (Figure 19B). Therefore, we decided to continue all further experiments with this cell number.

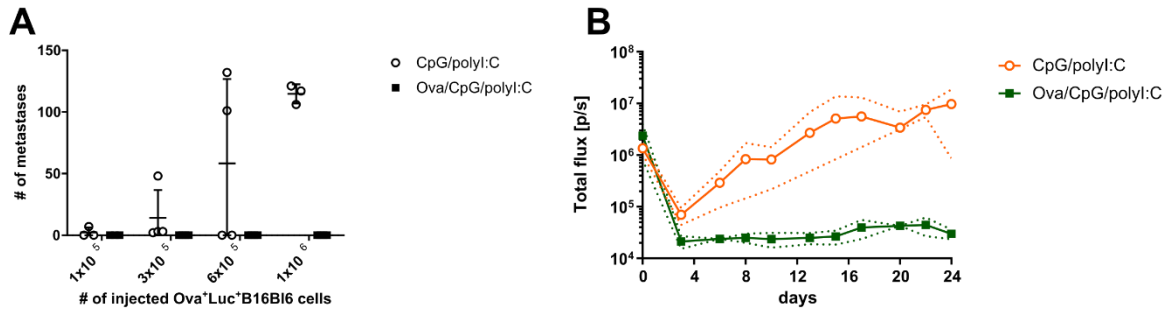

Figure 19: *in vivo* titration of Ova$^+$Luc$^+$B16BL6 cells. C57BL/6 mice (n=3-4) were immunized with the s.c. prime – i.n. boost immunization protocol using PLGA MS containing Ova/CpG which were co-administered together with PLGA MS containing polyI:C. Control groups were immunized with adjuvant-only PLGA MS (CpG/polyI:C). 6 days after the boost immunization mice were i.v. injected with different numbers of Ova$^+$Luc$^+$B16BL6 cells (OC, clone 7). (A) 24 days after injection of the cells, lungs were harvested and metastases counted. Results are shown as mean ± SD. (B) Total flux of tumor bioluminescence of 1x 10^6 injected Ova$^+$Luc$^+$B16BL6 cells shown as photons/second (ROI = 28.23 x 28.23 pix). Data are presented as mean ± S.D. with dotted lines in corresponding colors demonstrating the standard deviation.

4.1.5.2. T_{RM}-mediated protection from tumor growth at an early time point

Using this Ova^+Luc^+B16BL6 melanoma cell line, we next examined the capacity of vaccine-induced T_{RM} cells in the lung to protect mice from tumor growth even in the absence of circulating cells. For this purpose, mice were immunized using the "s.c. prime – i.n. boost" vaccination protocol to ensure the induction of a robust memory $CD8^+$ T cell response in the lung. 6 days after the boost immunization, at the peak of the T cell response, we injected Ova^+Luc^+B16BL6 intravenously. In order to decipher the protection offered by the local immune response in the lung, we included a group of mice that were treated with S1PR1-inhibitor FTY720. To allow enough time for local memory formation but prevent recruitment of circulating cells once tumor cells appeared in the lung, we commenced treatment with FTY720 two days before the injection of Ova^+Luc^+B16BL6 cells. Our results clearly demonstrate that at this early time point mice immunized with antigen-bearing PLGA MS were strongly protected from tumor growth and metastasis formation even without the contribution of circulating $CD8^+$ T cells (Figure 20A-C). Moreover, we observed that all groups of mice immunized with Ova exhibited an induction of T_{RM} cells in the lung as well as SIINFEKL-specific $CD8^+$ T cells in lung and spleen (Figure 20D-F). Interestingly, mice that were immunized with adjuvant-containing PLGA MS also benefited from some level of protection compared to mice immunized with empty microspheres even though protection was not as efficient. Hence, in combination with local antigen provided by the tumor cells, inflammation alone was sufficient to induce an antitumor response.

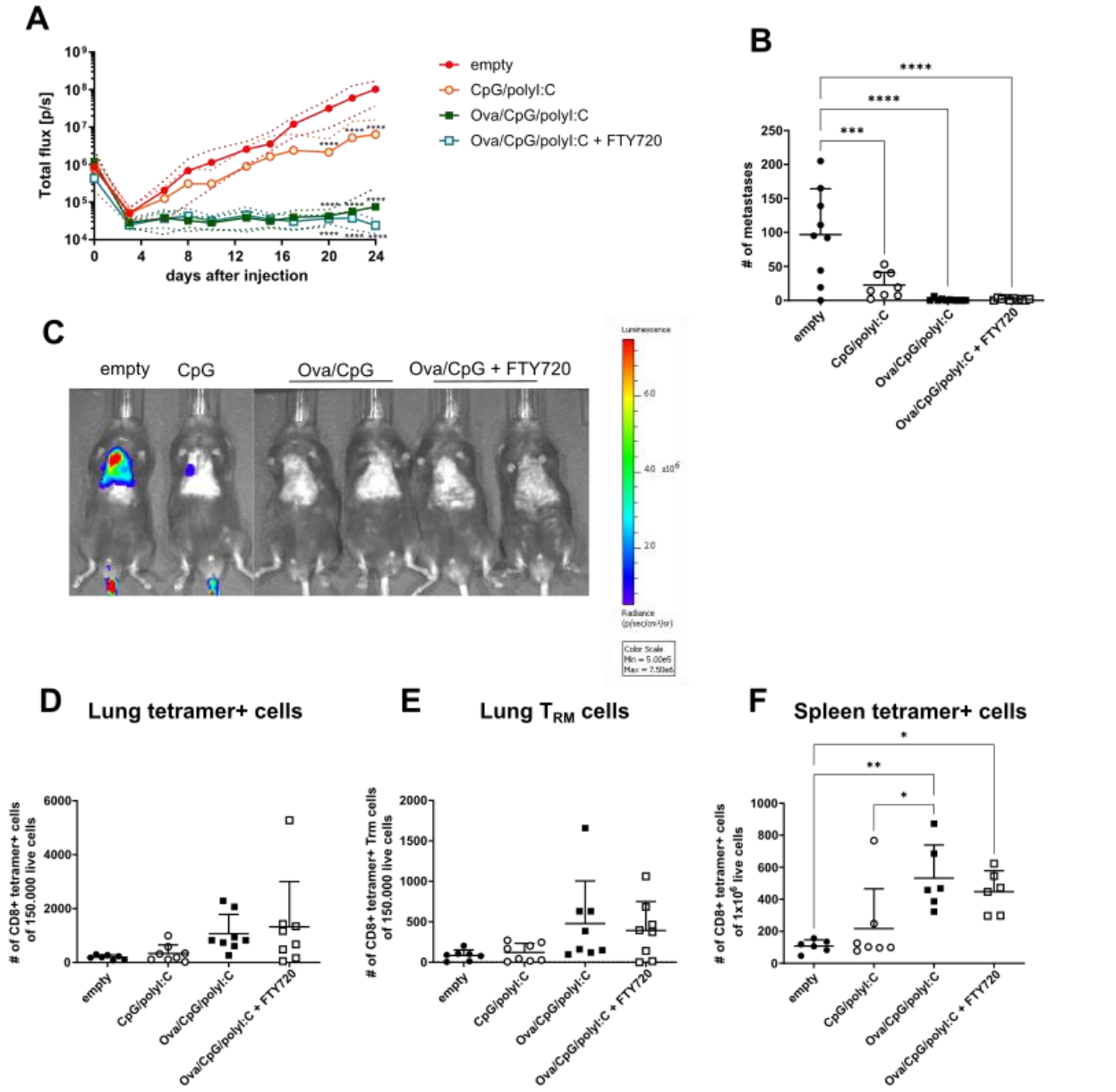

Figure 20: T_{RM} cells induced by PLGA MS protect mice from tumor growth. C57BL/6 mice (n=6-8) were immunized with the heterologous s.c. prime – i.n. boost immunization protocol using PLGA MS containing Ova/CpG which were co-administered together with PLGA MS containing polyI:C. Control groups were immunized with either empty PLGA MS or adjuvant-only PLGA MS (CpG/polyI:C). 6 days after the boost immunization Ova$^+$Luc$^+$B16BL6 melanoma cells were injected i.v. into the tail vain. FTY720 was added to the drinking water (7 µg/ml) of mice in the "Ova/CpG/polyI:C + FTY720" group 2 days before injection of the tumor cells. (A) Total flux of tumor bioluminescence of Ova$^+$Luc$^+$B16BL6 cells shown as photons/second (ROI = 28.23 x 28.23 pix). Data are presented as mean ± S.D. with dotted lines in corresponding colors demonstrating the standard deviation. Statistics: two-way ANOVA with a Tukey's multiple comparisons test. Statistical significances compared to "empty" group. (B) Number of metastases counted in the lung 24 days after injection of tumor cells. Statistics: one-way ANOVA with a Tukey's multiple comparisons test (C) Representative IVIS® images demonstrating tumor growth 24 days after PLGA MS boost immunization. Scaling of the bioluminescent pseudo-color code is shown and presented as photons/seconds/cm^2/steradian (p/sec/cm^2/sr). (D-F) Number of CD8$^+$ SIINFEKL-tetramer$^+$ cells in lung (D) and spleen (F) and CD8$^+$ SIINFEKL-tetramer$^+$ T_{RM} cells in the lung (E). Statistics: one-way ANOVA with a Tukey's multiple comparisons test. Results are shown as mean ± SD. *p < 0.05; **p < 0.01; ***p < 0.001; ****p < 0.0001.

4.1.5.3. In vivo protection from tumor growth following a boost vaccination without the antigen

Because we observed that mice immunized with adjuvant only PLGA MS were slightly protected from tumor growth compared to mice immunized with empty microspheres, we decided to analyze tumor growth in mice that had received a systemic, antigen-specific prime followed by a local, non-specific boost. We found that mice in the "boost w/o antigen" group were protected from tumor growth to a similar extent as mice that had received the antigen boost (Figure 21). However, since previous results had shown that the "boost w/o antigen" immunization strategy was not sufficient to induce the generation of T_{RM} cells (Figure 12), this protection was likely not due to the presence of T_{RM} cells. Most likely these mice were protected by antigen-specific circulating cells that had been stimulated following the antigen-prime. However, despite the fact that the protection we observed in the "boost w/o antigen" was almost certainly not mediated by T_{RM} cells, it nevertheless highlights that a systemic antigenic prime immunization with PLGA MS is capable of protecting mice from local tumor growth, at least at this early time point after immunization.

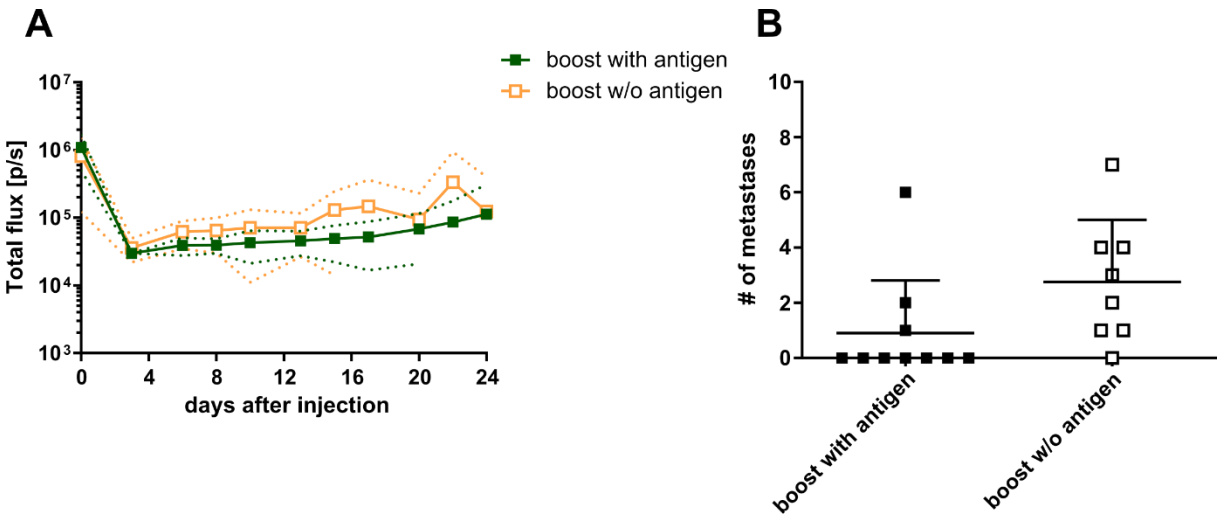

Figure 21: An antigen-specific prime followed by a non-specific boost is able to confer protection from tumor growth. C57BL/6 mice (n=8-10) were immunized with the heterologous s.c. prime – i.n. boost immunization protocol. Both groups received a s.c. prime immunization with PLGA MS containing Ova/CpG which were co-administered together with PLGA MS containing polyI:C. For the i.n. boost immunization the "boost with antigen" group received Ova/CpG + polyI:C PLGA MS, while the "boost w/o antigen" group was immunized with CpG + polyI:C PLGA MS. 6 days after the boost immunization Ova^+Luc^+B16BL6 melanoma cells were injected i.v. into the tail vain. (A) Total flux of tumor bioluminescence of Ova^+Luc^+B16BL6 cells shown as photons/second (ROI = 28.23 x 28.23 pix). Data are presented as mean ± S.D. with dotted lines in corresponding colors demonstrating the standard deviation. (B) Number of metastases counted in the lung 24 days after injection of tumor cells. Data are presented as mean ± SD.

T_{RM}-mediated protection from tumor growth at later time points

Next, we analyzed the protection offered by the local memory response in the lung at later time points. To this end, tumor cells were injected on day 18 (Figure 22A), 30 (Figure 22B) or 60 (Figure 22C) post boost. While we observed that the protection clearly diminished over time, even 60 days after the boost mice were still protected against tumor growth compared to "empty" controls indicating local long-term antitumor memory responses: basically no metastases were detected in mice that were able to make use of their local as well as their circulating vaccine-induced immune response even when the tumor challenge was performed 60 days post boost. Mice treated with FTY720 were protected from metastasis formation even when tumor cells were injected 30 days post boost, but were found to harbor some metastases in their lungs at the last time point analyzed (Figure 22A+B+C, middle graphs). This same tendency was also seen for the bioluminescence measurements (Figure 22A+B+C, left graphs). While lower bioluminescence signals were obtained in both groups immunized with Ova-bearing PLGA MS compared to unprotected mice, this effect grew smaller over time. Interestingly, all groups of mice that were immunized with at least the adjuvants displayed an increase in SIINFEKL-specific $CD8^+$ T cells in lung and spleen and T_{RM} cells in the lung compared to the "empty" control mice which suggested that inflammation alone strongly induces the formation of specific $CD8^+$ T cells as long as the antigen is provided by the tumor (Figure 22A+B+C, right graphs). Consequently, these results illustrated that the local memory response generated by a s.c. prime – i.n. boost immunization with PLGA MS was capable of inducing protective antitumor responses in mice.

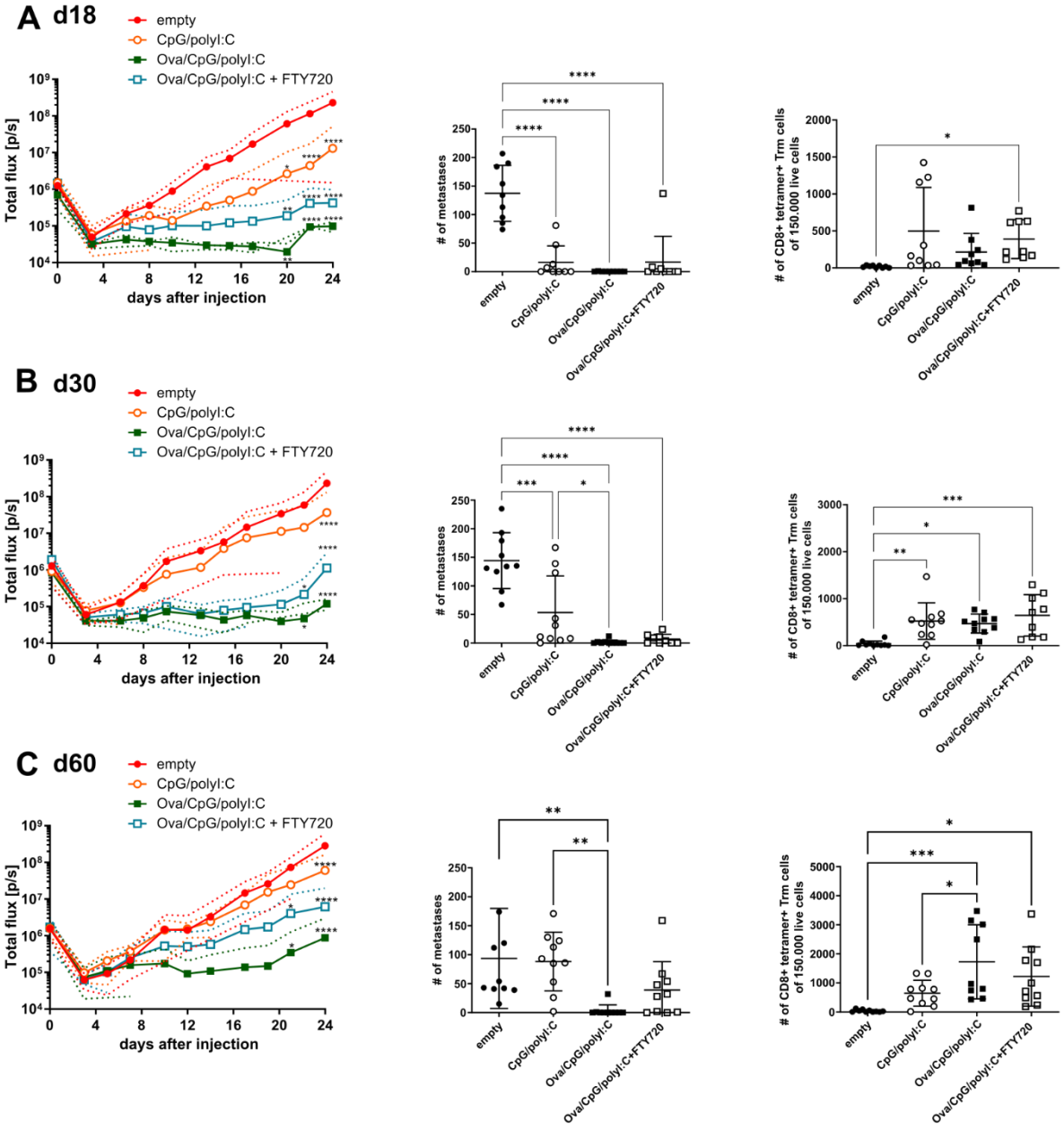

Figure 22: Immunization with PLGA-MS induces long-lasting protection from tumor growth. C57BL/6 mice (n=9-10) were immunized with the s.c. prime – i.n. boost immunization protocol using PLGA MS containing Ova/CpG which were co-administered together with PLGA MS containing polyI:C. Control groups were immunized with either empty PLGA MS or adjuvant-only PLGA MS (CpG/polyI:C). 18 (A), 30 (B) or 60 (C) days after the boost immunization Ova^+Luc^+B16BL6 melanoma cells were injected i.v. into the tail vain. FTY720 was added to the drinking water of mice in the "Ova/CpG/polyI:C + FTY720" group 2 days before injection of the tumor cells (7 µg/ml). (left graphs) Total flux of tumor bioluminescence of Ova^+Luc^+B16BL6 cells shown as photons/seconds (ROI = 28.23 x 28.23 pix). Data are presented as mean ± S.D. with dotted lines in corresponding colors demonstrating the standard deviation. Statistics: two-way ANOVA with a Tukey's multiple comparisons test. Statistical significances compared to "empty" group. (middle graphs) Number of metastases counted in the lung 24 days after injection of tumor cells. Statistics: one-way ANOVA with a Tukey's multiple comparisons test. (right graphs) Number of $CD8^+$SIINFEKL-tetramer$^+$ T_{RM} cells in the lung. Statistics: one-way ANOVA with a Tukey's multiple comparisons test. Results are shown as mean ± SD. *p < 0.05; **p < 0.01; ***p < 0.001; ****p < 0.0001.

4.1.6. Protection from infection with IAV

4.1.6.1. Infection of AAD mice with IAV

In addition to antitumor immunity, T_{RM} cells have long been known to play a major role in a myriad of infectious settings [113]. The induction of a long-lasting T_{RM} cell response directed at internal, conserved viral proteins might offer heterosubtypic protection from different influenza virus strains and is thus a desirable feature of a newly developed vaccine [358, 359]. Previous results from our lab have demonstrated that immunization with PLGA MS generated a strong cytotoxic T cell response in the lung that interfered with IAV infection. IFN-γ^+ $CD8^+$ T cells were induced after a s.c. prime followed by an i.n. boost 14 days later with PLGA MS bearing the $M1_{58-66}$ peptide (alone or in combination with the PA_{46-54} peptide) and the TLR9 ligand CpG that were co-administered together with PLGA MS containing the TLR3 ligand polyI:C [321]. However, the different subtypes of $CD8^+$ memory T cells were not analyzed in these experiments. Therefore, we decided to immunize mice with our established vaccination strategy and subsequently infect them with IAV at different time points after the boost vaccination. To be able to study the immune response to the HLA-A*0201-restricted $M1_{58-66}$ epitope, transgenic AAD mice were used for these experiments.

As a first measure to determine the protection from IAV infection, the viral titer in the lung was determined 48h after infection. Our results showed that when they were infected just 6 days after the boost immunization, mice that had received PLGA MS bearing the M1 epitope, showed a reduction in viral titer that was statistically significant compared to mice that had been immunized with CpG/polyI:C PLGA MS (Figure 23A). However, even though this reduction was statistically significant, it is questionable whether this reduction in viral titer is biologically relevant as the viral loads were high, nevertheless. Moreover, when mice were infected with IAV at later time points, no protection could be observed at all (Figure 23B-D). When we looked at survival and body weight of AAD mice that had been infected with IAV 6 days post boost, we were not able to reproduce the previously observed protection induced by $M1_{58-66}$-containing PLGA MS (Figure 23E+F). Weight loss and survival of mice was similar in all groups and immunization with the IAV epitope did not seem to offer any protection. Since not even the mice that were able to make use of the circulating cell populations were able to successfully prevent a lethal infection with IAV, it was not surprising that $M1_{58-66}$-immunized mice that had been treated with the S1PR1 inhibitor FTY720 were not protected either.

Since the employed immunization strategy followed by infection with $5x10^4$ PFU (= 10x LD_{50}) of the RB1 strain have previously been shown to induce protection from high viral loads as well as loss of bodyweight and death, we were not quite sure why we were not able to reproduce these findings [321]. We tried reducing the amount of virus used to infect the mice to 3x LD_{50},

however this merely changed the overall survival in all groups, even in mice that had only been immunized with adjuvant-bearing PLGA MS (data not shown). Therefore, we assumed that the ongoing construction next to the animal facility and the hereby induced stress, prevented an efficient immune response to the $M1_{58-66}$ peptide in AAD mice. Since the immune response in Ova-immunized C57BL/6 WT mice worked very well despite the ongoing disruptions, we decided to switch to a recombinant IAV strain. This strain, a PR8 strain, expressed SIINFEKL in the stalk of the neuraminidase surface protein [346].

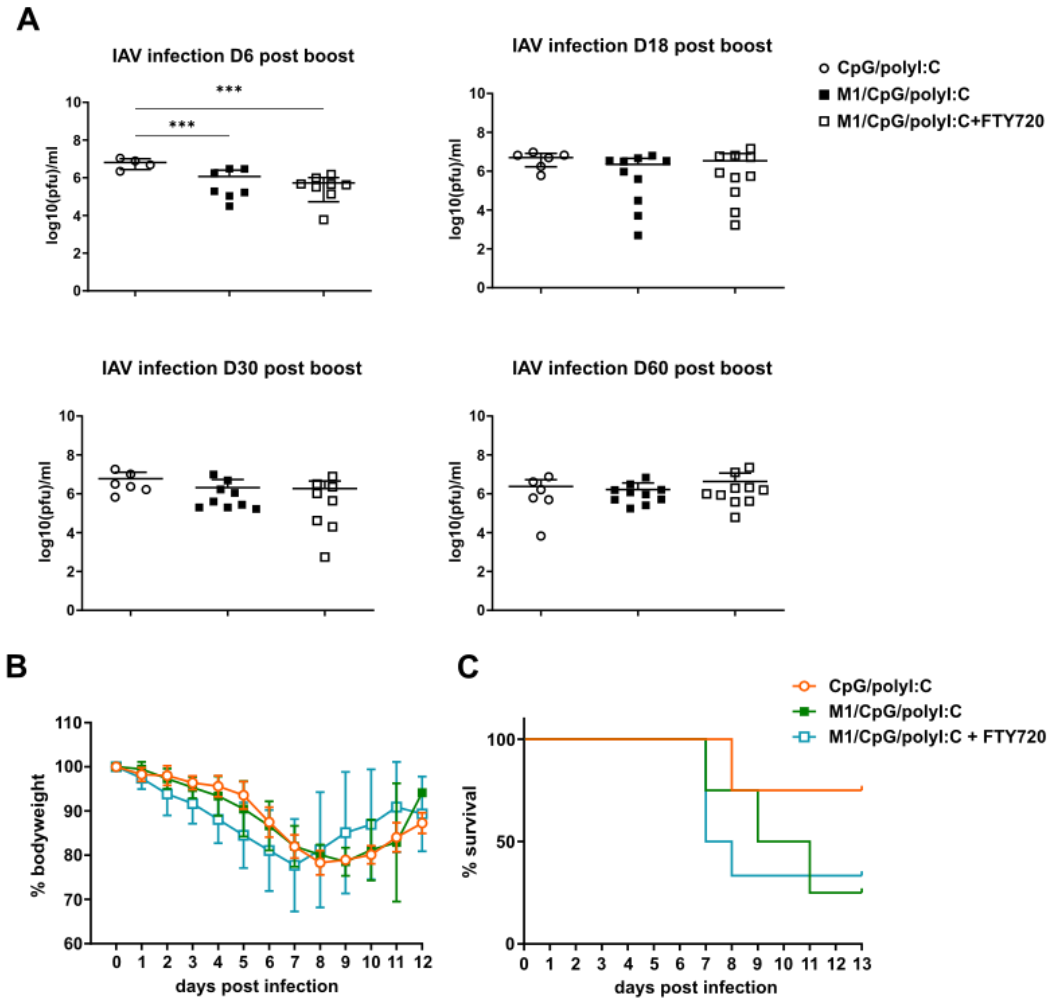

Figure 23: Analysis of protection from IAV in AAD mice immunized with $M1_{58-66}$-bearing PLGA MS. AAD mice (n=4-10) were immunized with the heterologous s.c. prime – i.n. boost immunization protocol using PLGA MS containing $M1_{58-66}$/CpG which were co-administered together with PLGA MS containing polyI:C. Control groups were immunized with adjuvant-only PLGA MS (CpG/polyI:C). FTY720 was added to the drinking water of mice in the "M1/CpG/polyI:C + FTY720" group 2 days before infection (7 µg/ml). (A) At different time points after the boost immunization (6, 18, 30 or 60 days) mice were intranasally infected with $5x10^4$ pfu of IAV (RB1). Virus titer in the lung of mice that were sacrificed 48h after infection. Statistics: one-way ANOVA with a Tukey's multiple comparisons test. ***$p < 0.001$. (B) Body weight of mice that were infected 6 days after the boost immunization was measured every day for a period of 13 days and obtained values were calculated in relation to the weight on the day of infection. Mice were sacrificed once they had lost 20% of the initial bodyweight. When mice were euthanized the last recorded bodyweight at the endpoint was used throughout the observation period. Statistics: two-way ANOVA with a Tukey's multiple comparisons test. (C) Kaplan-Meier survival curves of mice after infection with IAV. Statistics: Log-rank (Mantel–Cox) tests. Results are shown as mean ± SD. No significant differences were detected between any of the other groups.

4.1.6.2. Infection of C57BL/6 mice with recombinant IAV

Thus, following our established prime-boost immunization scheme we infected mice with the recombinant IAV strain expressing SIINFEKL in the stalk of the neuraminidase protein (insOva IAV). When mice were infected 6 days post boost, we observed a significant reduction in body weight loss compared to control mice which had received either “empty” PLGA MS or PLGA MS containing only “CpG/polyI:C” (Figure 24A). In line with this observation, mice immunized with antigen-bearing PLGA MS were protected from influenza-induced death, while in the control groups more than 50% of the mice had to be sacrificed due to excessive weight loss (Figure 24B). Mice immunized with Ova-containing PLGA MS also exhibited a significantly reduced viral titer in the lung 48h after infection confirming that prime-boost immunization with antigen-bearing PLGA MS resulted in a more rapid clearance of the virus than in control mice (Figure 24C). Importantly, mice that were treated with FTY720 to prevent the recruitment of circulating lymphocytes, showed no significant difference compared to mice that were able to make use of the recruitment of circulating lymphocytes, indicating that the locally established immune response in the lung was sufficient to avert virus infection.

To investigate whether the PLGA MS induced virus-specific immune response could also protect against IAV infection in the long term, we infected mice 30 days after the intranasal boost immunization. Our results showed that mice immunized with antigen-bearing PLGA MS treated with or without the inhibitor FTY720 exhibited a slightly improved protection against respiratory IAV challenge compared to control mice, although this protection was not significant and not sufficient to prevent virus-induced weight loss and death in the majority of mice (Figure 24D+E). Nevertheless, mice treated with FTY720 behaved in a in a similar manner to Ova-immunized mice not treated with the inhibitor suggesting that protection is mediated by lung resident memory $CD8^+$ T cells and does not rely on replenishment from the periphery. In summary, these results showed that PLGA MS are capable of inducing local memory responses sufficient to enhance viral clearance and protect mice from lethal IAV challenge at an early time point after immunization.

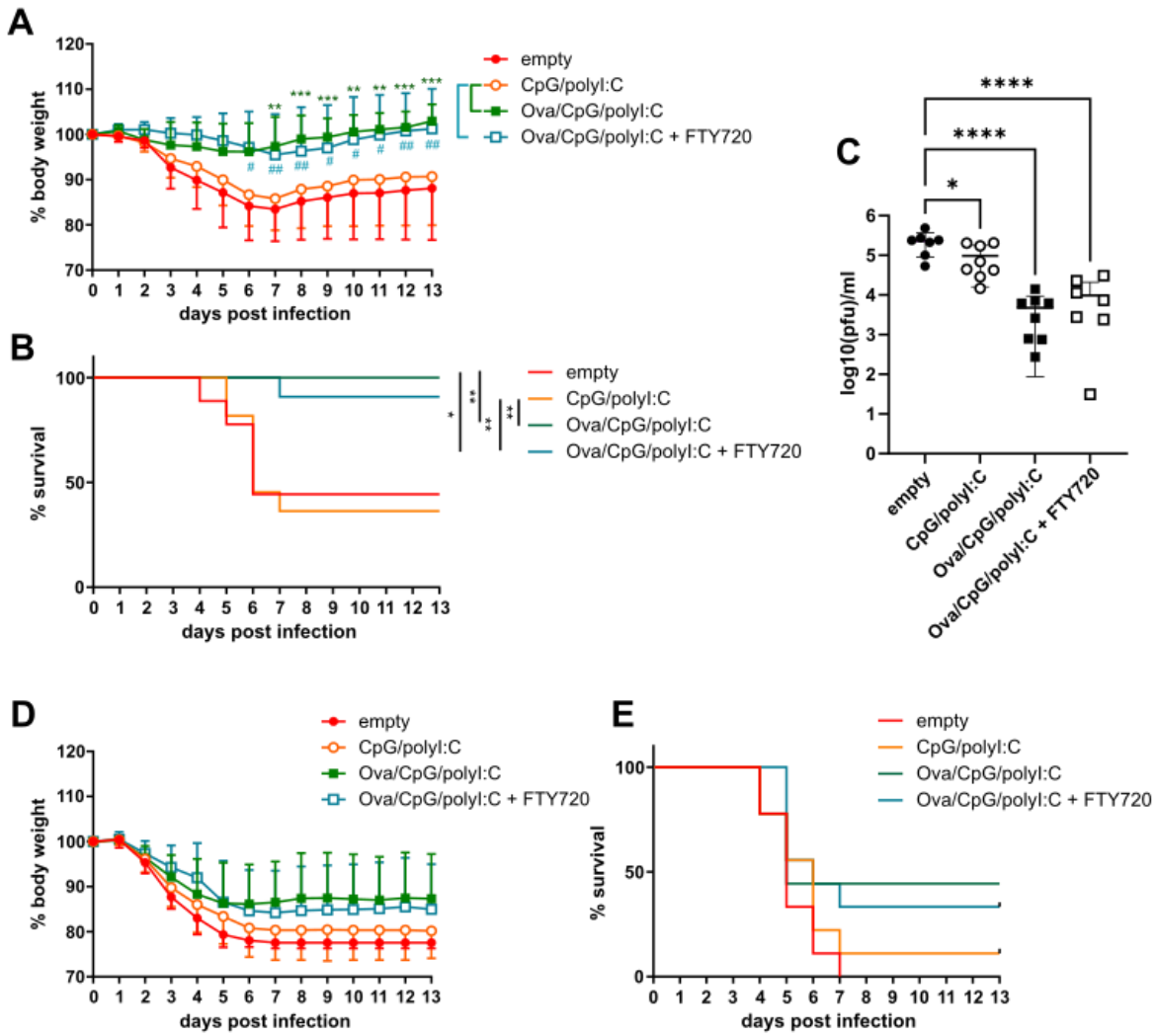

Figure 24: T_{RM} cells induced by PLGA MS protect mice from IAV infection. C57BL/6 mice (n=7-10) were immunized with the s.c. prime – i.n. boost immunization protocol using PLGA MS containing Ova/CpG which were co-administered together with PLGA MS containing polyI:C. Control groups were immunized with either empty PLGA MS or adjuvant-only PLGA MS (CpG/polyI:C). 6 (A-C) or 30 (D + E) days after the boost immunization mice were intranasally infected with 1000 PFU of insOva-IAV. FTY720 was added to the drinking water of mice in the "Ova/CpG/polyI:C + FTY720" group 2 days before infection (7 µg/ml). (A + D) Body weight was measured every day for a period of 13 days and obtained values were calculated in relation to the weight on the day of infection. Mice were sacrificed once they had lost 20% of the initial bodyweight. When mice were euthanized the last recorded bodyweight at the endpoint was used throughout the observation period. Statistical significances show results for the "Ova/CpG/polyI:C group (red) or the "Ova/CpG/polyI:C + FTY720" group (blue) compared to "CpG/polyI:C" group. Statistics: two-way ANOVA with a Tukey's multiple comparisons test. (B + E) Kaplan-Meier survival curves of mice after infection with IAV. Statistics: Log-rank (Mantel–Cox) tests. (C) Virus titer in the lung of mice that were sacrificed 48h after infection. Statistics: one-way ANOVA with a Tukey's multiple comparisons test. Results are shown as mean ± SD. *p < 0.05; **p < 0.01; ***p < 0.001; ****p < 0.0001.

4.2. Generation of PLGA MS bearing inactivated IAV

4.2.1. Comparison of different methods of inactivation

We have established that immunization with microspheres containing different epitopes of IAV proteins, such as $M1_{58-66}$ or PA_{46-54}, is capable of inducing a cytotoxic antiviral immune response in the lung. However, encapsulating only the $M1_{58-66}$ peptide, which is a $CD8^+$ T cell epitope, does not induce $CD4^+$ T cell or B cell responses. Moreover, because an immune response to a very limited number of epitopes is more susceptible to mutations in a new viral strain, we decided to encapsulate inactivated IAV into PLGA MS. As a first step, we compared four different inactivation methods that have been described in the literature [360, 361]. In the first method, the virus was simply heat inactivated (56°C for 30 minutes). The second method involved inactivation by UV irradiation for 30 minutes. The third and fourth method involved incubating the virus in either 0.1% β-propiolactone (BPL) or 0.02% formaldehyde (FA) over night. To analyze the efficacy of virus inactivation a plaque assay was performed. In the first experiment we saw in the microscope that the cells in the wells “infected” with the virus inactivated by BPL or FA had all died and that this effect decreased with the dilution of the virus sample. Since cells in the wells infected with untreated virus had not died, we assumed that this cell death was due to too high concentrations of the remaining BPL or FA. Therefore, despite the potential loss of (inactivated) virus, we decided to include a purification step to remove these substances to prevent any future adverse interactions in the mice. We subsequently performed another plaque assay with the purified virus samples and found that cell death had been minimized. Furthermore, our results showed that even though heat inactivation led to an approximately 100-fold reduction in viral titers, a non-negligible amount of active virus was still detectable in this sample (Figure 25A). In contrast, UV irradiation led to an approximately 10,000-fold reduction and no infectious virus was detectable in samples that had been treated with BPL or FA. Therefore, we decided to continue further experiments using these 3 methods of inactivation (BPL, FA and UV).

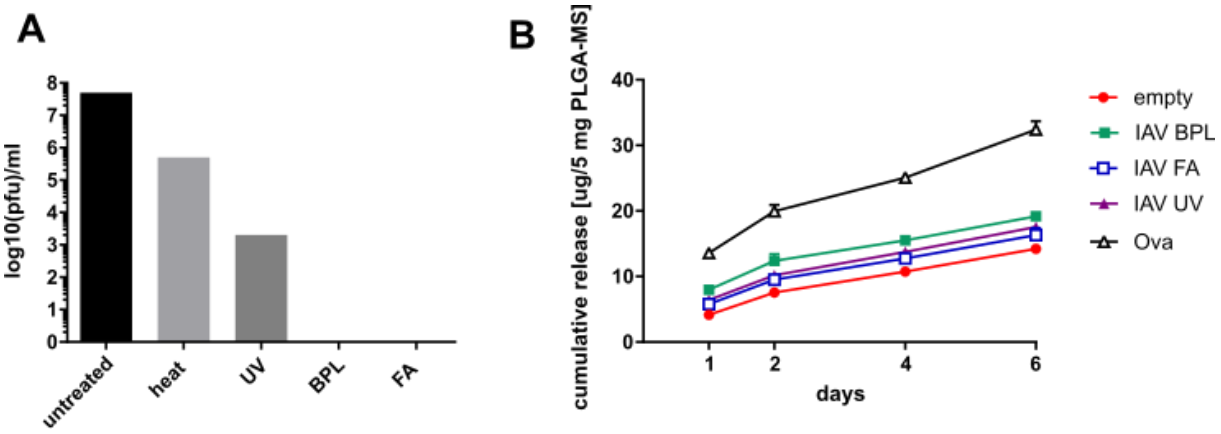

Figure 25: Characterization of PLGA MS encapsulating inactivated IAV. Influenza A virus (RB1 strain) was inactivated with heat (30 minutes at 56°C), UV irradiation (312nm, 30 minutes), 0.1% β-propiolactone (BPL; 4°C, o/n) or 0.02% formaldehyde (FA; 37°C, o/n). (A) Determination of the viral titer. (B) Cumulative *in vitro* protein release from 5mg PLGA MS (empty, IAV BPL/CpG, IAV FA/CpG, IAV UV/CpG, Ova/CpG) over 6 days analyzed by MicroBCA™ assay.

Subsequently, PLGA MS encapsulating inactivated virus together with the TLR9 ligand CpG were spray-dried and the release characteristics of these particles analyzed (Figure 25B+C). We found that the release of protein from microspheres containing the inactivated virus samples was only slightly higher than background levels (empty PLGA MS) and a lot lower than the release from microspheres encapsulating Ova. A silver staining of the release samples showed that, while Ova samples showed a typical burst release on day 1 followed by a continuous release over the next 5 days, all samples containing inactivated virus only showed the typical burst release on day 1, but no further release over the next few days. This typical burst release on the first day is usually due to protein that has been adsorbed on the surface of the particles instead of being encapsulated [3]. Therefore, we came to the conclusion that the inactivated virus had not been encapsulated into the PLGA MS, but only been bound to the surface.

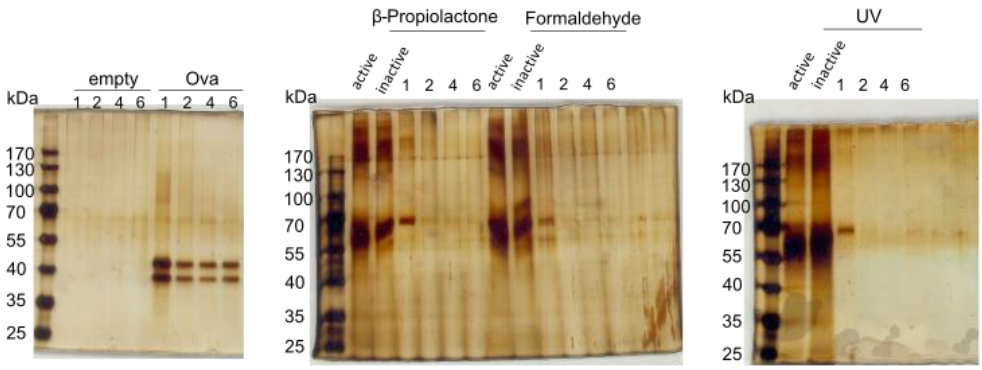

Figure 26: Protein release from PLGA MS encapsulating inactivated IAV. Influenza A virus (RB1 strain) was inactivated with heat (30 minutes at 56°C), UV irradiation (312nm, 30 minutes), 0.1% β-propiolactone (BPL; 4°C, o/n) or 0.02% formaldehyde (FA; 37°C, o/n). Silver staining of SDS-PAGE of supernatants of released content from PLGA MS collected on different days. For samples from BPL, FA and UV PLGA MS, untreated virus (active) and inactivated virus that had not been encapsulated into PLGA MS were used as a control

As a next measure, we decided to analyze the different particles by scanning electron microscopy (SEM) to determine if any differences in particle morphology could be observed (Figure 27). We found no obvious differences in morphology and particle size between the different PLGA MS, however, when the pictures were taken, it was very difficult to take pictures of the empty microspheres as these were very unstable. This was not observed with any of the other types of PLGA MS indicating that the particles with the inactivated virus samples did behave differently from empty particles. However, based on this observation we were not able to conclude the reason for this. It could have been due to the virus itself, adsorbed on the surface of the particle or encapsulated inside it, as well as the adjuvant CpG.

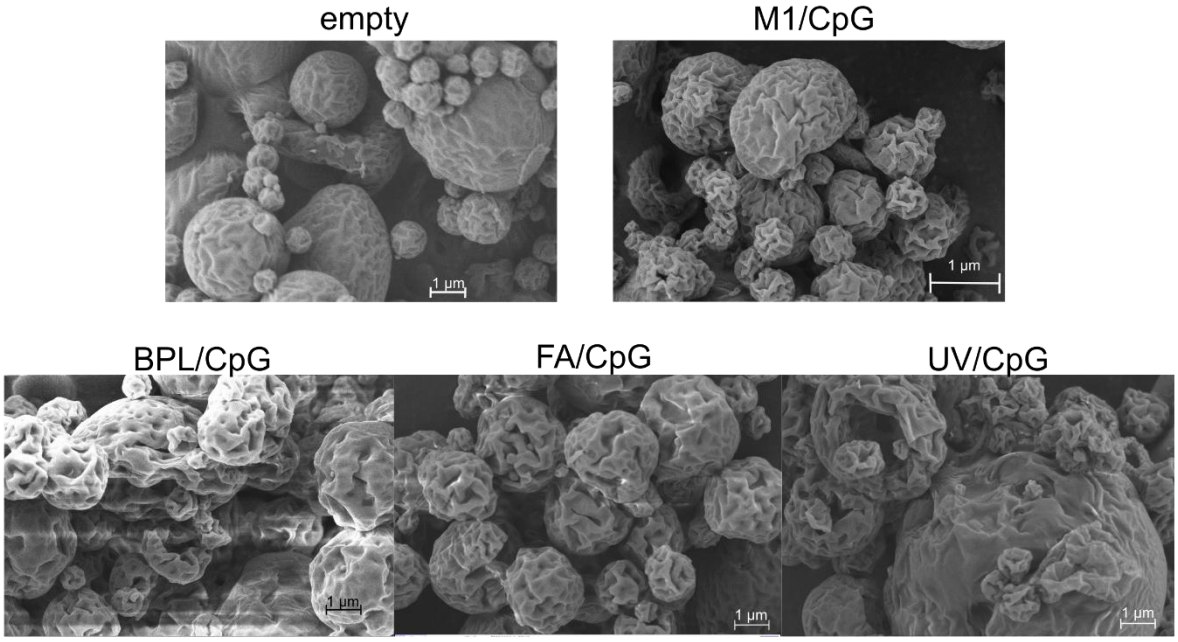

Figure 27: Visualization of different PLGA MS by scanning electron microscopy (SEM). PLGA MS were mounted on aluminum stubs and sputter-coated with a 6 nm thick layer of platinum by an argon beam sputter coater. PLGA MS were either empty or contained an antigen ($M1_{58-66}$ peptide or IAV inactivated with β-propiolactone (BPL), formaldehyde (FA) or UV irradiation) together with the adjuvant CpG. Scale bars, 1 µm.

4.2.2. *In vivo* analysis of PLGA MS bearing inactivated IAV

Finally, we decided to perform *in vivo* experiments to determine if the inactivated virus bound to the surface of the microspheres was sufficient to induce a specific immune response. First, we decided to check whether these PLGA MS were able to induce IFN-γ-producing $CD8^+$ cells in mice. For this purpose, mice were immunized with the s.c. prime – i.n. boost strategy. At the peak of the T cell response, 6 days after the intranasal boost, we sacrificed the mice and performed an ICS by restimulation of the single cell suspensions with different H-$2D^b$- or H-$2K^b$-restricted peptide epitopes of IAV, including the two immunodominant epitopes in C57BL/6 mice $PA_{224-233}$ and $NP_{366-374}$ [362, 363]. We found that none or only very limited amounts of

$CD8^+$ T cells had been formed in either lung (Figure 28) or spleen (Figure 29) that were specific for the peptides we tested for any of the groups. We also included samples that were stimulated with DC2.4 cells that had been infected with IAV to make sure that we would include all possible epitopes. However, also when samples were stimulated with virus-infected DC2.4 cells they did not produce IFN-γ. Together this data indicated that the virus bound to the surface of these PLGA MS was not sufficient to induce a specific immune response and that any virus that may have been encapsulated was not released during this period of time.

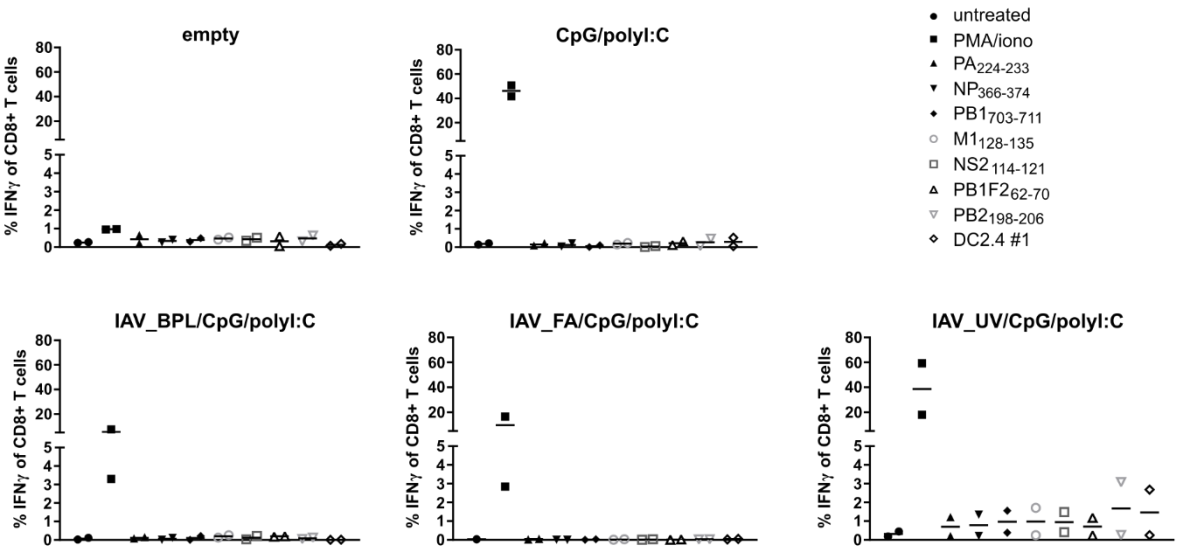

Figure 28: IFN-γ secretion of lung $CD8^+$ cells. C57BL/6 mice (n=2) were immunized with the s.c. prime – i.n. boost immunization protocol using PLGA MS containing IAV, that was inactivated with either β-propiolactone (BPL), formaldehyde (FA) or UV irradiation (UV), together with CpG which were co-administered together with PLGA MS containing polyI:C. Control groups were immunized with either empty PLGA MS or adjuvant-only PLGA MS (CpG/polyI:C). 6 days after the boost immunization mice were sacrificed and lungs harvested. Single cell suspensions of the lung were restimulated with the indicated peptides or with DC2.4 cells that had been infected with IAV. Cells that had not been restimulated were used as a negative control (untreated). As a positive control cells were restimulated with PMA/ionomycin. Subsequently, cells were stained extracellularly, followed by an intracellular staining for IFN-γ. Results are shown as mean ± SD.

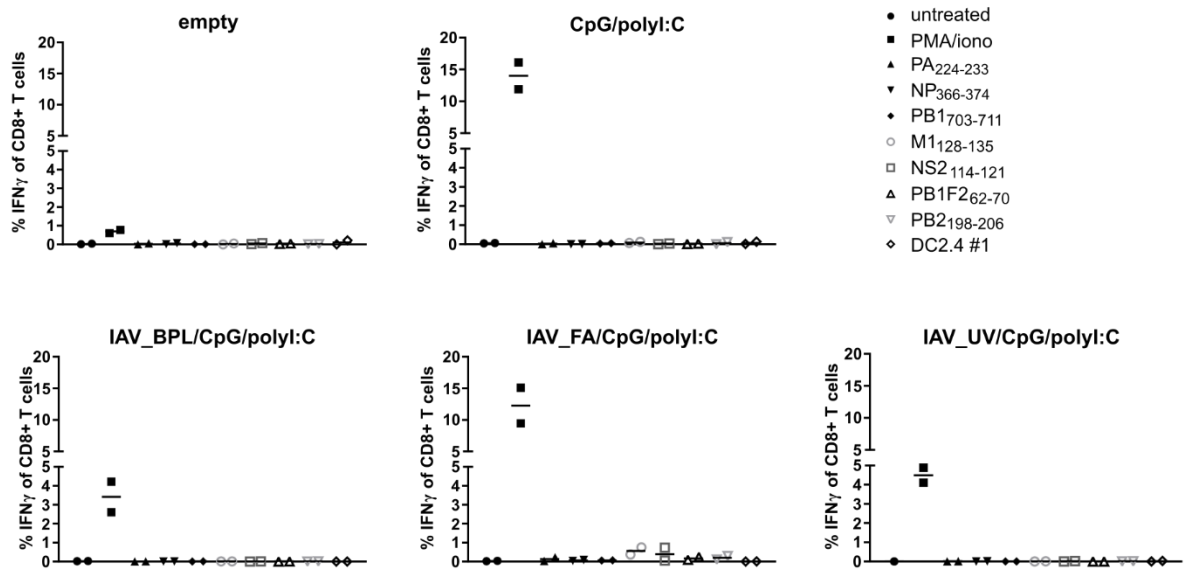

Figure 29: IFN-γ secretion of spleen CD8⁺ cells. C57BL/6 mice (n=2) were immunized with the s.c. prime – i.n. boost immunization protocol using PLGA MS containing IAV, that was inactivated with either β-propiolactone (BPL), formaldehyde (FA) or UV irradiation (UV), together with CpG which were co-administered together with PLGA MS containing polyI:C. Control groups were immunized with either empty PLGA MS or adjuvant-only PLGA MS (CpG/polyI:C). 6 days after the boost immunization mice were sacrificed and spleens harvested. Single cell suspensions of the spleen were restimulated with the indicated peptides or with DC2.4 cells that had been infected with IAV. Cells that had not been restimulated were used as a negative control (untreated). As a positive control cells were restimulated with PMA/ionomycin. Subsequently, cells were stained extracellularly, followed by an intracellular staining for IFN-γ. Results are shown as mean ± SD.

Nevertheless, as it was possible that the ICS would not capture the immune response induced, we decided to analyze whether immunization with these MS could protect mice from IAV infection. To this end, C57BL/6 mice were immunized according to the established immunization strategy with PLGA MS “containing” the different types of inactivated virus as the antigen. In line with our previous data, mice were infected with IAV 6 days after the boost immunization. This immunization strategy combined with an infection at this time point has proven to protect mice from IAV-induced weight loss and death in previous experiments (Figure 24, [321]). As a negative control we used mice immunized with empty or adjuvant-only PLGA MS. Unfortunately, we were not able to include a positive control, as we did not have PLGA MS that we could use to immunize C57BL/6 mice against the RB-1 IAV strain. We found no significant differences in weight loss and survival of mice immunized with either type of microspheres (Figure 30). Even when mice had been immunized with PLGA MS “containing” the inactivated virus, they were not protected from IAV-induced weight loss or death indicating once more that the virus bound to the surface of the PLGA microparticles was not sufficient to induce a strong antiviral immune response.

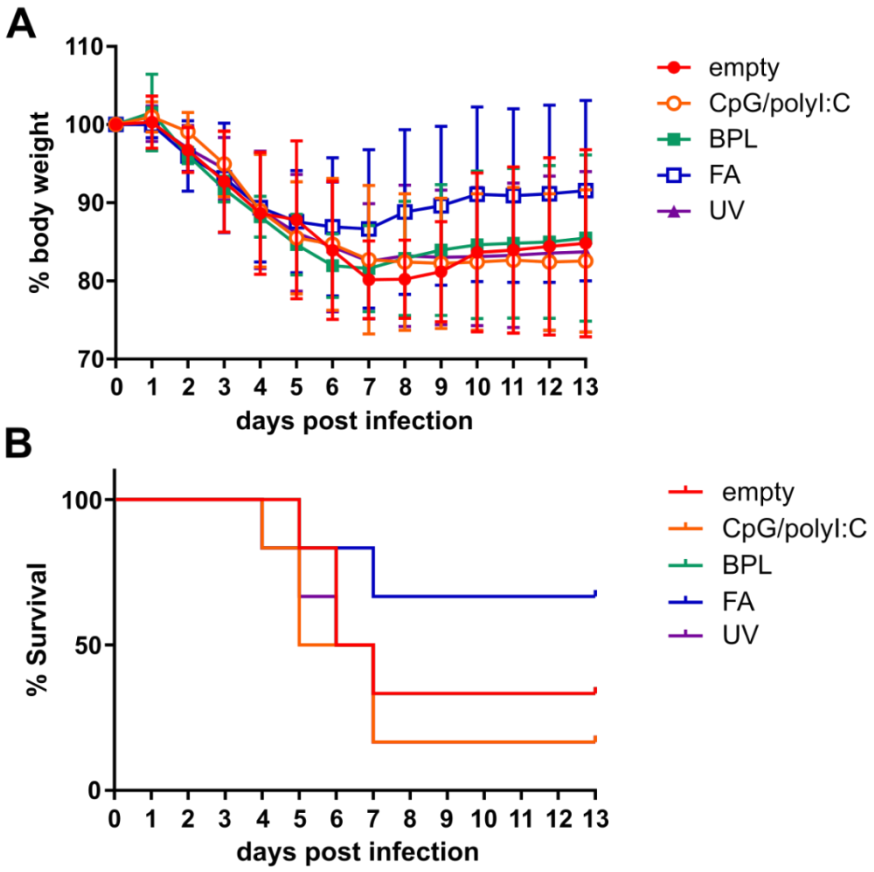

Figure 30: Analysis of protection from IAV infection in AAD mice immunized with $M1_{58-66}$-bearing PLGA MS. C57BL/6 mice (n=6) were immunized with the s.c. prime – i.n. boost immunization protocol using PLGA MS containing IAV, that was inactivated with either β-propiolactone (BPL), formaldehyde (FA) or UV irradiation (UV), together with CpG which were co-administered together with PLGA MS containing polyI:C. Control groups were immunized with either empty PLGA MS or adjuvant-only PLGA MS (CpG/polyI:C). 6 days after the boost immunization mice were intranasally infected with $5x10^4$ pfu of IAV (RB1). (A) Body weight was measured every day for a period of 13 days and obtained values were calculated in relation to the weight on the day of infection. Mice were sacrificed once they had lost 20% of the initial bodyweight. When mice were euthanized the last recorded bodyweight at the endpoint was used throughout the observation period. Statistics: two-way ANOVA with a Tukey's multiple comparisons test. (B) Kaplan-Meier survival curves of mice after infection with IAV. Statistics: Log-rank (Mantel–Cox) tests. Results are shown as mean ± SD. No significant differences detected between any of the groups.

5. Discussion

5.1. Generation of local CD8$^+$ memory T cells using PLGA MS

5.1.1. Immunization strategy

As a first step in this project we analyzed the best immunization strategy to induce a strong local memory response in the lung airways and interstitium with a special focus on T_{RM} cells due to their superior protective capacities compared to circulating memory T cells.

A number of studies have established that a mucosal vaccination strategy is required for the induction of T_{RM} cells in mucosal locations, such as the lung. Nizard *et al.* showed that in contrast to intramuscular immunization, intranasal immunization led to the generation of antigen-specific memory T cells in the lung mucosal tissue which expressed typical T_{RM} cell markers such as CD49a and CD103. Intramuscular immunization on the other hand induced effector-like T cells in the spleen which lacked expression of CD49a and CD103 [156]. In the setting of IAV infection, it has been demonstrated that i.n. administration of the live attenuated influenza vaccine (LAIV) is superior at inducing lung T_{RM} cells and thereby offers better heterosubtypic protection than parenteral injection of the inactivated influenza vaccine (IIV) which mostly induces strain-specific neutralizing antibodies [364]. Another study found that while i.m. influenza priming induced similar numbers of circulating antigen-specific memory CD8$^+$ T cells as i.n. priming, only the i.n. route of application was able to induce CD8$^+$ T_{RM} cells in the lung airways and parenchyma [83]. In general, it seems that mucosal vaccination strategies are better suited to induce a protective memory response at the sites of pathogen encounter [365]. However, with the exception of 9 vaccines that have been approved for application via the mucosal route (1x intranasal, 8x oral), the majority of protective vaccines to date are injected intramuscularly [365]. Because systemic protective immunity induced by i.m. vaccination is often not sufficient to protect against some pathogens, such as the respiratory pathogens *M.tuberculosis*, *B.pertussis* and influenza virus, improved vaccines are under development to enhance the suboptimal protection [365]. A preclinical study investigating the i.n. application of the Bacillus Calmette-Guerin vaccine for TB has given promising results while intranasally administered vaccines against *B.pertussis* have entered clinical phase II trials [366-368].Together these findings highlight the necessity for vaccines that can be applied via the mucosal route, to induce protective immunity directly at the sites of pathogen entry, and demonstrate that progress, albeit slow, is being made in this direction.

PLGA MS are an ideal candidate for such a vaccination strategy as they are approved for application via the mucosal route [3]. Previous work from our group has established that a s.c. prime followed by an i.n. boost immunization with PLGA MS induces a CD8$^+$ T cell response

capable of protecting mice from severe IAV infection [321]. Importantly, this protection was only observed when mice received both the s.c. prime as well as the i.n. boost. One immunization alone, either via the subcutaneous or via the intranasal route, was not sufficient to induce a specific protective immune response. However, as T_{RM} cells had not been examined in this study, we decided to investigate the generation of these cells after three different immunization protocols: i.n. prime only, i.n. prime – boost and s.c. prime – i.n. boost (Figure 8). Our results clearly showed that one intranasal immunization induced a very limited number of specific cells in the lung and basically no antigen-specific response in the spleen. An intranasal prime followed by a boost immunization via the intranasal route greatly enhanced the amount of tetramer$^+$ cells in the lung and, more importantly, the majority of the specific cells exhibited a T_{RM} cell phenotype but did not induce a SIINFEKL-specific response in the spleen. Conversely, a systemic (s.c.) prime followed by a local (i.n.) boost induced the highest percentage of both total tetramer$^+$ cells in lung and spleen as well as T_{RM} cells in the lung. While some vaccination strategies in the literature using different delivery vehicles, have been able to generate a robust T_{RM} cell response after an intranasal prime – boost vaccination [156, 348], other studies have confirmed our findings: a systemic “prime” followed by a local “pull” induces a superior response. Uddbäck *et al.* immunized mice using adenoviral vectors expressing flu nucleoprotein [369]. They found that, in contrast to s.c. or i.n. immunization alone, a simultaneous, combined immunization (s.c. + i.n.) induced the most robust protection against heterosubtypic IAV strains. From their data they concluded that together with T cells already present in the respiratory mucosal tissue, high numbers of antigen-specific CD8$^+$ T cells in the spleen are important for ideal protection. In the case of infection, this circulating antigen-specific T cell population is able to expand and infiltrate the lungs to aid the local memory cells in the antiviral immune responses. This finding emphasizes the importance of the circulating T cell response in addition to local T_{RM} cells and further points to our s.c. prime – i.n. boost immunization strategy which induced both a circulating as well as a local population.

In summary, our findings in combination with these data from the literature highlight the benefits of the s.c. prime – i.n. boost immunization strategy in inducing a local memory response that can be backed up by circulating antigen-specific cells when necessary. Since several studies have observed the induction of a sustained T_{RM} response after a simultaneous s.c. and i.n. immunization, it would be interesting to study this in the context of PLGA MS. In the context of a therapeutic tumor vaccination, recent work from our lab has demonstrated that a combined s.c. + i.n. immunization was necessary in order to induce sufficient antitumor immunity in the lung [265]. It would certainly be of advantage if also this simultaneous immunization strategy was able to generate T_{RM} cells likewise in a protective setting. In addition

to the expected better patient compliance of this strategy, inducing a T_{RM} cell response more rapidly should be highly beneficial in certain settings, such as the emergence of a new pandemic virus or a therapeutic cancer vaccination.

5.1.2. The memory $CD8^+$ T cell response in the lung

Once we had established an immunization strategy that efficiently induced T_{RM} cells we focused on the different types of generated memory $CD8^+$ T cells as well as their longevity. We found that, while T_{EM} cells were the dominating subtype in the spleen, in the lung airways and interstitium the majority of cells were T_{RM} cells (total), followed by T_{EM} cells (Figure 10). Since most of the T_{RM} cells in the lung have been reported to express the adhesion molecule CD103, we further subdivided this population into $CD103^+$ and $CD103^-$ T_{RM} cells. Our results show that even though many of $CD69^+$ T_{RM} cells co-expressed $CD103^+$, a sizable proportion was negative for this marker. It certainly would have been interesting to further analyze the phenotype of these $CD69^+$ T_{RM} cells using RNA sequencing. Although a core signature has been identified for T_{RM} cells across tissues in mice and humans, it is well established that T_{RM} cells show substantial heterogeneity across tissues and even within tissues [42, 46, 47, 76, 165, 370-372]. In this regard, further characterizing the T_{RM} cells established after PLGA MS immunization would certainly be a promising next step. Especially the comparison of $CD103^+$ to $CD103^-$ T_{RM} cell populations as well as cells in the airways vs the interstitium would be of interest.

Under certain circumstances $CD69^+CD103^-CD8^+$ T cells have been found to recirculate in mice [39, 50, 373]. In contrast, non-recirculating $CD69^-CD103^-CD8^+$ T cells have been detected in several murine tissues [151, 374]. Therefore, CD69 and CD103 have been designated “imperfect markers to infer tissue residency” [2]. For this reason, many studies use parabiosis experiments to fully confirm the residence of T_{RM} cells. However, in addition to being technically difficult to perform, this technique is ethically controversial and not approved by German regulatory authorities. It is therefore possible that some of the cells we identified as T_{RM} cells, either total or $CD103^+$ T_{RM}, were not truly resident. Nevertheless, we assume that the majority of cells identified as T_{RM} cells are non-recirculating $CD69^+$ cells as we prevented lymphocyte recirculation using FTY720 (Figure 11). This small molecule binds to S1PR1 and thereby sequesters lymphocytes in the LNs [356, 375]. Thus, we were able to study the local immune response in the lung without the contribution of circulating lymphocytes. When we compared the induction of T_{RM} cells in mice prime-boost immunized with antigen-bearing PLGA MS to mice immunized with the same strategy but additionally treated with FTY720, we found that both groups exhibited similar amounts of T_{RM} and T_{EM} cells in the lung airways and interstitium (Figure 12). At first it seems surprising that FTY720-treated mice display a similar amount of

T_{EM} cells in their lungs as FTY720-untreated mice because they are no longer able to recruit circulating cells, however it has been reported that FTY720 treatment leads to a transient increase of $CD69^-CD8^+$ T cells in the lung that is reversed when FTY720 treatment is stopped [91, 99]. Since the mice in the above mentioned experiments were treated with FTY720 for only two days, it is likely that the absence of a difference between FTY720-treated and - untreated groups is due to the inability of the T_{EM} cells, that were circulating through the lung, to leave the lung. Also, FTY720-treated mice displayed similar amounts of T_{EM} cells in the spleen as their untreated controls. Again, this is probably due to the impaired egress of these cells. Nevertheless, even though T_{EM} cell numbers were similar in FTY720-treated mice two days after we started the treatment, these mice were not able to recruit additional cells from the circulation when tumor cells or IAV were encountered in the lung, indicating that the majority of the response was performed by T_{RM} cells.

One major question that arises is whether starting the FTY720 treatment 2 days before the analysis (or injection of tumor cells or infection with IAV) is sufficient to prevent the recruitment of circulating cells at the time point of analysis (or injection of tumor cells or infection with IAV). In fact, when mice were treated with FTY720 for 26 days (for the tumor experiments in Figure 20 and Figure 22), the amount of $CD3^+$ cells in the blood was reduced by 80-85% (data not shown) compared to the 70% reduction observed when mice were treated for 2 days indicating that a longer treatment period further reduces the number of circulating cells. It is possible that the higher number of circulating $CD3^+$ cells at the beginning might have skewed the obtained data slightly compared to an earlier treatment regimen. However, starting the treatment with FTY720 two days (in some cases even less) before analysis of the memory response is a frequently used kinetic in the literature [88, 156, 376]. Moreover, at the earliest time point we analyzed (day 6 post boost) mice were already treated with the inhibitor just 4 days after the boost immunization. Adding the inhibitor to the drinking water at an even earlier time point could have interfered with the recruitment of antigen-specific cells to the lung and the development of a local memory response. Therefore, we decided to commence treatment with FTY720 two days before analysis (or injection of tumor cells or infection with IAV), similar to other published studies.

In summary, our results showed that a s.c. prime – i.n. boost immunization strategy with PLGA MS induces T_{RM} cells in lung and airways as well as a substantial population of T_{EM} cells in the circulation. The importance of an antigen-specific memory T cell population in the circulation in addition to the local memory response has been confirmed in multiple studies. In several murine tumor models the presence of both circulating and resident memory T cell populations has been found to improve protection from tumor growth compared to either population alone [156, 166]. This is also confirmed by our findings: Ova-immunized mice were better protected

from tumor growth than Ova-immunized mice additionally treated with FTY720, especially when the tumor challenge was performed at later time points. Considering that one of the main mechanisms by which T_{RM} cells are known to offer protection from reinfection is via the recruitment of circulating immune cells, this is not an unexpected finding [62]. These findings further corroborate the benefit of our systemic prime – local boost immunization strategy as it ensures the generation of both local and circulating memory responses.

After having established which $CD8^+$ memory T cell subtypes are generated in response to PLGA MS immunization we focused on the longevity of the local memory response in the lung. In line with prior work, we observed that even though a memory response was still detectable at later time points, numbers of T_{RM} cells had declined substantially (Figure 13). This is a common theme for lung T_{RM} cells: airway T_{RM}, which are especially short-lived, have been found to possess a half-life of only 14 days which is likely due to the inhospitable environment in the airways and the rapid removal of cells via phagocytic cells or mucociliary clearance [101, 105]. But also interstitial T_{RM} cells have mostly disappeared 7 months after influenza infection and are much less long-lived than T_{RM} cells in other tissues, such as the skin where they can persist up to a lifetime in mice [100, 112]. This loss of T_{RM} cells in the lung seems to be due to apoptosis rather than migration out of the lung [112]. While T_{RM} cells in the skin occupy niches that offer ideal conditions for these cells, $CD8^+$ T_{RM} cells in the lung are enriched in specific niches created at the site of tissue regeneration after injury. These niches have been termed repair-associated memory depots (RAMDs) and slowly shrink over time until they finally disappear with the recovery of the tissue [99, 103]. Since the tissue injury induced by immunization with PLGA MS is clearly not as prominent as that induced in an infectious or tumorous setting this might offer an explanation for the faster decline in numbers in our vaccination setting. Even though we could still detect antigen-specific cells in the lungs 60 days after the boost immunization, their numbers had already decreased substantially. Furthermore, we also observed a strong decrease in the percentage of SIINFEKL-specific cells among all $CD8^+$ T cells between day 30 and day 60 post boost in lung and airways (Figure 13D). This further indicates that the specific cells induced via PLGA MS immunization are already lost at a much earlier time point than those induced after influenza infection. A histological or microscopical comparison of the RAMDs generated in response to PLGA MS immunization to those generated by a more severe pulmonary “injury”, such as a respiratory virus infection, could further corroborate this hypothesis.

In addition, it has been suggested that the availability of cognate antigen and APCs in the RAMDs is the limiting factor for the number of $CD8^+$ T_{RM} cells generated [91]. A recent study in mice showed that $CD8^+$ T_{RM} in the lung can persist for at least 1 year post vaccination. In this study the authors used an adenovirus expressing influenza nucleoprotein which was

administered via airway vaccination. By this means antigen was present in the lung interstitium and airways for more than 3 months post vaccination and the $CD8^+$ T_{RM} pool was maintained by *in situ* proliferation as well as replenishment from the circulating T cell pool [377]. Prolonging the presence of antigen in the lung could also be achieved with PLGA MS by adjusting the release characteristics based on the composition of the polymer (the LA/GA ratio). Increasing the percentage of the hydrophobic lactic acid units would prolong the release of the antigen from the microparticles. This might lead to increased antigen persistence in the lung and thereby an improved persistence of lung $CD8^+$ T_{RM} populations.

Another method to prolong the presence of T_{RM} cells in the lung is via boost immunizations. A prior study demonstrated that repeated influenza infections were able to induce T_{RM} cells that persisted in larger numbers and were resistant to apoptosis [378]. Moreover, we have previously shown that a boost immunization 8 weeks after the prime strongly enhances the diminished $CD8^+$ T cell IFN-γ response [321]. Slütter *et al.* identified circulating T_{EM} cells as the precursors for lung T_{RM} cells and showed that a systemic boost with recombinant *L.monocytogenes* expressing the same antigen as the influenza virus which was used to infect mice 45 days previously, increased the specific T_{EM} population which in turn led to an increase in lung T_{RM} cells [112]. Over time however, the T_{EM} population in the circulation lost its capacity to differentiate into lung T_{RM} cells. This finding further highlights the benefits of the induction of both local T_{RM} and circulating T_{EM} cells after PLGA MS immunization as seen in our experimental setup.

Collectively, these results suggest that an additional boost vaccination at later time points might be necessary and might lead to a sustained T_{RM} cell response. Based on the above mentioned data, it would certainly be worthwhile to compare the efficacy of an additional systemic (s.c.) boost to one administered locally (i.n.). However, it is important to keep in mind that the strong decline in T_{RM} cell numbers in the lung in comparison to other tissues seems to fulfill a protective function. The main function of the lung is gas exchange which might be compromised by the accumulation of vast numbers of immune cells [91]. Additionally, persistent antigen due to repeated boost immunizations or prolonged release from PLGA particles could potentially induce persistent inflammation and immunopathology [377]. Therefore, the consequences of inducing a more long-lasting T cell population in the lung through boost immunizations have to be carefully studied.

In experimental mice the time point of primary antigen encounter can be determined precisely, thus enabling researchers to study the duration of T_{RM} persistence in different tissues. Because humans are constantly in contact with many different pathogens, it is not possible to determine the exact time point when someone encountered an antigen. However, data from human HLA-

disparate lung transplant recipients has found donor T_{RM} to persist in the donor lung for more than 15 months hinting that human T_{RM} cells are more long-lived than their murine counterparts [189]. In the context of influenza vaccinations this timeframe would be sufficient to offer protection for the duration of one influenza season. It will certainly be interesting to analyze the persistence of T_{RM} cells in other human organs and tissues to see whether the kinetics are similar to those observed in mice. Possibly, the COVID-19 pandemic and the associated close monitoring of infections might enable researchers to study the maintenance of SARS-CoV-2-specific T_{RM} cells in the lungs of previously infected individuals.

5.1.3. T_{RM} cells in antitumor immunity

The importance of T_{RM} cells in the immune response to a variety of malignancies has been well analyzed in a myriad of studies in mice. Likewise, data from human cancer patients indicate that the presence of T_{RM} cells is correlated to an improved outcome in multiple types of cancer, indicating a similar importance of T_{RM} cells in humans [150]. Therefore, we decided to analyze the capacity of PLGA MS-induced $CD8^+$ T_{RM} cells to protect mice from tumor growth. Using the generated Ova^+Luc^+B16BL6 melanoma cell line, we were able to improve the obtained data by monitoring *in vivo* growth of the tumor cell lines rather than only counting the metastases at a defined endpoint. Our results showed that tumor antigen-immunized mice were protected from tumor growth even at the latest time point analyzed (Figure 20, Figure 22), confirming previous studies from our group that had analyzed the *in vivo* antitumor response after PLGA MS immunization [265, 323, 324]. Importantly, we were able to show that the local antitumor response was sufficient to protect mice from tumor growth at an early time point. When tumor cells were injected 6 days after the boost, mice treated with FTY720 were protected to the same extent as antigen-immunized, but FTY720-untreated mice. While this antitumor effect declined over time, FTY720-treated mice still harbored significantly less metastases in the lung than mice immunized with empty PLGA MS even when tumor cells were injected on day 30 post boost. By day 60 the number of metastases in FTY720-treated mice was no longer significantly reduced compared to “empty” controls, yet a tendency could still be observed. We were also able to observe an increase in lung $CD8^+$ T_{RM} cells in antigen-immunized mice that seemed to inversely correlate with the reduction in lung metastases. Collectively, our data allows us to speculate that the T_{RM} cells play a pivotal role in the antitumor immune response also in the setting of PLGA MS immunization. The capability of this vaccination delivery system to induce T_{RM} cells further adds to its advantages. Moreover, we were able to show that an antigen-specific systemic prime vaccination followed by a nonspecific local boost immunization (boost w/o antigen) was able to protect mice to a similar extent as an antigen-specific prime *and* boost immunization (boost with antigen) (Figure 21). However, when we analyzed the different subsets generated in response to different

immunization strategies (Figure 12), we found that this “boost w/o antigen” strategy did not induce T_{RM} cells. Even though the application of PLGA MS containing at least the adjuvants slightly increased the infiltration of $CD8^+$ T cells into the airways compared to empty MS, it did not lead to an induction of SIINFEKL-specific $CD8^+$ T cells in either lung or airways. Therefore, the antitumor protection in the lung in the “boost w/o antigen” group was most likely mediated by antigen-specific circulating cells that had been induced following the antigen-prime. To follow this hypothesis, it would have been good to include a “boost w/o antigen + FTY720” group. This way mice would have received the antigen-specific prime followed by the nonspecific boost to allow the induction of a specific immune response. Subsequently, mice would have been treated with FTY720 starting two days before the injection of the Ova^+Luc^+B16BL6 tumor cells. These mice would not have possessed antigen-specific T cells in the lungs and airways and would not have been able to recruit circulating antigen-specific cells to the lung to combat the tumor cells. Thus, a lack of protection of these mice compared to “boost with antigen + FTY720” (i.e. Ova/CpG/polyI:C + FTY720) mice could have underscored the ability of PLGA MS immunization to induce a protective circulating antitumor response with just one systemic prime.

In addition to the correlation of T_{RM} cell numbers and patient survival, the presence of T_{RM} cells has also been linked to the clinical benefit of immune checkpoint inhibitors [150]. Recent data suggests that T_{RM} cells, or T_{RM}-like TILs as they are often called in a tumor setting, may be (one of) the major targets for immune checkpoint blockade due to their high expression levels of immune checkpoint molecules [111, 379]. In line with this, a study in melanoma patients found an expansion of T_{RM}-like TILs following anti-PD-1 therapy [137]. In general, cancer immunotherapy seems to be improved greatly when several approaches are combined, such as cancer vaccination and immune checkpoint blockade [225, 262-264]. To this end, we have recently shown that combination cancer immunotherapy consisting of the induction of tumor-specific cells via PLGA MS immunization and the subsequent inhibition of immune checkpoints on these cells via anti-CTLA-4 and anti-PD-1 treatment significantly enhanced the antitumor response in comparison to one method alone [265]. It would certainly be interesting to study the contribution of T_{RM} cells to the efficacy of immune checkpoint therapy in the setting of PLGA MS vaccination.

In addition to increasing the efficacy of immune checkpoint therapy, T_{RM} cells may also protect individuals from tumors due to their ability to migrate to draining LNs. In mice T_{RM} cells have been found to migrate to draining LNs following secondary infection [39]. Furthermore, stimulating T_{RM} cells in the lung also provoked responses in LNs draining the lung. Together, these findings indicate that T_{RM} cells may additionally protect from tumor growth by taking up residence in the tissue-draining LNs and thus preventing metastases formation [163]. In this

way, T_{RM} cells in the LNs could also prevent a relapse after successful cancer therapy [111]. Moreover, inducing T_{RM} cells in the affected tissue as well as the draining LNs by PLGA MS vaccination may help to hinder tumors from reappearing. Therefore, as a next step in analyzing T_{RM}-mediated antitumor immunity, the formation of T_{RM} cells in lung-draining LNs could be studied.

While our results are promising in showing that PLGA MS immunization leads to the formation of T_{RM} cells in the lung that are capable of protecting from tumor growth, they also highlight that efficient antitumor immunity requires both resident as well as circulating memory T cells. Especially when mice were challenged with tumor cells on day 60 post boost, the local memory response was not sufficient to prevent the formation of metastases. This effect has also been observed by others [156, 348]. In a model of murine head and neck tumor, treating mice with the lymphocyte recirculation-inhibitor FTY720 uncovered that T_{RM} cells play a pivotal role in protecting mice from tumor growth. However, the authors also discovered that tumor protection was improved when mice were able to make use of circulating lymphocytes [156]. Nevertheless, even though FTY720-treated mice did not have significantly reduced numbers of metastases in their lungs compared to “empty” or adjuvant-only-immunized mice, the tendency was still observable and the number was not significantly increased compared to Ova-immunized FTY720-untreated mice. Together, our data are in line with other findings underscoring the excellent antitumor capacity of local tumor-specific memory T cells which ideally can be backed-up by a circulating population.

In a clinical setting, cancer vaccinations are usually given in a therapeutic, rather than a prophylactic manner. In this study we focused on T_{RM} cells induced by prophylactic vaccination. However, other studies from our group have established that PLGA MS immunization is also able to protect mice from tumor growth in a therapeutic setting. As previously mentioned, following the i.v. injection of $Ova^{+}Luc^{+}$B16BL6 cells, mice were immunized simultaneously via the s.c. and the i.n. route as soon as tumor growth could be detected in the lung. This therapeutic strategy significantly reduced pulmonary metastases [265].

At large however, therapeutic cancer vaccinations, at least when they are administered alone, do not show a great success rate [225, 259]. As mentioned above, it is believed that this is due, in part, to the immunosuppressive microenvironment in advanced malignancies and the associated difficulties of monotherapy to overcome this suppression. In contrast, the two established prophylactic vaccines for cancer prevention, namely the vaccines against human papillomavirus (HPV) and hepatitis B virus (HBV), show outstanding success rates. In 1984 a national immunization program against HBV was initiated in Taiwan which has resulted in a significant reduction in the incidence of hepatocellular carcinoma in a 20-year follow-up study [380]. More recently, in 2006, a vaccine protecting against chronic HPV infection and thereby

cervical cancer, was first approved for use in females aged 11-26, later also for males aged 11-21. Since then, a number of clinical trials has given us a first indication of the reduced prevalence of HPV infections in vaccinated individuals [381, 382]. It is expected that a significant reduction in the incidence of HPV-induced cancers will be observed in future decades [225, 383]. Ideally, of course this would be possible for all types of cancers, but finding an antigen to vaccinate against in a prophylactic setting, that is not expressed by healthy cells, is more difficult with tumors that are not induced by viral infections. The risks associated with immunizing healthy individuals against a self-antigen that may potentially be overexpressed by tumor cells in the future, outweigh the benefits. However, it has been suggested that people at risk of developing malignant tumors, such as patients with pre-malignant lesions or individuals with certain mutations (such as women with mutations in *Brca1* or *Brca2*) could be vaccinated against tumor-associated antigens at an earlier time point to enhance immunosurveillance and inhibit cancer development – before the environment becomes too immunosuppressive [225]. Our data has clearly shown that PLGA MS are well suited for this type of cancer vaccination. Since PLGA is completely biodegradable and broken down into non-toxic products, PLGA particles are an ideal delivery system. Moreover, it is possible to encapsulate a wide variety of proteins and peptides into these particles and previous work from our group has established that encapsulation of more than one peptide into the same microparticle does not weaken the immune response to either one epitope [321].

In the era of personalized medicine, identifying personal tumor neo-antigens to encapsulate would certainly be a viable option and could greatly improve cancer vaccination efficacy [220, 249]. Furthermore, using tumor lysate to immunize patients could widen the repertoire of tumor-specific T cell clones, thereby reducing the risk of immune escape by the tumor, without the need to identify the tumor antigens in advance. Several studies have proven that tumor lysates which are administered in particulate forms, such as in PLGA microparticles, are superior at inducing immune responses than soluble tumor lysate [384]. In line with this idea, members from our group have tried to encapsulate tumor lysate into PLGA MS. While this previously seemed to induce antitumor immune responses in a therapeutic setting [323], more recent data shows that the amount of antigen in the lysate preparations is not sufficient to induce strong immune responses (Bachelorthesis Isabel Hölzl, 2021).

In addition to optimizing the timing of cancer vaccinations, a more relevant modification could be the application route. Many cancers occur in mucosal tissues and as previously mentioned the majority of currently approved vaccines are administered into the muscle. Preclinical studies in mice have indicated that a systemic i.m. prime followed by a vaginal boost with an HPV vaccine induced local T_{RM} cells more efficiently. Moreover, compared to an i.m. boost, the vaginal boost correlated with better survival [385]. Another major drawback of the HPV

vaccines, which are highly successful in a prophylactic setting, is the inability to induce an immune response against already established tumors. One possible reason for this observation is the fact that the currently employed HPV vaccines work mainly by inducing neutralizing antibodies that prevent the virus from infecting host cells in the first place. However, once host cells have been infected, the humoral arm of the adaptive immune response is no longer able to kill large amounts of virus-infected cancer cells [249]. A vaccine that can be administered via the mucosal route and that efficiently induces a local memory T cell response could solve many of the current problems associated with the reduced efficacy of cancer vaccines. In this project we have shown that both of these requirements can be fulfilled by our PLGA MS immunization strategy, further corroborating their advantages as vaccine delivery systems. In summary, our data indicate that PLGA MS may serve as delivery systems for cancer vaccines – in a prophylactic or a therapeutic setting – and certainly justify further research.

5.1.4. T_{RM} cells in viral infection

Even though current research has mainly focused on vaccinations against tumors, the majority of vaccinations to date are still performed to prevent infections. The importance of developing vaccines that activate the cellular arm of the adaptive immune response is gaining more attention. Thus far, influenza vaccines usually comprise different inactivated viral strains that are injected intramuscularly, thereby inducing mostly a humoral immune response against the viral surface proteins HA and NA. However, due to antigenic drift these proteins constantly change, rendering the developed antibodies less effective. For this reason, in recent years the focus has been placed on the T cell response to influenza virus. Studies in mice have shown that, in contrast to i.m. injection of the inactivated influenza vaccine, intranasal administration of the LAIV is able to induce $CD4^+$ and $CD8^+$ T_{RM} responses in the lung that are able to offer heterosubtypic protection [364]. Analysis of the human lung has revealed a large population of T_{RM} cells among influenza-specific cells [117, 386]. Similar to mice, these resident T cells have been reported to offer cross-strain protection making them an ideal target for vaccination [387]. Using the s.c. prime – i.n. boost immunization strategy, we analyzed the protection offered by thus generated T_{RM} cells in the setting of PLGA MS vaccination. Unfortunately, we were not able to observe a protection in $M1_{58-66}$-immunized AAD mice, regardless of whether they had been treated with the inhibitor or not (Figure 23). It is not surprising that FTY720-treated mice were not protected, as not even the combination of resident and circulating specific T cells was able to prevent high viral loads and IAV-induced death. Therefore, we decided to switch to the recombinant IAV strain. Although this system is slightly more artificial, we were able to induce antigen-specific protection via vaccination and study the protective effects of the local T_{RM} response. When mice were infected on day 6 post boost, we observed a significant difference

in viral loads as well as inhibition of bodyweight loss and death, in both groups of mice immunized with Ova-bearing PLGA MS (Figure 24). In accordance with the literature, we therefore concluded that T_{RM} cells were able to offer substantial protection from IAV infection. Unfortunately, this protection did not extend to later time points. When mice were infected on day 30 post boost, the differences between antigen-immunized mice and control groups were no longer significant even though a slight tendency could still be observed. It is interesting that the protection in the infectious setting declined much quicker than in our tumor model. This may be due to the absence of $CD4^+$ T cell help. A study in mice established that without the help from $CD4^+$ T cells, $CD8^+$ T_{RM} cells do not upregulate the typical residency markers CD103 and CD69 to the same extent. Moreover, the ability of unhelped $CD8^+$ T_{RM} cells to localize to the airway epithelium was significantly impaired [51]. In our tumor model mice were immunized with PLGA MS containing the whole protein ovalbumin. The tumor cell line was transduced with the whole cytosolic part of the protein. It can therefore be assumed that in our tumor model Ova-immunized mice also developed an immune response to $CD4^+$ epitopes, such as Ova $_{323 - 339}$, as well as a B cell response. The activation of $CD4^+$ T cells probably also induced antigen-specific $CD4^+$ T_{RM} cells that were able to support the $CD8^+$ T_{RM} in combating the tumor. In contrast, in our influenza model, even though mice were immunized with MS containing the whole protein (ovalbumin), the recombinant virus (insOva IAV) only expressed the $CD8^+$ T cell epitope SIINFEKL. Therefore, the Ova-specific $CD4^+$ T cells were not able to recognize their epitope on the virus and thus not able to help the $CD8^+$ T cells in combating the virus. These findings highlight the importance of including more than just one epitope in the PLGA MS. Moreover, our AAD mice were immunized with the short peptide $M1_{58-66}$. This peptide can be bound directly to MHC molecules on the surface rather than being processed first. Therefore, these short peptides also fail to activate $CD4^+$ T cells which might be another reason for the difficulties we observed with the AAD mice [249].

In addition to the importance of lung T_{RM} cells in preventing influenza infection, $CD8^+$ T_{RM} cells in the nasal mucosa have been found to be essential for limiting the spread of influenza virus to the lower respiratory tract [388]. This is important, as it prevents the development of severe cases of influenza disease. Interestingly, this study found that in addition to persisting much longer than lung T_{RM} cells, nasal T_{RM} cells did not require the presence of local antigen for their maintenance. We only looked at the immune response in the lung and airways, however considering that the boost was applied by administering the PLGA MS solution onto the nostrils and we were able to detect an induction of T_{RM} cells in the lung, we can assume that nasal T_{RM} cells were induced too. It would certainly be interesting to analyze the PLGA MS-induced specific response in the nasal mucosa, although this might be more challenging.

As previously mentioned, the decline in memory responses in the lung is most likely due to protective measures. Interestingly, a recent study observed that the reduction of lung $CD8^+$ T_{RM} cells following influenza infection was accompanied by an egress of $CD69^+CD103^+CD8^+$ T_{RM} cells to the draining mediastinal LNs [389]. In the LNs these cells retained typical markers of T_{RM} cells, maintained expression of granzyme B and did not equilibrate between parabiotic mice. The authors proposed that this “retrograde migration” provides longer-lived regional memory [389]. This might provide a mechanism to offer local memory protection without compromising the respiratory function of the lung. It would certainly be interesting to analyze the specific response in the LNs at a memory time point after PLGA MS immunization.

Even despite the fact that T_{RM} cell numbers and protection declined, immunization using PLGA MS still offers some great potential. One of the main challenges regarding vaccination against influenza viruses is the need for a yearly reformulation of the vaccine due to the high mutation rate of the epitopes recognized by the antibodies which are elicited by the currently employed influenza vaccines. This requires the prediction of the most likely circulating virus strains a few months before the start of the next influenza season. In the case of a mismatch between the vaccine and the circulating strain, the efficacy of the vaccine is considerably lower [1]. Since $CD8^+$ T cells have been shown to offer heterosubtypic protection from influenza virus and PLGA MS are able to induce a strong influenza-specific $CD8^+$ T cell response, this suggests that the same vaccine formulation could be used for a yearly boost immediately before the season, thus circumventing the problem of a potential vaccine – strain mismatch. Moreover, we have previously shown that several epitopes can be encapsulated into the same PLGA MS, further reducing the risk of a potential loss of vaccination efficacy due to antigenic drift of the influenza virus [321].

In light of the COVID-19 pandemic, the importance of vaccines and vaccination strategies that are able to protect from coronaviruses has gained much attention. Similar to influenza viruses, the cellular immune response is also very important for efficient protection from SARS-CoV-2 as antibodies alone are not able to get rid of cells already infected by the virus and thus require assistance by CTLs. Moreover, the antibody response to SARS-CoV-2 decays rapidly and is not as long-lived as the memory T cell response [104]. In addition, mutations acquired in the spike protein of SARS-CoV-2 often render antibodies less suitable to prevent infection. A strong T cell response against more conserved viral epitopes might nevertheless counteract severe infection even if new mutations arise, highlighting the need for vaccines that induce strong memory T cell responses. Similar to influenza, preclinical studies using SARS-CoV-1 have found an important role for T cells in controlling infection [94, 390]. In line with this, analysis of samples from SARS-CoV-2-infected individuals showed an inverse correlation of disease severity and the presence of memory $CD8^+$ T cells with a tissue-resident phenotype

in bronchoalveolar lavage fluids [391]. Furthermore, SARS-CoV-2-specific T_{RM} cells were detected in convalescent patients 10 months after infection [392].Together, these findings highlight the importance of resident cellular memory in controlling different respiratory viral infections and further reinforce the importance of developing vaccines that induce sustained T cell responses.

5.1.5. Conclusion

In this project we were able to show that a systemic prime followed by a local boost immunization with PLGA MS generated a strong and sustained resident memory $CD8^+$ T cell response in the lung. Importantly, the local memory response was able to protect mice from tumor growth in a tumor model as well as high viral loads and death in an infectious model. In accordance with our data, two other groups have found that T_{RM} can be induced after immunization with PLGA-based particles. Gola *et al.* showed that a heterologous prime-boost vaccination consisting of an i.m. prime with human adenovirus-5 expressing Ova followed by an i.v. boost with PLGA nanoparticles containing Ova generated liver antigen-specific $CD8^+$ T cells protected mice from liver-stage malaria disease [393]. A second study made use of PLGA-based cationic pathogen-like particles (PLPs) loaded with TLR agonists that were delivered intranasally. The authors found that this strategy induced $CD4^+$ and $CD8^+$ T_{RM} cells in the lungs of vaccinated mice [394].

Although vaccines have played an important role in modern medicine, there is still much room for improvement. For some devastating pathogens, such as HIV and TB, no (effective) vaccines exist to date [395, 396]. A growing body of literature is emphasizing the importance of the local immune response, especially that of T_{RM} cells. Data from HIV-positive patients found high frequencies of $CD8^+$ T_{RM} cells in individuals who naturally control the infection [120]. These findings indicate that new vaccines should place their focus on cellular responses along with humoral responses. Another major possibility for improvement is the route of administration. A number of recent studies have underlined the advantages of a mucosal immunization – alone or in combination with a systemic one. However, vaccines that are administered intranasally need to be deemed safe for this route of administration [365]. PLGA has been approved for mucosal routes and our results clearly show that in this preclinical study intranasal vaccination was feasible.

One of the few vaccines approved for mucosal administration in humans is the live attenuated influenza vaccine [365]. Although studies in mice have indicated that the intranasal administration of this vaccine induces lung T_{RM} cells, this vaccine cannot be used in immunocompromised individuals [304]. In contrast, PLGA MS encapsulating different viral peptides together with adjuvants pose no threat for immunocompromised individuals. In

addition to this advantage, PLGA MS do not require a cold-chain storage (as mRNA-based vaccines do), do not induce anti-vector immunity (as viral vector-based vaccines do) and could circumvent the need for frequent boost immunizations due to the depot effect created at the site of administration.

In conclusion, we further corroborate the use of PLGA MS as a potent vaccine delivery system. Based on our data and the ever-growing body of literature on T_{RM} cells, it would certainly be interesting to further study different aspects of the local T cell memory response. This could include the exact phenotype of the different populations of T_{RM} cells ($CD103^+$ vs $CD103^-$, airway vs interstitium), analysis of $CD4^+$ memory response, the T_{RM} response in draining LNs as well as the nasal mucosa and the possibility of increasing the persistence of T_{RM} cells via additional boost immunization or different PLGA MS.

5.2. Generation of PLGA MS bearing inactivated IAV

We have clearly shown that PLGA MS can be used successfully to immunize mice against IAV. However, to date, we have only immunized mice with MS encapsulating different peptide epitopes of IAV. The major disadvantage of this strategy is the failure to induce $CD4^+$ T cell as well as B cell responses that can support the $CD8^+$ T cell response. Additionally, an immune response against only one epitope is at a higher risk of immune escape through mutation of the virus. Moreover, whole inactivated virus is more immunogenic than purified proteins or peptides which require the addition of an adjuvant to induce an immune reaction [365]. To counter these disadvantages, we tried to encapsulate whole inactivated virus (WIV) into PLGA MS. Based on the literature we tested four different strategies for inactivation of the virus: heat, FA, BPL and UV irradiation. While heat inactivation is based on denaturing the proteins, the other three methods cause inactivation by targeting viral proteins or nucleic acids (in the case of influenza viruses: RNA). FA mostly induces cross-linking of proteins, BPL leads to an irreversible alkylation of the nucleic acid bases and UV radiation stimulates photodimer formation between nucleic acid bases [397]. These methods are also applied for vaccines currently in use: inactivated influenza virus vaccines are often based on influenza viruses inactivated with FA and the two SARS-CoV-2 vaccines by Sinovac and Sinopharm are both based on corona viruses inactivated with BPL [398, 399]. Our titration experiments showed that apart from the heat inactivation method, all strategies led to a strong inactivation of the virus (Figure 25). The disadvantages of the two methods involving the chemicals is that they had to be removed or strongly diluted due to their toxicity before we were able to encapsulate them in PLGA MS for *in vivo* use. In addition to this step being more time-consuming, it is likely, that some of the virus particles were lost in this purification step. The titration experiment we performed to check for remaining infectivity of the virus simply inferred that no infectious virus

remained but not how much of the initial virus was still present after inactivation and purification.

As a next step we characterized the release from the spray-dried particles over a period of 6 days. We observed that virus was only released during the first 24h with no further release during the next 5 days (Figure 26). This indicates that the viral particles are only adsorbed on the surface of the PLGA MS. One explanation for this observation could be that the viruses are simply too large to be encapsulated efficiently. IAVs are approximately 80-120nm in size, while PLGA microparticles are very heterogeneous in size and can vary from the nanometer range up to a few micrometers [1, 3]. It is possible that only the largest particles were able to encapsulate virus at all, while all the smaller particles were left empty or only encapsulated the adjuvant CpG. Moreover, when PLGA is hydrolyzed in aqueous solution, this creates small pores in the particles through which the encapsulated content can be released [400]. Most likely the pores created during the 6-day incubation period were not large enough for the viral particles to be released. This could possibly have been countered by analyzing the release once the particles had completely disintegrated, which is probably much later since the particles degrade within 30 days [265]. However, the major advantage of PLGA particles, namely the slow release over time and the depot effect, is surely lost in this case.

When viruses are inactivated using the methods described above, there is always the risk of the viral antigens being affected and changed too much to be recognized by the immune system [399]. FA in particular seems to induce alterations of the viral epitopes that can have unwanted effects on the efficacy of the vaccine [401, 402]. BPL seems to target mainly nucleic acids, however, amino acids can also be affected, especially when the experimental conditions are not optimized [397, 403]. Interestingly, on the SDS gels of our samples of protein release from the PLGA MS, active and inactivated virus were used as a control. A comparison of the samples of active virus to FA-inactivated virus shows a band that can be seen in the inactivated sample (approximately 80-90 kDa) which is not present in the active virus (Figure 26). This was always present in this type of sample (data not shown), indicating that this band is likely some cross-linked protein of the virus.

Nevertheless, we decided to analyze the immune response induced *in vivo* in response to immunization with these PLGA MS. First, we performed an intracellular cytokine staining to analyze whether any specific IFN-γ-producing cells had been generated (Figure 28, Figure 29). Our results showed that we were not able to detect a strong response for any of the epitopes analyzed. Since it was not clear which epitopes would be presented by APCs due to the inactivation step, we checked for several different ones. We also included DC2.4 cells that had been infected with IAV as a control, hoping to see whether these APCs, presenting all kinds of IAV epitopes, could stimulate any specific $CD8^+$ T cells. However, we saw no

responses for any of the epitopes in mice immunized with PLGA MS containing virus inactivated with either FA or BPL in both lung and spleen. There were some IFN-γ-producing $CD8^+$ T cells detectable in the lung, but not the spleen, of one mouse immunized with microparticles "containing" virus inactivated by UV irradiation. One possible explanation for this effect could be the fact that after UV irradiation small amounts of infectious virus were still present in quantities sufficient to induce a small response in this one mouse. Since the response did not extend to the spleen, it is also possible that the observed response was simply an artefact.

To check whether the PLGA MS were nevertheless capable of inducing a protective antiviral immune response in mice, we decided to infect immunized mice with IAV and monitor their bodyweight as a readout for protection (Figure 30). Our results showed no significant protection for any of the virus-immunized groups compared to empty mice, thus underscoring the lack of vaccine-induced immunity.

One possibility to improve the encapsulation of inactivated virus is to increase the amount of virus to be encapsulated. In the aforementioned experiments we aimed to encapsulate the same amount of virus in 5mg of PLGA MS (i.e. the amount one mouse receives for the s.c. prime) as we typically use for infection ($5x10^4$ PFU). Using a higher amount of virus might lead to more virus being encapsulated although it most likely would not circumvent the problem of the virus being too large to exit through the small pores. Possibly it would lead to more virus being adsorbed on the surface of the PLGA particles which might increase the observed immune response although it would not bring along the typical advantage of PLGA, the depot effect. Moreover, since inactivation of the virus with UV irradiation was not complete, a higher amount of encapsulated virus could potentially lead to an infection of the mice when they are immunized with the PLGA particles. For safety reasons, this method could obviously not be applied in humans, especially not in immunocompromised individuals.

Another way to improve encapsulation of the virus would be to split the virus into smaller units. When the first influenza vaccine was developed in the 1940s, it consisted of whole inactivated virus [1]. However, in the past decades the method of production has been improved in several ways, one of which is treating the whole virus with diethyl ether or detergent to disrupt the particles and create split vaccines. The organization and RNA of the virus are disrupted, but all of the viral proteins are still present [404]. This vaccine induces similar beneficial immune responses as the WIV, while being more tolerable [405]. It would certainly be interesting to investigate whether this method of production could improve the encapsulation and release efficacy. In fact, one study using PLGA MS-encapsulated IAV that had been disintegrated using Tween/ether treatment followed by inactivation of the virus using formalin, found that this vaccination strategy induced better antibody titers in mice than the fluid vaccine did [406].

Moreover, another study showed that administration of an H5N1 influenza split vaccine together with adjuvant-loaded PLGA microparticles improved immune responses compared to empty PLGA microparticles [407].

In summary, we were not able to induce protective immune responses with PLGA MS containing whole inactivated IAV which is most likely due to the virus not being encapsulated and/or released from the particles. Splitting the virus into smaller units and using higher amounts of virus might solve this issue, however it would be critical to find the optimal balance between inducing a strong immune response while preventing the overproduction of proinflammatory cytokines and lung immunopathology.

6. Abbreviations

AAD	HLA-A*0201 transgenic mice
ACT	Adoptive cell transfer
AMP	Adenosine monophosphate
APC	Allophycyanin
APCs	Antigen-presenting cells
APS	Ammonium persulfate
ATP	Adenosine triphosphate
BA	Bovine albumine
BAL	Bronchoalveolar lavage
BALF	Bronchoalveolar lavage fluid
Batf3	Basic leucine zipper ATF-like transcription factor 3
BCG	Bacillus Calmette–Guérin
BPL	B-propiolactone
BFA	Brefeldin A
Blimp-1	B-Lymphocyte-Induced maturation protein 1
BM	Bone marrow
BV	Brilliant Violet
CAR	Chimeric antigen receptor
CCR7	CC chemokine receptor type 7
CD	Cluster of Differentiation
cDCs	Conventional dendritic cells
CDH-1	Gene encoding E-cadherin (CD103)
CTL	Cytotoxic T lymphocytes
CMV	Cytomegalovirus
COVID-19	Coronavirus disease 2019
CTLA-4	cytotoxic T-lymphocyte-associated protein 4 (CD152)
DAMPs	Danger-associated molecular pattern
DCs	Dendritic cells
DCM	dichlormethane
DETC	Dendritic epidermal T cells
DMEM	Dulbecco’s modified Eagle medium
DMSO	Dimethyl sulfoxide
dNTPs	Deoxyribonucleotide triphosphate
dsRNA	Double-stranded RNA
EDTA	Ethylenediaminetetraacetic acid
Eomes	Eomesodermin

ER	Endoplasmic reticulum
FA	Formaldehyde
FABP4	Fatty acid binding protein 4
FACS	Fluorescence-activated cell sorting
FCS	Fetal calf serum
FDA	U.S. Food and Drug administration
FVS	Fixable viability stain
FRT	Female reproductive tract
GA	Glycolic acid
GFP	Green fluorescent protein
GMP	Good manufacturing practice
GM-CSF	Granulocyte-macrophage colony-stimulating factor
GvHD	Graft-versus-host-disease
HA	Hemagglutinin (protein of IAV)
HBV	Hepatitis B virus
HCV	Hepatitis C virus
HDM	House dust mite
HEK	Human embryonic kidney cells
HIV	Human immunodeficiency virus
HLA	Human leukocyte antigen
HPV	Human papillomavirus
HSV	Herpes simplex virus
Hobit	Homolog of Blimp-1 in T cells
IAV	Influenza A virus
iBALT	inducible bronchus-associated lymphoid tissues
IBV	Influenza B virus
IBD	Inflammatory bowel disease
ICB	Immune checkpoint blockade
ICS	Intracellular cytokine staining
IFN- γ	Interferon-γ
IIV	Inactivated influenza vaccine
IL	Interleukin
ILC	Innate lymphoid cell
i.m.	intramuscular
IMDM	Iscove's modified Dulbecco's medium
i.n.	intranasal
IRES	internal ribosome entry site
ITGA4	Integrin alpha-4 (CD49)
ITGAE	Integrin alpha-E (CD103)

IVIS	*In vivo* imaging system
KLF2	Krüppel-like factor 2
KLRG1	Killer cell lectin-like receptor subfamily G member 1
LA	Lactic acid
LAG3	Lymphocyte-activation gene 3 (CD223)
LAIV	Live-attenuated influenza vaccine
LB	Lysogeny broth
LCMV	Lymphocytic choriomeningitis virus
LFA-1	lymphocyte function-associated antigen-1
LN	Lymph node
M1	Matrix protein of IAV
M2	Membrane protein of IAV
mAb	Monoclonal antibody
MDCK	Madin-Darby canine kidney cells
MDSC	Myeloid-derived suppressor cell
MEM	Minimum essential medium
MHC	Major histocompatibility complex
MLD_{50}	50% mouse lethal dose
MOI	Multiplicity of infection
MPECs	Memory precursor effector cells
MS	Microspheres
NA	Neuraminidase
NEP	Nuclear export protein
NK cells	Natural killer cells
NLT	Non-lymphoid tissues
NP	Nucleoprotein
Nr4a1	nuclear receptor subfamily 4 group A member 1
NS1	Non-structural protein 1
NSCLC	Non-small-cell lung carcinoma
o/n	overnight
OD_{600nm}	Optical density at 600 nm
ODN	Oligodeoxynucleotides
Ova	Ovalbumin
PA	Polymerase acidic protein
PAMPs	Pathogen-associated molecular patterns
PAP	Prostatic acid phosphatase
PB1	polymerase basic protein 1
PB2	polymerase basic protein 2
PBMC	peripheral blood mononuclear cell

PBS	Phosphate buffered saline
PCR	Polymerase chain reaction
pDC	Plasmacytoid dendritic cell
PD-1	Programmed cell death protein 1 (CD279)
PD-L1	Programmed cell death protein ligand 1
PE	Phycoerythrin
PEI	Polyethylenimine
PFA	Paraformaldehyde
PFU	Plaque forming units
PLA	Polylactic acid
PLGA	poly(lactic-*co*-glycolic acid)
PMA	Phorbol myristate acetate
PR8	Influenza virus strain A/Puerto Rico/8/1934
PRR	Pathogen-recognition receptor
RAMDs	Repair-associated memory depots
RB1	Influenza virus strain A/Regensburg/D6/09
RIG-I	retinoic acid-inducible gene I
RSV	Respiratory syncytial virus
RT	Room temperature
Runx3	Runt-related transcription factor 3
S1PR1	Sphingosine-1-phosphate receptor 1
SARS	severe acute respiratory syndrome
SARS-CoV-2	severe acute respiratory syndrome coronavirus type 2
s.c.	subcutaneous
SD	Standard deviation
SDS	Sodium dodecyl sulfate
SEM	Scanning electron microscopy
SLECs	Short-lived effector cells
SLO	Secondary lymphoid organ
SPF	Specific-pathogen-free
ssRNA	Single-stranded RNA
TAA	Tumor-associated antigen
TAE	Tris-acetate-EDTA
TAM	Tumor-associated macrophages
TAP	Transporter associated with antigen processing
T_{CM}	Central memory T cells
T_{EFF}	Effector T cells
T_{EM}	Effector memory T cells
TEMED	Tetramethylethylenediamine

T_{FH}	Follicular T helper cells
T_{PM}	Peripheral memory T cells
Tregs	Regulatory T cells
T_{RM}	Tissue-resident memory T cells
T_{SCM}	Stem cell-like memory T cells
TB	Tuberculosis
TCR	T cell receptor
TGF-β	Transforming growth factor β
TIL	Tumor infiltrating lymphocyte
TIM-3	T-cell immunoglobulin and mucin-domain containing-3
TLR	Toll-like receptor
TME	Tumor microenvironment
TNF	Tumour necrosis factor
VCAM-1	vascular cell adhesion molecule 1
VLA-1	Very late antigen 1 (CD49a)
VZV	Varicella-zoster virus
w/o	without
WIV	Whole inactivated virus
WT	Wild-type

7. References

1. Krammer, F., et al., *Influenza.* Nat Rev Dis Primers, 2018. **4**(1): p. 3.
2. Kok, L., D. Masopust, and T.N. Schumacher, *The precursors of CD8+ tissue resident memory T cells: from lymphoid organs to infected tissues.* Nature Reviews Immunology, 2021.
3. Koerner, J., D. Horvath, and M. Groettrup, *Harnessing Dendritic Cells for Poly (D,L-lactide-co-glycolide) Microspheres (PLGA MS)-Mediated Anti-tumor Therapy.* Front Immunol, 2019. **10**: p. 707.
4. Behr, F.M., et al., *Armed and Ready: Transcriptional Regulation of Tissue-Resident Memory CD8 T Cells.* Frontiers in Immunology, 2018. **9**(1770).
5. Banchereau, J. and R.M. Steinman, *Dendritic cells and the control of immunity.* Nature, 1998. **392**(6673): p. 245-52.
6. Guilliams, M., et al., *Unsupervised High-Dimensional Analysis Aligns Dendritic Cells across Tissues and Species.* Immunity, 2016. **45**(3): p. 669-684.
7. Eisenbarth, S.C., *Dendritic cell subsets in T cell programming: location dictates function.* Nature Reviews Immunology, 2019. **19**(2): p. 89-103.
8. Swiecki, M. and M. Colonna, *The multifaceted biology of plasmacytoid dendritic cells.* Nat Rev Immunol, 2015. **15**(8): p. 471-85.
9. Kumar, H., T. Kawai, and S. Akira, *Pathogen Recognition by the Innate Immune System.* International Reviews of Immunology, 2011. **30**(1): p. 16-34.
10. Joffre, O.P., et al., *Cross-presentation by dendritic cells.* Nature Reviews Immunology, 2012. **12**(8): p. 557-569.
11. Embgenbroich, M. and S. Burgdorf, *Current Concepts of Antigen Cross-Presentation.* Frontiers in Immunology, 2018. **9**(1643).
12. Guermonprez, P., et al., *Antigen presentation and T cell stimulation by dendritic cells.* Annu Rev Immunol, 2002. **20**: p. 621-67.
13. Gourley, T.S., et al., *Generation and maintenance of immunological memory.* Semin Immunol, 2004. **16**(5): p. 323-33.
14. Kaech, S.M. and E.J. Wherry, *Heterogeneity and cell-fate decisions in effector and memory CD8+ T cell differentiation during viral infection.* Immunity, 2007. **27**(3): p. 393-405.
15. Sallusto, F., et al., *Two subsets of memory T lymphocytes with distinct homing potentials and effector functions.* Nature, 1999. **401**(6754): p. 708-12.
16. Kim, S.-K., K.S. Schluns, and L. Lefrançois, *Induction and Visualization of Mucosal Memory CD8 T Cells Following Systemic Virus Infection.* The Journal of Immunology, 1999. **163**(8): p. 4125.
17. Reinhardt, R.L., et al., *Visualizing the generation of memory CD4 T cells in the whole body.* Nature, 2001. **410**(6824): p. 101-5.
18. Masopust, D., et al., *Preferential localization of effector memory cells in nonlymphoid tissue.* Science, 2001. **291**(5512): p. 2413-7.
19. Hogan, R.J., et al., *Activated antigen-specific CD8+ T cells persist in the lungs following recovery from respiratory virus infections.* J Immunol, 2001. **166**(3): p. 1813-22.
20. Wiley, J.A., et al., *Antigen-Specific CD8+ T Cells Persist in the Upper Respiratory Tract Following Influenza Virus Infection.* The Journal of Immunology, 2001. **167**(6): p. 3293.
21. Woodland, D.L. and J.E. Kohlmeier, *Migration, maintenance and recall of memory T cells in peripheral tissues.* Nat Rev Immunol, 2009. **9**(3): p. 153-61.

22. Wherry, E.J., et al., *Lineage relationship and protective immunity of memory CD8 T cell subsets.* Nature Immunology, 2003. **4**(3): p. 225-234.
23. Bachmann, M.F., et al., *Functional Properties and Lineage Relationship of CD8+ T Cell Subsets Identified by Expression of IL-7 Receptor α and CD62L.* The Journal of Immunology, 2005. **175**(7): p. 4686-4696.
24. Martin, M.D. and V.P. Badovinac, *Defining Memory CD8 T Cell.* Frontiers in Immunology, 2018. **9**(2692).
25. Klonowski, K.D., et al., *Dynamics of blood-borne CD8 memory T cell migration in vivo.* Immunity, 2004. **20**(5): p. 551-62.
26. Gebhardt, T., et al., *Memory T cells in nonlymphoid tissue that provide enhanced local immunity during infection with herpes simplex virus.* Nat Immunol, 2009. **10**(5): p. 524-30.
27. Masopust, D., et al., *Dynamic T cell migration program provides resident memory within intestinal epithelium.* J Exp Med, 2010. **207**(3): p. 553-64.
28. Schenkel, J.M. and D. Masopust, *Tissue-resident memory T cells.* Immunity, 2014. **41**(6): p. 886-97.
29. Gerlach, C., et al., *The Chemokine Receptor CX3CR1 Defines Three Antigen-Experienced CD8 T Cell Subsets with Distinct Roles in Immune Surveillance and Homeostasis.* Immunity, 2016. **45**(6): p. 1270-1284.
30. Szabo, P.A., M. Miron, and D.L. Farber, *Location, location, location: Tissue resident memory T cells in mice and humans.* Science immunology, 2019. **4**(34): p. eaas9673.
31. Sathaliyawala, T., et al., *Distribution and Compartmentalization of Human Circulating and Tissue-Resident Memory T Cell Subsets.* Immunity, 2013. **38**(1): p. 187-197.
32. Gattinoni, L., et al., *T memory stem cells in health and disease.* Nature Medicine, 2017. **23**(1): p. 18-27.
33. Schenkel, J.M., K.A. Fraser, and D. Masopust, *Cutting edge: resident memory CD8 T cells occupy frontline niches in secondary lymphoid organs.* J Immunol, 2014. **192**(7): p. 2961-4.
34. Wakim, L.M., et al., *Dendritic Cell–Induced Memory T Cell Activation in Nonlymphoid Tissues.* Science, 2008. **319**: p. 198-202.
35. Wakim, L.M., A. Woodward-Davis, and M.J. Bevan, *Memory T cells persisting within the brain after local infection show functional adaptations to their tissue of residence.* Proc Natl Acad Sci U S A, 2010. **107**(42): p. 17872-9.
36. Anderson, K.G., et al., *Cutting edge: intravascular staining redefines lung CD8 T cell responses.* J Immunol, 2012. **189**(6): p. 2702-6.
37. Jiang, X., et al., *Skin infection generates non-migratory memory CD8+ T(RM) cells providing global skin immunity.* Nature, 2012. **483**(7388): p. 227-31.
38. Fernandez-Ruiz, D., et al., *Liver-Resident Memory CD8(+) T Cells Form a Front-Line Defense against Malaria Liver-Stage Infection.* Immunity, 2016. **45**(4): p. 889-902.
39. Beura, L.K., et al., *T Cells in Nonlymphoid Tissues Give Rise to Lymph-Node-Resident Memory T Cells.* Immunity, 2018. **48**(2): p. 327-338 e5.
40. Bankovich, A.J., L.R. Shiow, and J.G. Cyster, *CD69 suppresses sphingosine 1-phosophate receptor-1 (S1P1) function through interaction with membrane helix 4.* The Journal of biological chemistry, 2010. **285**(29): p. 22328-22337.
41. El-Asady, R., et al., *TGFbeta-dependent CD103 expression by CD8(+) T cells promotes selective destruction of the host intestinal epithelium during graft-versus-host disease.* The Journal of experimental medicine, 2005. **201**(10): p. 1647-1657.

42. Mackay, L.K., et al., *The developmental pathway for CD103(+)CD8+ tissue-resident memory T cells of skin.* Nat Immunol, 2013. **14**(12): p. 1294-301.
43. Kumar, B.V., et al., *Human Tissue-Resident Memory T Cells Are Defined by Core Transcriptional and Functional Signatures in Lymphoid and Mucosal Sites.* Cell Rep, 2017. **20**(12): p. 2921-2934.
44. Ray, S.J., et al., *The collagen binding alpha1beta1 integrin VLA-1 regulates CD8 T cell-mediated immune protection against heterologous influenza infection.* Immunity, 2004. **20**(2): p. 167-79.
45. Pan, Y., et al., *Survival of tissue-resident memory T cells requires exogenous lipid uptake and metabolism.* Nature, 2017. **543**(7644): p. 252-256.
46. Hombrink, P., et al., *Programs for the persistence, vigilance and control of human CD8+ lung-resident memory T cells.* Nature Immunology, 2016. **17**(12): p. 1467-1478.
47. Mackay, L.K., et al., *Hobit and Blimp1 instruct a universal transcriptional program of tissue residency in lymphocytes.* Science, 2016. **352**(6284): p. 459-463.
48. Behr, F.M., et al., *Blimp-1 Rather Than Hobit Drives the Formation of Tissue-Resident Memory CD8+ T Cells in the Lungs.* Frontiers in Immunology, 2019. **10**(400).
49. Milner, J.J., et al., *Runx3 programs CD8+ T cell residency in non-lymphoid tissues and tumours.* Nature, 2017. **552**(7684): p. 253-257.
50. Mackay, L.K., et al., *T-box Transcription Factors Combine with the Cytokines TGF-beta and IL-15 to Control Tissue-Resident Memory T Cell Fate.* Immunity, 2015. **43**(6): p. 1101-11.
51. Laidlaw, B.J., et al., *CD4+ T cell help guides formation of CD103+ lung-resident memory CD8+ T cells during influenza viral infection.* Immunity, 2014. **41**(4): p. 633-45.
52. Bai, A., et al., *Kruppel-like factor 2 controls T cell trafficking by activating L-selectin (CD62L) and sphingosine-1-phosphate receptor 1 transcription.* J Immunol, 2007. **178**(12): p. 7632-9.
53. Skon, C.N., et al., *Transcriptional downregulation of S1pr1 is required for the establishment of resident memory CD8+ T cells.* Nat Immunol, 2013. **14**(12): p. 1285-93.
54. Masopust, D. and A.G. Soerens, *Tissue-Resident T Cells and Other Resident Leukocytes.* Annu Rev Immunol, 2019. **37**: p. 521-546.
55. Milner, J.J., et al., *Heterogenous Populations of Tissue-Resident CD8(+) T Cells Are Generated in Response to Infection and Malignancy.* Immunity, 2020. **52**(5): p. 808-824.e7.
56. Omilusik, K.D. and A.W. Goldrath, *Remembering to remember: T cell memory maintenance and plasticity.* Curr Opin Immunol, 2019. **58**: p. 89-97.
57. Mora-Buch, R. and S.K. Bromley, *Discipline in Stages: Regulating CD8+ Resident Memory T Cells.* Frontiers in Immunology, 2021. **11**(3942).
58. Christo, S.N., et al., *Discrete tissue microenvironments instruct diversity in resident memory T cell function and plasticity.* Nature Immunology, 2021. **22**(9): p. 1140-1151.
59. Chen, Y., et al., *Single-Cell Transcriptomics Reveals Core Regulatory Programs That Determine the Heterogeneity of Circulating and Tissue-Resident Memory CD8(+) T Cells.* Cells, 2021. **10**(8).
60. Qiu, Z., T.H. Chu, and B.S. Sheridan, *TGF-β: Many Paths to CD103(+) CD8 T Cell Residency.* Cells, 2021. **10**(5).

61. Schenkel, J.M., et al., *T cell memory. Resident memory CD8 T cells trigger protective innate and adaptive immune responses.* Science (New York, N.Y.), 2014. **346**(6205): p. 98-101.
62. Schenkel, J.M., et al., *Sensing and alarm function of resident memory CD8(+) T cells.* Nat Immunol, 2013. **14**(5): p. 509-13.
63. Ariotti, S., et al., *T cell memory. Skin-resident memory CD8 + T cells trigger a state of tissue-wide pathogen alert.* Science, 2014. **346**(6205): p. 101-5.
64. Ariotti, S., et al., *Tissue-resident memory CD8+ T cells continuously patrol skin epithelia to quickly recognize local antigen.* Proc Natl Acad Sci U S A, 2012. **109**(48): p. 19739-44.
65. Beura, L.K., et al., *Intravital mucosal imaging of CD8(+) resident memory T cells shows tissue-autonomous recall responses that amplify secondary memory.* Nat Immunol, 2018. **19**(2): p. 173-182.
66. Park, S.L., et al., *Local proliferation maintains a stable pool of tissue-resident memory T cells after antiviral recall responses.* Nat Immunol, 2018. **19**(2): p. 183-191.
67. Fonseca, R., et al., *Developmental plasticity allows outside-in immune responses by resident memory T cells.* Nat Immunol, 2020. **21**(4): p. 412-421.
68. Smith-Garvin, J.E., et al., *T-cell receptor signals direct the composition and function of the memory CD8+ T-cell pool.* Blood, 2010. **116**(25): p. 5548-59.
69. Rosato, P.C., et al., *Integrating resident memory into T cell differentiation models.* Current Opinion in Immunology, 2020. **63**: p. 35-42.
70. Joshi, N.S., et al., *Inflammation directs memory precursor and short-lived effector CD8(+) T cell fates via the graded expression of T-bet transcription factor.* Immunity, 2007. **27**(2): p. 281-95.
71. Kaech, S.M., et al., *Selective expression of the interleukin 7 receptor identifies effector CD8 T cells that give rise to long-lived memory cells.* Nat Immunol, 2003. **4**(12): p. 1191-8.
72. Sheridan, B.S., et al., *Oral infection drives a distinct population of intestinal resident memory CD8(+) T cells with enhanced protective function.* Immunity, 2014. **40**(5): p. 747-57.
73. Stemberger, C., et al., *A Single Naive CD8+ T Cell Precursor Can Develop into Diverse Effector and Memory Subsets.* Immunity, 2007. **27**(6): p. 985-997.
74. Gerlach, C., et al., *One naive T cell, multiple fates in CD8+ T cell differentiation.* J Exp Med, 2010. **207**(6): p. 1235-46.
75. Gaide, O., et al., *Common clonal origin of central and resident memory T cells following skin immunization.* Nat Med, 2015. **21**(6): p. 647-53.
76. Kurd, N.S., et al., *Early precursors and molecular determinants of tissue-resident memory CD8(+) T lymphocytes revealed by single-cell RNA sequencing.* Sci Immunol, 2020. **5**(47).
77. Kok, L., et al., *A committed tissue-resident memory T cell precursor within the circulating CD8+ effector T cell pool.* J Exp Med, 2020. **217**(10).
78. Richmond, J.M., et al., *Antibody blockade of IL-15 signaling has the potential to durably reverse vitiligo.* Sci Transl Med, 2018. **10**(450).
79. Muschaweckh, A., et al., *Antigen-dependent competition shapes the local repertoire of tissue-resident memory CD8+ T cells.* Journal of Experimental Medicine, 2016. **213**(13): p. 3075-3086.
80. Wakim, L.M., et al., *Antibody-targeted vaccination to lung dendritic cells generates tissue-resident memory CD8 T cells that are highly protective against influenza virus infection.* Mucosal Immunol, 2015. **8**(5): p. 1060-71.

81. Khan, T.N., et al., *Local antigen in nonlymphoid tissue promotes resident memory CD8+ T cell formation during viral infection.* J Exp Med, 2016. **213**(6): p. 951-66.
82. Lauron, E.J., et al., *Viral MHCI inhibition evades tissue-resident memory T cell formation and responses.* Journal of Experimental Medicine, 2018. **216**(1): p. 117-132.
83. McMaster, S.R., et al., *Pulmonary antigen encounter regulates the establishment of tissue-resident CD8 memory T cells in the lung airways and parenchyma.* Mucosal Immunol, 2018. **11**: p. 1071–1078.
84. Adachi, T., et al., *Hair follicle-derived IL-7 and IL-15 mediate skin-resident memory T cell homeostasis and lymphoma.* Nat Med, 2015. **21**(11): p. 1272-9.
85. McGill, J., N. Van Rooijen, and K.L. Legge, *IL-15 trans-presentation by pulmonary dendritic cells promotes effector CD8 T cell survival during influenza virus infection.* The Journal of experimental medicine, 2010. **207**(3): p. 521-534.
86. Hirai, T., et al., *Keratinocyte-Mediated Activation of the Cytokine TGF-β Maintains Skin Recirculating Memory CD8(+) T Cells.* Immunity, 2019. **50**(5): p. 1249-1261.e5.
87. Mohammed, J., et al., *Stromal cells control the epithelial residence of DCs and memory T cells by regulated activation of TGF-β.* Nat Immunol, 2016. **17**(4): p. 414-21.
88. Iborra, S., et al., *Optimal Generation of Tissue-Resident but Not Circulating Memory T Cells during Viral Infection Requires Crosspriming by DNGR-1(+) Dendritic Cells.* Immunity, 2016. **45**(4): p. 847-860.
89. Kim, T.S., et al., *Distinct dendritic cell subsets dictate the fate decision between effector and memory CD8(+) T cell differentiation by a CD24-dependent mechanism.* Immunity, 2014. **40**(3): p. 400-13.
90. Mani, V., et al., *Migratory DCs activate TGF-β to precondition naïve CD8(+) T cells for tissue-resident memory fate.* Science, 2019. **366**(6462).
91. Takamura, S., *Persistence in Temporary Lung Niches: A Survival Strategy of Lung-Resident Memory CD8+ T Cells.* Viral Immunology, 2017. **30**(6): p. 438-450.
92. McMaster, S.R., et al., *Airway-Resident Memory CD8 T Cells Provide Antigen-Specific Protection against Respiratory Virus Challenge through Rapid IFN-gamma Production.* J Immunol, 2015. **195**(1): p. 203-9.
93. Jozwik, A., et al., *RSV-specific airway resident memory CD8+ T cells and differential disease severity after experimental human infection.* Nat Commun, 2015. **6**: p. 10224.
94. Zhao, J., et al., *Airway Memory CD4(+) T Cells Mediate Protective Immunity against Emerging Respiratory Coronaviruses.* Immunity, 2016. **44**(6): p. 1379-91.
95. Gilchuk, P., et al., *A Distinct Lung-Interstitium-Resident Memory CD8(+) T Cell Subset Confers Enhanced Protection to Lower Respiratory Tract Infection.* Cell Rep, 2016. **16**(7): p. 1800-9.
96. Wu, T., et al., *Lung-resident memory CD8 T cells (TRM) are indispensable for optimal crossprotection against pulmonary virus infection.* J Leukoc Biol, 2014. **95**: p. 215-24.
97. Mackay, L.K., et al., *Long-lived epithelial immunity by tissue-resident memory T (TRM) cells in the absence of persisting local antigen presentation.* Proc Natl Acad Sci U S A, 2012. **109**(18): p. 7037-7042.

98. Shin, H. and A. Iwasaki, *A vaccine strategy that protects against genital herpes by establishing local memory T cells.* Nature, 2012. **491**.
99. Takamura, S., et al., *Specific niches for lung-resident memory CD8+ T cells at the site of tissue regeneration enable CD69-independent maintenance.* J Exp Med, 2016. **213**(13): p. 3057-3073.
100. Zaid, A., et al., *Persistence of skin-resident memory T cells within an epidermal niche.* Proc Natl Acad Sci U S A, 2014. **111**(14): p. 5307–5312.
101. Ely, K.H., et al., *Memory T Cell Populations in the Lung Airways Are Maintained by Continual Recruitment.* The Journal of Immunology, 2006. **176**(1): p. 537.
102. Moyron-Quiroz, J.E., et al., *Role of inducible bronchus associated lymphoid tissue (iBALT) in respiratory immunity.* Nat Med, 2004. **10**(9): p. 927-34.
103. Takamura, S., *Niches for the Long-Term Maintenance of Tissue-Resident Memory T Cells.* Frontiers in Immunology, 2018. **9**(1214).
104. Qian, Y., et al., *Legend of the Sentinels: Development of Lung Resident Memory T Cells and Their Roles in Diseases.* Frontiers in Immunology, 2021. **11**(3769).
105. Hayward, S.L., et al., *Environmental cues regulate epigenetic reprogramming of airway-resident memory CD8(+) T cells.* Nat Immunol, 2020. **21**(3): p. 309-320.
106. Hogan, R.J., et al., *Long-Term Maintenance of Virus-Specific Effector Memory CD8+ T Cells in the Lung Airways Depends on Proliferation.* The Journal of Immunology, 2002. **169**(9): p. 4976.
107. Zammit, D.J., et al., *Residual antigen presentation after influenza virus infection affects CD8 T cell activation and migration.* Immunity, 2006. **24**(4): p. 439-49.
108. Wein, A.N., et al., *CXCR6 regulates localization of tissue-resident memory CD8 T cells to the airways.* J Exp Med, 2019. **216**(12): p. 2748-2762.
109. Day, C., et al., *The chemokine CXCL16 is highly and constitutively expressed by human bronchial epithelial cells.* Exp Lung Res, 2009. **35**(4): p. 272-83.
110. Takamura, S., et al., *Interstitial-resident memory CD8(+) T cells sustain frontline epithelial memory in the lung.* J Exp Med, 2019. **216**(12): p. 2736-2747.
111. Marceaux, C., et al., *Holding our breath: the promise of tissue-resident memory T cells in lung cancer.* Transl Lung Cancer Res, 2021. **10**: p. 819-2829.
112. Slütter, B., et al., *Dynamics of influenza-induced lung-resident memory T cells underlie waning heterosubtypic immunity.* Sci Immunol, 2017. **2**(7): p. eaag2031.
113. Muruganandah, V., et al., *A Systematic Review: The Role of Resident Memory T Cells in Infectious Diseases and Their Relevance for Vaccine Development.* Frontiers in Immunology, 2018. **9**(1574).
114. Clark, R.A., *Resident memory T cells in human health and disease.* Sci Transl Med, 2015. **7**(269): p. 269rv1.
115. Gebhardt, T. and L.K. Mackay, *Local immunity by tissue-resident CD8(+) memory T cells.* Frontiers in immunology, 2012. **3**: p. 340-340.
116. Gebhardt, T., et al., *Tissue-resident memory T cells in tissue homeostasis, persistent infection, and cancer surveillance.* Immunol Rev, 2018. **283**(1): p. 54-76.

117. Pizzolla, A., et al., *Influenza-specific lung-resident memory T cells are proliferative and polyfunctional and maintain diverse TCR profiles.* J Clin Invest, 2018. **128**(2): p. 721-733.
118. Zarnitsyna, V.I., et al., *Mathematical Model Reveals the Role of Memory CD8 T Cell Populations in Recall Responses to Influenza.* Frontiers in immunology, 2016. **7**: p. 165-165.
119. Kadoki, M., et al., *Organism-Level Analysis of Vaccination Reveals Networks of Protection across Tissues.* Cell, 2017. **171**(2): p. 398-413.e21.
120. Kiniry, B.E., et al., *Detection of HIV-1-specific gastrointestinal tissue resident CD8(+) T-cells in chronic infection.* Mucosal Immunol, 2018. **11**(3): p. 909-920.
121. Wilk, M.M., et al., *Lung CD4 Tissue-Resident Memory T Cells Mediate Adaptive Immunity Induced by Previous Infection of Mice with Bordetella pertussis.* The Journal of Immunology, 2017. **199**(1): p. 233.
122. Haddadi, S., et al., *Expression and role of VLA-1 in resident memory CD8 T cell responses to respiratory mucosal viral-vectored immunization against tuberculosis.* Scientific Reports, 2017. **7**(1): p. 9525.
123. Jeyanathan, M., A. Heriazon, and Z. Xing, *Airway luminal T cells: a newcomer on the stage of TB vaccination strategies.* Trends Immunol, 2010. **31**(7): p. 247-52.
124. Santosuosso, M., et al., *Mechanisms of mucosal and parenteral tuberculosis vaccinations: adenoviral-based mucosal immunization preferentially elicits sustained accumulation of immune protective CD4 and CD8 T cells within the airway lumen.* J Immunol, 2005. **174**(12): p. 7986-94.
125. Wang, J., et al., *Single mucosal, but not parenteral, immunization with recombinant adenoviral-based vaccine provides potent protection from pulmonary tuberculosis.* J Immunol, 2004. **173**(10): p. 6357-65.
126. Connor, L.M., et al., *A key role for lung-resident memory lymphocytes in protective immune responses after BCG vaccination.* Eur J Immunol, 2010. **40**(9): p. 2482-92.
127. Perdomo, C., et al., *Mucosal BCG Vaccination Induces Protective Lung-Resident Memory T Cell Populations against Tuberculosis.* mBio, 2016. **7**(6).
128. Hu, Z., et al., *Sendai Virus Mucosal Vaccination Establishes Lung-Resident Memory CD8 T Cell Immunity and Boosts BCG-Primed Protection against TB in Mice.* Mol Ther, 2017. **25**(5): p. 1222-1233.
129. Moliva, J.I., J. Turner, and J.B. Torrelles, *Immune Responses to Bacillus Calmette-Guérin Vaccination: Why Do They Fail to Protect against Mycobacterium tuberculosis?* Front Immunol, 2017. **8**: p. 407.
130. Pichyangkul, S., et al., *Chemoprophylaxis with sporozoite immunization in P. knowlesi rhesus monkeys confers protection and elicits sporozoite-specific memory T cells in the liver.* PLOS ONE, 2017. **12**(2): p. e0171826.
131. Glennie, N.D., S.W. Volk, and P. Scott, *Skin-resident CD4+ T cells protect against Leishmania major by recruiting and activating inflammatory monocytes.* PLOS Pathogens, 2017. **13**(4): p. e1006349.
132. Glennie, N.D., et al., *Skin-resident memory CD4+ T cells enhance protection against Leishmania major infection.* J Exp Med, 2015. **212**(9): p. 1405-14.
133. Rodrigues, A., et al., *Leishmania infantum antigens modulate memory cell subsets of liver resident T lymphocyte.* Immunobiology, 2017. **222**(2): p. 409-422.
134. Landrith, T.A., et al., *CD103(+) CD8 T Cells in the Toxoplasma-Infected Brain Exhibit a Tissue-Resident Memory Transcriptional Profile.* Front Immunol, 2017. **8**: p. 335.

135. Han, S.J., et al., *White Adipose Tissue Is a Reservoir for Memory T Cells and Promotes Protective Memory Responses to Infection.* Immunity, 2017. **47**(6): p. 1154-1168.e6.
136. Boddupalli, C.S., et al., *Interlesional diversity of T cell receptors in melanoma with immune checkpoints enriched in tissue-resident memory T cells.* JCI Insight, 2016. **1**(21): p. e88955.
137. Edwards, J., et al., *CD103(+) Tumor-Resident CD8(+) T Cells Are Associated with Improved Survival in Immunotherapy-Naive Melanoma Patients and Expand Significantly During Anti-PD-1 Treatment.* Clin Cancer Res, 2018. **24**(13): p. 3036-3045.
138. Salerno, E.P., et al., *T cells in the human metastatic melanoma microenvironment express site-specific homing receptors and retention integrins.* Int J Cancer, 2014. **134**(3): p. 563-74.
139. Djenidi, F., et al., *CD8+CD103+ tumor-infiltrating lymphocytes are tumor-specific tissue-resident memory T cells and a prognostic factor for survival in lung cancer patients.* J Immunol, 2015. **194**(7): p. 3475-86.
140. Ganesan, A.P., et al., *Tissue-resident memory features are linked to the magnitude of cytotoxic T cell responses in human lung cancer.* Nat Immunol, 2017. **18**(8): p. 940-950.
141. Wang, B., et al., *CD103+ Tumor Infiltrating Lymphocytes Predict a Favorable Prognosis in Urothelial Cell Carcinoma of the Bladder.* J Urol, 2015. **194**(2): p. 556-62.
142. Wang, Z.Q., et al., *CD103 and Intratumoral Immune Response in Breast Cancer.* Clin Cancer Res, 2016. **22**(24): p. 6290-6297.
143. Hartana, C.A., et al., *Tissue-resident memory T cells are epigenetically cytotoxic with signs of exhaustion in human urinary bladder cancer.* Clin Exp Immunol, 2018. **194**(1): p. 39-53.
144. Webb, J.R., et al., *Tumor-infiltrating lymphocytes expressing the tissue resident memory marker CD103 are associated with increased survival in high-grade serous ovarian cancer.* Clin Cancer Res, 2014. **20**(2): p. 434-44.
145. Webb, J.R., et al., *Profound elevation of CD8+ T cells expressing the intraepithelial lymphocyte marker CD103 (alphaE/beta7 Integrin) in high-grade serous ovarian cancer.* Gynecol Oncol, 2010. **118**(3): p. 228-36.
146. Bösmüller, H.C., et al., *Combined Immunoscore of CD103 and CD3 Identifies Long-Term Survivors in High-Grade Serous Ovarian Cancer.* Int J Gynecol Cancer, 2016. **26**(4): p. 671-9.
147. Komdeur, F.L., et al., *CD103+ tumor-infiltrating lymphocytes are tumor-reactive intraepithelial CD8+ T cells associated with prognostic benefit and therapy response in cervical cancer.* Oncoimmunology, 2017. **6**(9): p. e1338230.
148. Savas, P., et al., *Single-cell profiling of breast cancer T cells reveals a tissue-resident memory subset associated with improved prognosis.* Nat Med, 2018. **24**(7): p. 986-993.
149. Quinn, E., et al., *CD103+ intraepithelial lymphocytes--a unique population in microsatellite unstable sporadic colorectal cancer.* Eur J Cancer, 2003. **39**(4): p. 469-75.
150. Craig, D.J., et al., *Resident Memory T Cells and Their Effect on Cancer.* Vaccines (Basel), 2020. **8**(4).
151. Park, S.L., T. Gebhardt, and L.K. Mackay, *Tissue-Resident Memory T Cells in Cancer Immunosurveillance.* Trends Immunol, 2019. **40**(8): p. 735-747.

152. Malik, B.T., et al., *Resident memory T cells in the skin mediate durable immunity to melanoma.* Sci Immunol, 2017. **2**(10).
153. Park, S.L., et al., *Tissue-resident memory CD8(+) T cells promote melanoma-immune equilibrium in skin.* Nature, 2019. **565**(7739): p. 366-371.
154. Murray, T., et al., *Very Late Antigen-1 Marks Functional Tumor-Resident CD8 T Cells and Correlates with Survival of Melanoma Patients.* Front Immunol, 2016. **7**: p. 573.
155. Gálvez-Cancino, F., et al., *Vaccination-induced skin-resident memory CD8(+) T cells mediate strong protection against cutaneous melanoma.* Oncoimmunology, 2018. **7**(7): p. e1442163.
156. Nizard, M., et al., *Induction of resident memory T cells enhances the efficacy of cancer vaccine.* Nat Commun, 2017. **8**: p. 15221.
157. Cibrián, D. and F. Sánchez-Madrid, *CD69: from activation marker to metabolic gatekeeper.* Eur J Immunol, 2017. **47**(6): p. 946-953.
158. Labiano, S., et al., *CD69 is a direct HIF-1α target gene in hypoxia as a mechanism enhancing expression on tumor-infiltrating T lymphocytes.* Oncoimmunology, 2017. **6**(4): p. e1283468.
159. Le Floc'h, A., et al., *Alpha E beta 7 integrin interaction with E-cadherin promotes antitumor CTL activity by triggering lytic granule polarization and exocytosis.* J Exp Med, 2007. **204**(3): p. 559-70.
160. Thomas, D.A. and J. Massagué, *TGF-beta directly targets cytotoxic T cell functions during tumor evasion of immune surveillance.* Cancer Cell, 2005. **8**(5): p. 369-80.
161. Duhen, T., et al., *Co-expression of CD39 and CD103 identifies tumor-reactive CD8 T cells in human solid tumors.* Nature Communications, 2018. **9**(1): p. 2724.
162. Deaglio, S., et al., *Adenosine generation catalyzed by CD39 and CD73 expressed on regulatory T cells mediates immune suppression.* Journal of Experimental Medicine, 2007. **204**(6): p. 1257-1265.
163. Okła, K., D.L. Farber, and W. Zou, *Tissue-resident memory T cells in tumor immunity and immunotherapy.* J Exp Med, 2021. **218**(4).
164. Sharma, P. and J.P. Allison, *Immune checkpoint targeting in cancer therapy: toward combination strategies with curative potential.* Cell, 2015. **161**(2): p. 205-14.
165. Clarke, J., et al., *Single-cell transcriptomic analysis of tissue-resident memory T cells in human lung cancer.* Journal of Experimental Medicine, 2019. **216**(9): p. 2128-2149.
166. Enamorado, M., et al., *Enhanced anti-tumour immunity requires the interplay between resident and circulating memory CD8(+) T cells.* Nat Commun, 2017. **8**: p. 16073.
167. Tokura, Y., et al., *Pathophysiology of Skin Resident Memory T Cells.* Frontiers in Immunology, 2021. **11**(3789).
168. Ryan, G.E., J.E. Harris, and J.M. Richmond, *Resident Memory T Cells in Autoimmune Skin Diseases.* Frontiers in Immunology, 2021. **12**(1337).
169. Schunkert, E.M., P.N. Shah, and S.J. Divito, *Skin Resident Memory T Cells May Play Critical Role in Delayed-Type Drug Hypersensitivity Reactions.* Frontiers in Immunology, 2021. **12**(3410).
170. Cheuk, S., et al., *CD49a Expression Defines Tissue-Resident CD8(+) T Cells Poised for Cytotoxic Function in Human Skin.* Immunity, 2017. **46**(2): p. 287-300.

171. Kurihara, K., et al., *Significance of IL-17A-producing CD8+CD103+ skin resident memory T cells in psoriasis lesion and their possible relationship to clinical course.* Journal of Dermatological Science, 2019. **95**(1): p. 21-27.
172. Boniface, K., et al., *Vitiligo Skin Is Imprinted with Resident Memory CD8 T Cells Expressing CXCR3.* J Invest Dermatol, 2018. **138**(2): p. 355-364.
173. Zhou, M., et al., *JAK/STAT signaling controls the fate of CD8(+)CD103(+) tissue-resident memory T cell in lupus nephritis.* J Autoimmun, 2020. **109**: p. 102424.
174. Sibaud, V., et al., *Dermatologic complications of anti-PD-1/PD-L1 immune checkpoint antibodies.* Current Opinion in Oncology, 2016. **28**(4).
175. Freeman-Keller, M., et al., *Nivolumab in Resected and Unresectable Metastatic Melanoma: Characteristics of Immune-Related Adverse Events and Association with Outcomes.* Clin Cancer Res, 2016. **22**(4): p. 886-94.
176. Brunner, P.M., et al., *Nonlesional atopic dermatitis skin shares similar T-cell clones with lesional tissues.* Allergy, 2017. **72**(12): p. 2017-2025.
177. Divito, S.J., et al., *Peripheral host T cells survive hematopoietic stem cell transplantation and promote graft-versus-host disease.* The Journal of Clinical Investigation, 2020. **130**(9): p. 4624-4636.
178. Campbell, J.J., et al., *Sezary syndrome and mycosis fungoides arise from distinct T-cell subsets: a biologic rationale for their distinct clinical behaviors.* Blood, 2010. **116**(5): p. 767-71.
179. Clark, R.A., et al., *Skin effector memory T cells do not recirculate and provide immune protection in alemtuzumab-treated CTCL patients.* Sci Transl Med, 2012. **4**(117): p. 117ra7.
180. Watanabe, R., et al., *Human skin is protected by four functionally and phenotypically discrete populations of resident and recirculating memory T cells.* Sci Transl Med, 2015. **7**(279): p. 279ra39.
181. Rahimi, R.A., et al., *Distinct functions of tissue-resident and circulating memory Th2 cells in allergic airway disease.* J Exp Med, 2020. **217**(9).
182. Hondowicz, B.D., et al., *Interleukin-2-Dependent Allergen-Specific Tissue-Resident Memory Cells Drive Asthma.* Immunity, 2016. **44**(1): p. 155-166.
183. Turner, D.L., et al., *Biased Generation and In Situ Activation of Lung Tissue-Resident Memory CD4 T Cells in the Pathogenesis of Allergic Asthma.* J Immunol, 2018. **200**(5): p. 1561-1569.
184. Kleinschek, M.A., et al., *Circulating and gut-resident human Th17 cells express CD161 and promote intestinal inflammation.* J Exp Med, 2009. **206**(3): p. 525-34.
185. Zundler, S., et al., *Hobit- and Blimp-1-driven CD4(+) tissue-resident memory T cells control chronic intestinal inflammation.* Nat Immunol, 2019. **20**(3): p. 288-300.
186. Afeltra, A., et al., *Expression of CD69 antigen on synovial fluid T cells in patients with rheumatoid arthritis and other chronic synovitis.* Ann Rheum Dis, 1993. **52**(6): p. 457-60.
187. Sasaki, K., et al., *Relapsing–Remitting Central Nervous System Autoimmunity Mediated by GFAP-Specific CD8 T Cells.* The Journal of Immunology, 2014. **192**(7): p. 3029.
188. Kuric, E., et al., *Demonstration of Tissue Resident Memory CD8 T Cells in Insulitic Lesions in Adult Patients with Recent-Onset Type 1 Diabetes.* Am J Pathol, 2017. **187**(3): p. 581-588.
189. Snyder, M.E., et al., *Generation and persistence of human tissue-resident memory T cells in lung transplantation.* Sci Immunol, 2019. **4**(33).

190. Nguyen, Q.P., et al., *Origins of CD4+ circulating and tissue-resident memory T-cells.* Immunology, 2019. **157**(1): p. 3-12.
191. Iijima, N. and A. Iwasaki, *A local macrophage chemokine network sustains protective tissue-resident memory CD4 T cells.* Science, 2014. **346**(6205): p. 93-98.
192. Stary, G., et al., *A mucosal vaccine against Chlamydia trachomatis generates two waves of protective memory T cells.* Science, 2015. **348**(6241): p. aaa8205.
193. Park, C.O., et al., *Staged development of long-lived T-cell receptor αβ TH17 resident memory T-cell population to Candida albicans after skin infection.* Journal of Allergy and Clinical Immunology, 2018. **142**(2): p. 647-662.
194. Teijaro, J.R., et al., *Cutting edge: Tissue-retentive lung memory CD4 T cells mediate optimal protection to respiratory virus infection.* J Immunol, 2011. **187**(11): p. 5510-4.
195. Turner, D.L., et al., *Lung niches for the generation and maintenance of tissue-resident memory T cells.* Mucosal Immunol, 2014. **7**(3): p. 501-10.
196. Allen, A.C., et al., *Sustained protective immunity against Bordetella pertussis nasal colonization by intranasal immunization with a vaccine-adjuvant combination that induces IL-17-secreting TRM cells.* Mucosal Immunology, 2018. **11**(6): p. 1763-1776.
197. Hondowicz, B.D., et al., *IL-2 is required for the generation of viral-specific CD4+ Th1 tissue-resident memory cells and B cells are essential for maintenance in the lung.* European Journal of Immunology, 2018. **48**(1): p. 80-86.
198. Smith, N.M., et al., *Regionally compartmentalized resident memory T cells mediate naturally acquired protection against pneumococcal pneumonia.* Mucosal Immunology, 2018. **11**(1): p. 220-235.
199. Romagnoli, P.A., et al., *Differentiation of distinct long-lived memory CD4 T cells in intestinal tissues after oral Listeria monocytogenes infection.* Mucosal Immunology, 2017. **10**(2): p. 520-530.
200. Benoun, J.M., et al., *Optimal protection against Salmonella infection requires noncirculating memory.* Proceedings of the National Academy of Sciences, 2018. **115**(41): p. 10416-10421.
201. Siracusa, F., et al., *Nonfollicular reactivation of bone marrow resident memory CD4 T cells in immune clusters of the bone marrow.* Proceedings of the National Academy of Sciences, 2018. **115**(6): p. 1334-1339.
202. Sakai, S., et al., *Cutting Edge: Control of Mycobacterium tuberculosis Infection by a Subset of Lung Parenchyma–Homing CD4 T Cells.* The Journal of Immunology, 2014. **192**(7): p. 2965.
203. Iijima, N., et al., *Dendritic cells and B cells maximize mucosal Th1 memory response to herpes simplex virus.* Journal of Experimental Medicine, 2008. **205**(13): p. 3041-3052.
204. Feinen, B., et al., *Critical role of Th17 responses in a murine model of Neisseria gonorrhoeae genital infection.* Mucosal Immunology, 2010. **3**(3): p. 312-321.
205. Scurlock Amy, M., et al., *Interleukin-17 Contributes to Generation of Th1 Immunity and Neutrophil Recruitment during Chlamydia muridarum Genital Tract Infection but Is Not Required for Macrophage Influx or Normal Resolution of Infection.* Infection and Immunity, 2011. **79**(3): p. 1349-1362.

206. Hirahara, K., et al., *The Role of CD4(+) Resident Memory T Cells in Local Immunity in the Mucosal Tissue - Protection Versus Pathology.* Frontiers in immunology, 2021. **12**: p. 616309-616309.
207. Swarnalekha, N., et al., *T resident helper cells promote humoral responses in the lung.* Sci Immunol, 2021. **6**(55).
208. Son, Y.M., et al., *Tissue-resident CD4(+) T helper cells assist the development of protective respiratory B and CD8(+) T cell memory responses.* Sci Immunol, 2021. **6**(55).
209. Collins, N., et al., *Skin CD4 (+) memory T cells exhibit combined cluster-mediated retention and equilibration with the circulation. Nat Commun 7: 11514*. 2016.
210. Beura, L.K., et al., *CD4(+) resident memory T cells dominate immunosurveillance and orchestrate local recall responses.* J Exp Med, 2019. **216**(5): p. 1214-1229.
211. Turner, D.L., C.L. Gordon, and D.L. Farber, *Tissue-resident T cells, in situ immunity and transplantation.* Immunological Reviews, 2014. **258**(1): p. 150-166.
212. Gebhardt, T., et al., *Different patterns of peripheral migration by memory CD4+ and CD8+ T cells.* Nature, 2011. **477**(7363): p. 216-219.
213. Farber, D.L., N.A. Yudanin, and N.P. Restifo, *Human memory T cells: generation, compartmentalization and homeostasis.* Nat Rev Immunol, 2014. **14**(1): p. 24-35.
214. Ross, S.H. and D.A. Cantrell, *Signaling and Function of Interleukin-2 in T Lymphocytes.* Annu Rev Immunol, 2018. **36**: p. 411-433.
215. Chatzileontiadou, D.S.M., et al., *The Many Faces of CD4+ T Cells: Immunological and Structural Characteristics.* International Journal of Molecular Sciences, 2021. **22**(1).
216. Takahara, M., et al., *IL-7 promotes long-term in vitro survival of unique long-lived memory subset generated from mucosal effector memory CD4+ T cells in chronic colitis mice.* Immunology Letters, 2013. **156**(1): p. 82-93.
217. Boyman, O., et al., *Spontaneous Development of Psoriasis in a New Animal Model Shows an Essential Role for Resident T Cells and Tumor Necrosis Factor-α.* Journal of Experimental Medicine, 2004. **199**(5): p. 731-736.
218. Owczarczyk Saczonek, A., et al., *Immunological Memory of Psoriatic Lesions.* Int J Mol Sci, 2020. **21**(2).
219. Waldman, A.D., J.M. Fritz, and M.J. Lenardo, *A guide to cancer immunotherapy: from T cell basic science to clinical practice.* Nature Reviews Immunology, 2020. **20**(11): p. 651-668.
220. Esfahani, K., et al., *A review of cancer immunotherapy: from the past, to the present, to the future.* Current oncology (Toronto, Ont.), 2020. **27**(Suppl 2): p. S87-S97.
221. Hegde, P.S. and D.S. Chen, *Top 10 Challenges in Cancer Immunotherapy.* Immunity, 2020. **52**(1): p. 17-35.
222. Matsushita, H., et al., *Cancer exome analysis reveals a T-cell-dependent mechanism of cancer immunoediting.* Nature, 2012. **482**(7385): p. 400-404.
223. Schreiber, R.D., L.J. Old, and M.J. Smyth, *Cancer immunoediting: integrating immunity's roles in cancer suppression and promotion.* Science, 2011. **331**(6024): p. 1565-70.
224. DuPage, M., et al., *Expression of tumour-specific antigens underlies cancer immunoediting.* Nature, 2012. **482**(7385): p. 405-9.

225. Finn, O.J., *The dawn of vaccines for cancer prevention.* Nature Reviews Immunology, 2018. **18**(3): p. 183-194.
226. Gabrilovich, D.I., *Myeloid-Derived Suppressor Cells.* Cancer Immunol Res, 2017. **5**(1): p. 3-8.
227. Gurusamy, D., et al., *Novel "Elements" of Immune Suppression within the Tumor Microenvironment.* Cancer Immunol Res, 2017. **5**(6): p. 426-433.
228. Tanaka, A. and S. Sakaguchi, *Regulatory T cells in cancer immunotherapy.* Cell Res, 2017. **27**(1): p. 109-118.
229. Quail, D.F. and J.A. Joyce, *Microenvironmental regulation of tumor progression and metastasis.* Nature Medicine, 2013. **19**(11): p. 1423-1437.
230. Baitsch, L., et al., *Exhaustion of tumor-specific CD8⁺ T cells in metastases from melanoma patients.* J Clin Invest, 2011. **121**(6): p. 2350-60.
231. Ahmadzadeh, M., et al., *Tumor antigen-specific CD8 T cells infiltrating the tumor express high levels of PD-1 and are functionally impaired.* Blood, 2009. **114**(8): p. 1537-1544.
232. Cha, J.H., et al., *New Approaches on Cancer Immunotherapy.* Cold Spring Harb Perspect Med, 2020. **10**(8).
233. Rosenberg, S.A., *IL-2: The First Effective Immunotherapy for Human Cancer.* The Journal of Immunology, 2014. **192**(12): p. 5451.
234. Rosenberg, S.A., *Interleukin 2 for patients with renal cancer.* Nature clinical practice. Oncology, 2007. **4**(9): p. 497-497.
235. Atkins, M.B., et al., *High-dose recombinant interleukin 2 therapy for patients with metastatic melanoma: analysis of 270 patients treated between 1985 and 1993.* J Clin Oncol, 1999. **17**(7): p. 2105-16.
236. Krummel, M.F. and J.P. Allison, *CD28 and CTLA-4 have opposing effects on the response of T cells to stimulation.* J Exp Med, 1995. **182**(2): p. 459-65.
237. Ishida, Y., et al., *Induced expression of PD-1, a novel member of the immunoglobulin gene superfamily, upon programmed cell death.* Embo j, 1992. **11**(11): p. 3887-95.
238. Freeman, G.J., et al., *Engagement of the PD-1 immunoinhibitory receptor by a novel B7 family member leads to negative regulation of lymphocyte activation.* J Exp Med, 2000. **192**(7): p. 1027-34.
239. Nishimura, H., et al., *Immunological studies on PD-1 deficient mice: implication of PD-1 as a negative regulator for B cell responses.* Int Immunol, 1998. **10**(10): p. 1563-72.
240. Nishimura, H., et al., *Development of lupus-like autoimmune diseases by disruption of the PD-1 gene encoding an ITIM motif-carrying immunoreceptor.* Immunity, 1999. **11**(2): p. 141-51.
241. Smyth, M.J. and M.W. Teng, *2018 Nobel Prize in physiology or medicine.* Clinical & translational immunology, 2018. **7**(10): p. e1041-e1041.
242. Wherry, E.J. and M. Kurachi, *Molecular and cellular insights into T cell exhaustion.* Nat Rev Immunol, 2015. **15**(8): p. 486-99.
243. Rosenberg, S.A. and N.P. Restifo, *Adoptive cell transfer as personalized immunotherapy for human cancer.* Science, 2015. **348**(6230): p. 62-8.
244. Huston, J.S., et al., *Protein engineering of antibody binding sites: recovery of specific activity in an anti-digoxin single-chain Fv analogue produced in Escherichia coli.* Proceedings of the National Academy of Sciences of the United States of America, 1988. **85**(16): p. 5879-5883.
245. Chandran, S.S. and C.A. Klebanoff, *T cell receptor-based cancer immunotherapy: Emerging efficacy and pathways of resistance.* Immunological reviews, 2019. **290**(1): p. 127-147.

246. Dotti, G., et al., *Design and development of therapies using chimeric antigen receptor-expressing T cells.* Immunological reviews, 2014. **257**(1): p. 107-126.
247. Sadelain, M., R. Brentjens, and I. Rivière, *The promise and potential pitfalls of chimeric antigen receptors.* Curr Opin Immunol, 2009. **21**(2): p. 215-23.
248. D'Aloia, M.M., et al., *CAR-T cells: the long and winding road to solid tumors.* Cell Death & Disease, 2018. **9**(3): p. 282.
249. Hollingsworth, R.E. and K. Jansen, *Turning the corner on therapeutic cancer vaccines.* npj Vaccines, 2019. **4**(1): p. 7.
250. Goydos, J.S., et al., *A phase I trial of a synthetic mucin peptide vaccine. Induction of specific immune reactivity in patients with adenocarcinoma.* J Surg Res, 1996. **63**(1): p. 298-304.
251. Marchand, M., et al., *Tumor regressions observed in patients with metastatic melanoma treated with an antigenic peptide encoded by gene MAGE-3 and presented by HLA-A1.* Int J Cancer, 1999. **80**(2): p. 219-30.
252. Disis, M.L., et al., *Generation of immunity to the HER-2/neu oncogenic protein in patients with breast and ovarian cancer using a peptide-based vaccine.* Clin Cancer Res, 1999. **5**(6): p. 1289-97.
253. Grunwitz, C. and L.M. Kranz, *mRNA Cancer Vaccines-Messages that Prevail.* Curr Top Microbiol Immunol, 2017. **405**: p. 145-164.
254. Yu, M. and O.J. Finn, *DNA vaccines for cancer too.* Cancer Immunol Immunother, 2006. **55**(2): p. 119-30.
255. Coughlin, C.M. and R.H. Vonderheide, *Targeting adult and pediatric cancers via cell-based vaccines and the prospect of activated B lymphocytes as a novel modality.* Cancer Biol Ther, 2003. **2**(5): p. 466-70.
256. Palucka, K. and J. Banchereau, *Dendritic-cell-based therapeutic cancer vaccines.* Immunity, 2013. **39**(1): p. 38-48.
257. Bol, K.F., et al., *Dendritic Cell–Based Immunotherapy: State of the Art and Beyond.* Clinical Cancer Research, 2016. **22**(8): p. 1897.
258. Kantoff, P.W., et al., *Sipuleucel-T immunotherapy for castration-resistant prostate cancer.* N Engl J Med, 2010. **363**(5): p. 411-22.
259. Finn, O.J., *Cancer vaccines: between the idea and the reality.* Nat Rev Immunol, 2003. **3**(8): p. 630-41.
260. Tan, A.C., A. Goubier, and H.E. Kohrt, *A quantitative analysis of therapeutic cancer vaccines in phase 2 or phase 3 trial.* J Immunother Cancer, 2015. **3**: p. 48.
261. Lu, L., et al., *Cross-sectional and longitudinal analysis of cancer vaccination trials registered on the US Clinical Trials Database demonstrates paucity of immunological trial endpoints and decline in registration since 2008.* Drug Des Devel Ther, 2014. **8**: p. 1539-53.
262. Karaki, S., et al., *Is There Still Room for Cancer Vaccines at the Era of Checkpoint Inhibitors.* Vaccines (Basel), 2016. **4**(4).
263. Garg, A.D., et al., *Integrating Next-Generation Dendritic Cell Vaccines into the Current Cancer Immunotherapy Landscape.* Trends Immunol, 2017. **38**(8): p. 577-593.
264. Vreeland, T.J., et al., *Gaining ground on a cure through synergy: combining checkpoint inhibitors with cancer vaccines.* Expert Rev Clin Immunol, 2016. **12**(12): p. 1347-1357.
265. Koerner, J., et al., *PLGA-particle vaccine carrying TLR3/RIG-I ligand Riboxxim synergizes with immune checkpoint blockade for effective anti-cancer immunotherapy.* Nat Commun, 2021. **12**(1): p. 2935.

266. Yoko Matsuzaki, et al., *Clinical Features of Influenza C Virus Infection in Children.* JID, 2006. **193**.
267. Ron A. M. Fouchier, et al., *Characterization of a Novel Influenza A Virus Hemagglutinin Subtype (H16) Obtained from Black-Headed Gulls.* Journal of Virology, 2005. **79**(5): p. 2814–2822.
268. Suxiang Tong, et al., *A distinct lineage of influenza A virus from bats.* Proc Natl Acad Sci U S A, 2012. **109**(11).
269. Wenjun Ma, Adolfo García-Sastre, and M. Schwemmle, *Expected and Unexpected Features of the Newly Discovered Bat Influenza A-like Viruses.* PLoS One, 2015.
270. Petrova, V.N. and C.A. Russell, *The evolution of seasonal influenza viruses.* Nat Rev Microbiol, 2018. **16**(1): p. 47-60.
271. Yumi Kanegae, et al., *Evolutionary Pattern of the Hemagglutinin Gene of Influenza B Viruses Isolated in Japan: Cocirculating Lineages in the Same Epidemic Season.* Journal of Virology, 1990. **64**(6).
272. Biere, B., B. Bauer, and B. Schweiger, *Differentiation of Influenza B Virus Lineages Yamagata and Victoria by Real-Time PCR.* Journal of Clinical Microbiology, 2010. **48**(4).
273. Webster, R.G., et al., *Evolution and Ecology of Influenza A Viruses.* Microbiological Reviews, 1992. **56**(1): p. 152-79.
274. Björn Olsen, et al., *Global Patterns of Influenza A Virus in Wild Birds.* Science, 2006. **312**.
275. Gavin J. D. Smith, D.V., Justin Bahl, , et al., *Origins and evolutionary genomics of the 2009 swine-origin H1N1 influenza A epidemic.* Nature, 2009. **459**.
276. Ignacio Mena, et al., *Origins of the 2009 H1N1 influenza pandemic in swine in Mexico.* eLife, 2016. **5**.
277. Smith, D.J., et al., *Mapping the Antigenic and Genetic Evolution of Influenza Virus.* Science, 2004. **305**(5682): p. 371-6.
278. Nobusawa, E. and K. Sato, *Comparison of the mutation rates of human influenza A and B viruses.* J Virol, 2006. **80**(7).
279. Garten, R.J., et al., *Antigenic and genetic characteristics of swine-origin 2009 A(H1N1) influenza viruses circulating in humans.* Science, 2009. **325**(5937): p. 197-201.
280. E. G. M. Berkhoff, et al., *Functional Constraints of Influenza A Virus Epitopes Limit Escape from Cytotoxic T Lymphocytes.* Journal of Virology, 2005. **79**(17): p. 11239–11246.
281. G.F. Rimmelzwaan, et al., *Sequence variation in the influenza A virus nucleoprotein associated with escape from cytotoxic T lymphocytes.* Virus Research, 2004. **103**: p. 97-100.
282. Kendal, A.P., et al., *Antigenic similarity of influenza A (H1N1) viruses from epidemics in 1977--1978 to "Scandinavian" strains isolated in epidemics of 1950 -- 1951.* Virology, 1978. **89**(2): p. 632-6.
283. Marios Koutsakos, et al., *Influenza lineage extinction during the COVID-19 pandemic?* Nat rev Microbiol, 2021.
284. Rafael Lozano, et al., *Global and regional mortality from 235 causes of death for 20 age groups in 1990 and 2010: a systematic analysis for the Global Burden of Disease Study 2010.* The Lancet, 2010.
285. Iuliano, A.A., et al., *Estimates of global seasonal influenza-associated respiratory mortality: a modelling study.* The Lancet, 2018. **391**(10127): p. 1285-1300.

286. Arun Kumar and S.B. Trine Sundebo Meldgaard, *Novel Platforms for the Development of a Universal influenza vaccine.* Front Immunol, 2018. **9**.
287. Mameli, C., et al., *Influenza Vaccination: Effectiveness, Indications, and Limits in the Pediatric Population.* Frontiers in pediatrics, 2019. **7**: p. 317-317.
288. Mameli, C., et al., *Influenza vaccine response: future perspectives.* Expert Opin Biol Ther, 2018. **18**(1): p. 1-5.
289. Han, T. and W.A. Marasco, *Structural basis of influenza virus neutralization.* Ann. N.Y. Acad. Sci., 2011(The Year in Immunology).
290. Ampofo, W.K., et al., *Improving influenza vaccine virus selection. Report of a WHO informal consultation held at WHO headquarters, Geneva, Switzerland, 14–16 June 2010.* 2010.
291. WHO. *Recommended composition of influenza virus vaccines for use in the 2020-2021 northern hemisphere influenza season*. 2020.
292. Barr, I.G., et al., *WHO recommendations for the viruses used in the 2013–2014 Northern Hemisphere influenza vaccine: Epidemiology, antigenic and genetic characteristics of influenza A(H1N1)pdm09, A(H3N2) and B influenza viruses collected from October 2012 to January 2013.* Vaccine, 2014. **32**: p. 4713–4725.
293. de Jong, J.C., et al., *Mismatch Between the 1997/1998 Influenza Vaccine and the Major Epidemic A(H3N2) Virus Strain as the Cause of an Inadequate Vaccine-Induced Antibody Response to This Strain in the Elderly.* Journal of Medical Virology, 2000. **61**: p. 94-99.
294. Seth J. Zost, et al., *Contemporary H3N2 influenza viruses have a glycosylation site that alters binding of antibodies elicited by egg-adapted vaccine strains.* Proc Natl Acad Sci U S A, 2017. **114**(47).
295. Ilaria Manini, et al., *Egg-Independent Influenza Vaccines and Vaccine Candidates.* Vaccines (Basel), 2017. **5**(18).
296. Barr, I.G., et al., *Cell culture-derived influenza vaccines in the severe 2017–2018 epidemic season: a step towards improved influenza vaccine effectiveness.* npj Vaccines, 2018. **3**(44).
297. Prevention, C.f.D.C.a. *Recombinant Influenza (Flu) Vaccine* 2021; Available from: https://www.cdc.gov/flu/protect/vaccine/qa_flublok-vaccine.htm.
298. Irina Isakova-Sivak, et al., *Genetic bases of the temperature-sensitive phenotype of a master donor virus used in live attenuated influenza vaccines: A/Leningrad/134/17/57 (H2N2).* Virology, 2011. **412**.
299. Fischer, W.A., 2nd, et al., *Restricted replication of the live attenuated influenza A virus vaccine during infection of primary differentiated human nasal epithelial cells.* Vaccine, 2015. **33**(36): p. 4495-504.
300. Belshe, R.B., et al., *Efficacy of vaccination with live attenuated, coldadapted, trivalent, intranasal influenza virus vaccine against a variant (A/Sydney) not contained in the vaccine.* The Journal of Pediatrics, 1999. **136**(2).
301. Daniel F. Hoft, et al., *Live and Inactivated Influenza Vaccines Induce Similar Humoral Responses, but Only Live Vaccines Induce Diverse T-Cell Responses in Young Children.* JID, 2011. **204**.
302. Herve Caspard, et al., *Live-Attenuated Influenza Vaccine Effectiveness in Children From 2009 to 2015–2016: A Systematic Review and Meta-Analysis.* Open Forum Infectious Diseases, 2017.
303. Herve Casparda, et al., *Effectiveness of live attenuated influenza vaccine and inactivated influenza vaccine in children 2–17 years of age in 2013–2014 in the United States.* Vaccine, 2016. **34**: p. 77-82.

304. Schmidt, A. and D. Lapuente, *T Cell Immunity against Influenza: The Long Way from Animal Models Towards a Real-Life Universal Flu Vaccine.* Viruses, 2021. **13**(2).
305. D J Topham, R A Tripp, and P.C. Doherty, *CD8+ T cells clear influenza virus by perforin or Fas-dependent processes.* J Immunol, 1997. **159**: p. 5197-5200.
306. Doherty, P.C., et al., *Effector CD4+ and CD8+ T-cell mechanisms in the control of respiratory virus infections.* Immunological Reviews, 1997. **159**: p. 105-117.
307. Jacob E. Kohlmeier, et al., *Type I Interferons Regulate Cytolytic Activity of Memory CD8+ T Cells in the Lung Airways during Respiratory Virus Challenge.* Immunity, 2010. **33**: p. 96-105.
308. Saranya Sridhar, et al., *Cellular immune correlates of protection against symptomatic pandemic influenza.* Nat Med, 2013. **19**(10).
309. Butreddy, A., et al., *PLGA/PLA-Based Long-Acting Injectable Depot Microspheres in Clinical Use: Production and Characterization Overview for Protein/Peptide Delivery.* Int J Mol Sci, 2021. **21**(8884).
310. Gander, B., *Trends in particulate antigen and DNA delivery systems for vaccines.* Adv Drug Deliv Rev, 2005. **57**(3): p. 321-3.
311. Li, S., *Hydrolytic degradation characteristics of aliphatic polyesters derived from lactic and glycolic acids.* Journal of Biomedical Materials Research, 1999. **48**(3): p. 342-353.
312. Piperno, A., et al., *Recent Advances and Challenges in Gene Delivery Mediated by Polyester-Based Nanoparticles.* Int J Nanomedicine, 2021. **16**: p. 5981-6002.
313. Lagreca, E., et al., *Recent advances in the formulation of PLGA microparticles for controlled drug delivery.* Progress in Biomaterials, 2020. **9**: p. 153-174.
314. Gentile, P., et al., *An Overview of Poly(lactic-co-glycolic) Acid (PLGA)-Based Biomaterials for Bone Tissue Engineering.* International Journal of Molecular Sciences, 2014. **15**(3): p. 3640-3659.
315. Jain, A., et al., *Injectable formulations of poly(lactic acid) and its copolymers in clinical use.* Advanced Drug Delivery Reviews, 2016. **107**: p. 213-227.
316. Johansen, P., et al., *Immunogenicity of single-dose diphtheria vaccines based on PLA/PLGA microspheres in guinea pigs.* Vaccine, 1999. **18**(3-4): p. 209-15.
317. Peyre, M., et al., *An experimental divalent vaccine based on biodegradable microspheres induces protective immunity against tetanus and diphtheria.* Journal of Pharmaceutical Sciences, 2003. **92**(5): p. 957-966.
318. Eldridge, J.H., et al., *Vaccine-containing biodegradable microspheres specifically enter the gut-associated lymphoid tissue following oral administration and induce a disseminated mucosal immune response.* Adv Exp Med Biol, 1989. **251**: p. 191-202.
319. Yeh, M. and C. Chiang, *Inactive Vibrio cholerae whole-cell vaccine-loaded biodegradable microparticles: in vitro release and oral vaccination.* J Microencapsul, 2004. **21**(1): p. 91-106.
320. Yeh, M.K., et al., *Oral immunogenicity of the inactivated Vibrio cholerae whole-cell vaccine encapsulated in biodegradable microparticles.* J Control Release, 2002. **82**(2-3): p. 237-47.
321. Herrmann, V.L., et al., *Cytotoxic T cell vaccination with PLGA microspheres interferes with influenza A virus replication in the lung and suppresses the infectious disease.* J Control Release, 2015. **216**: p. 121-31.
322. Herrmann, V.L., et al., *The STEAP1262–270 Peptide Encapsulated into PLGA Microspheres Elicits Strong Cytotoxic T Cell Immunity in HLA-A*0201*

Transgenic Mice—A New Approach to Immunotherapy Against Prostate Carcinoma. The Prostate, 2016. **76**: p. 456-468.
323. Mueller, M., et al., *Coencapsulation of tumor lysate and CpG-ODN in PLGA-microspheres enables successful immunotherapy of prostate carcinoma in TRAMP mice.* J Control Release, 2012. **162**(1): p. 159-66.
324. Mueller, M., et al., *Tumor eradication by immunotherapy with biodegradable PLGA microspheres--an alternative to incomplete Freund's adjuvant.* Int J Cancer, 2011. **129**(2): p. 407-16.
325. Schlosser, E., et al., *TLR ligands and antigen need to be coencapsulated into the same biodegradable microsphere for the generation of potent cytotoxic T lymphocyte responses.* Vaccine, 2008. **26**(13): p. 1626-37.
326. Waeckerle-Men, Y., et al., *Encapsulation of proteins and peptides into biodegradable poly(D,L-lactide-co-glycolide) microspheres prolongs and enhances antigen presentation by human dendritic cells.* Vaccine, 2006. **24**(11): p. 1847-57.
327. Waeckerle-Men, Y. and M. Groettrup, *PLGA microspheres for improved antigen delivery to dendritic cells as cellular vaccines.* Adv Drug Deliv Rev, 2005. **57**(3): p. 475-82.
328. Jiang, W., et al., *Biodegradable poly(lactic-co-glycolic acid) microparticles for injectable delivery of vaccine antigens.* Adv Drug Deliv Rev, 2005. **57**(3): p. 391-410.
329. Cleland, J.L., *Single-administration vaccines: controlled-release technology to mimic repeated immunizations.* Trends Biotechnol, 1999. **17**(1): p. 25-9.
330. Langer, R., J.L. Cleland, and J. Hanes, *New advances in microsphere-based single-dose vaccines.* Adv Drug Deliv Rev, 1997. **28**(1): p. 97-119.
331. Aguado, M.T., *Future approaches to vaccine development: single-dose vaccines using controlled-release delivery systems.* Vaccine, 1993. **11**(5): p. 596-7.
332. Coombes, A.G., et al., *Single dose, polymeric, microparticle-based vaccines: the influence of formulation conditions on the magnitude and duration of the immune response to a protein antigen.* Vaccine, 1996. **14**(15): p. 1429-38.
333. Gupta, R.K., M. Singh, and D.T. O'Hagan, *Poly(lactide-co-glycolide) microparticles for the development of single-dose controlled-release vaccines.* Adv Drug Deliv Rev, 1998. **32**(3): p. 225-246.
334. Lin, C.-Y., et al., *Biodegradable polymeric microsphere-based vaccines and their applications in infectious diseases.* Human Vaccines & Immunotherapeutics, 2015. **11**(3): p. 650-656.
335. Men, Y., et al., *A single administration of tetanus toxoid in biodegradable microspheres elicits T cell and antibody responses similar or superior to those obtained with aluminum hydroxide.* Vaccine, 1995. **13**(7): p. 683-689.
336. I Ré, M., *Microencapsulation by spray drying.* Drying Technology, 1998. **16**(6): p. 1195-1236.
337. Patel, R.P., M.P. Patel, and A.M. Suthar, *Spray drying technology: An overview.* Indian Journal of Science and Technology, 2009. **2**: p. 44-47.
338. Giunchedi, P. and U. Conte, *Spray-drying as a preparation method of microparticulate drug delivery systems: an overview.* Stp Pharma Sciences, 1995. **5**: p. 276-290.
339. Giteau, A., et al., *How to achieve sustained and complete protein release from PLGA-based microparticles?* Int J Pharm, 2008. **350**: p. 14-26.

340. Shen, H., et al., *Enhanced and prolonged cross-presentation following endosomal escape of exogenous antigens encapsulated in biodegradable nanoparticles.* Immunology, 2006. **117**(1): p. 78-88.
341. Waeckerle-Men, Y., et al., *Phenotype and functional analysis of human monocyte-derived dendritic cells loaded with biodegradable poly(lactide-co-glycolide) microspheres for immunotherapy.* J Immunol Methods, 2004. **287**(1-2): p. 109-124.
342. Heit, A., et al., *Antigen co-encapsulated with adjuvants efficiently drive protective T cell immunity.* Eur J Immunol, 2007. **37**(8): p. 2063-74.
343. Schliehe, C., et al., *CD8- dendritic cells and macrophages cross-present poly(D,L-lactate-co-glycolate) acid microsphere-encapsulated antigen in vivo.* J Immunol, 2011. **187**(5): p. 2112-21.
344. Shen, L. and K.L. Rock, *Cellular protein is the source of cross-priming antigen in vivo.* Proc Natl Acad Sci U S A, 2004. **101**(9): p. 3035-3040.
345. Nakamura, K., et al., *Characterization of mouse melanoma cell lines by their mortal malignancy using an experimental metastatic model.* Life Sciences, 2002. **70**(7): p. 791-798.
346. Dolan, B.P., et al., *Defective ribosomal products are the major source of antigenic peptides endogenously generated from influenza A virus neuraminidase.* J Immunol, 2010. **184**(3): p. 1419-24.
347. Matrosovich, M., et al., *New low-viscosity overlay medium for viral plaque assays.* Virology Journal, 2006. **3**(1): p. 63.
348. Sandoval, F., et al., *Mucosal Imprinting of Vaccine-Induced CD8+ T Cells Is Crucial to Inhibit the Growth of Mucosal Tumors.* Sci Transl Med, 2013. **5**.
349. Cuburu, N., et al., *Intravaginal immunization with HPV vectors induces tissue-resident CD8+ T cell responses.* J Clin Invest, 2012. **122**(12): p. 4606-20.
350. Decrausaz, L., et al., *Intravaginal live attenuated Salmonella increase local antitumor vaccine-specific CD8(+) T cells.* Oncoimmunology, 2013. **2**(1): p. e22944.
351. Butcher, E.C. and L.J. Picker, *Lymphocyte Homing and Homeostasis.* Science, 1996. **272**(5258): p. 60-67.
352. Mackay, L.K., et al., *Cutting edge: CD69 interference with sphingosine-1-phosphate receptor function regulates peripheral T cell retention.* J Immunol, 2015. **194**(5): p. 2059-63.
353. Topham, D.J. and E.C. Reilly, *Tissue-Resident Memory CD8(+) T Cells: From Phenotype to Function.* Front Immunol, 2018. **9**: p. 515.
354. Mueller, S.N. and L.K. Mackay, *Tissue-resident memory T cells: local specialists in immune defence.* Nat Rev Immunol, 2016. **16**(2): p. 79-89.
355. Brinkmann, V., et al., *The immune modulator FTY720 targets sphingosine 1-phosphate receptors.* J Biol Chem, 2002. **277**(24): p. 21453-7.
356. Morris, M.A., et al., *Transient T cell accumulation in lymph nodes and sustained lymphopenia in mice treated with FTY720.* Eur J Immunol, 2005. **35**(12): p. 3570-80.
357. Casey, K.A., et al., *Antigen-independent differentiation and maintenance of effector-like resident memory T cells in tissues.* J Immunol, 2012. **188**(10): p. 4866-75.
358. Gotch, F.M., et al., *Identification of viral molecules recognized by Influenza-specific human cytotoxic T lymphocytes.* Journal of Experimental Medicine, 1987. **165**: p. 408-416.
359. McMichael, A.J., et al., *Cytotoxic T-Cell Immunity to Influenza.* N Engl J Med, 1983. **309**: p. 13-17.

360. Jonges, M., et al., *Influenza virus inactivation for studies of antigenicity and phenotypic neuraminidase inhibitor resistance profiling.* Journal of clinical microbiology, 2010. **48**(3): p. 928-940.
361. Herrera-Rodriguez, J., et al., *Inactivated or damaged? Comparing the effect of inactivation methods on influenza virions to optimize vaccine production.* Vaccine, 2019. **37**(12): p. 1630-1637.
362. Zhong, W., et al., *Genome-wide Characterization of a Viral Cytotoxic T Lymphocyte Epitope Repertoire *.* Journal of Biological Chemistry, 2003. **278**(46): p. 45135-45144.
363. Chen, W., et al., *Immunoproteasomes Shape Immunodominance Hierarchies of Antiviral Cd8+ T Cells at the Levels of T Cell Repertoire and Presentation of Viral Antigens.* Journal of Experimental Medicine, 2001. **193**(11): p. 1319-1326.
364. Zens, K.D., J.K. Chen, and D.L. Farber, *Vaccine-generated lung tissue-resident memory T cells provide heterosubtypic protection to influenza infection.* JCI Insight, 2016. **1**(10).
365. Lavelle, E.C. and R.W. Ward, *Mucosal vaccines — fortifying the frontiers.* Nature Reviews Immunology, 2021.
366. Jahnmatz, M., et al., *Safety and immunogenicity of the live attenuated intranasal pertussis vaccine BPZE1: a phase 1b, double-blind, randomised, placebo-controlled dose-escalation study.* Lancet Infect Dis, 2020. **20**(11): p. 1290-1301.
367. Lin, A., et al., *Live attenuated pertussis vaccine BPZE1 induces a broad antibody response in humans.* J Clin Invest, 2020. **130**(5): p. 2332-2346.
368. Bull, N.C., et al., *Enhanced protection conferred by mucosal BCG vaccination associates with presence of antigen-specific lung tissue-resident PD-1(+) KLRG1(-) CD4(+) T cells.* Mucosal Immunol, 2019. **12**(2): p. 555-564.
369. Uddback, I.E.M., et al., *Combined local and systemic immunization is essential for durable T-cell mediated heterosubtypic immunity against influenza A virus.* Scientific Reports, 2016. **6**(1): p. 20137.
370. Kumar, B.V., et al., *Functional heterogeneity of human tissue-resident memory T cells based on dye efflux capacities.* JCI insight, 2018. **3**(22): p. e123568.
371. Wakim, L.M., et al., *The molecular signature of tissue resident memory CD8 T cells isolated from the brain.* J Immunol, 2012. **189**(7): p. 3462-71.
372. Szabo, P.A., et al., *Single-cell transcriptomics of human T cells reveals tissue and activation signatures in health and disease.* Nature Communications, 2019. **10**(1): p. 4706.
373. Park, S.L., L.K. Mackay, and T. Gebhardt, *Distinct recirculation potential of CD69(+)CD103(-) and CD103(+) thymic memory CD8(+) T cells.* Immunol Cell Biol, 2016. **94**(10): p. 975-980.
374. Steinert, Elizabeth M., et al., *Quantifying Memory CD8 T Cells Reveals Regionalization of Immunosurveillance.* Cell, 2015. **161**(4): p. 737-749.
375. Mandala, S., et al., *Alteration of lymphocyte trafficking by sphingosine-1-phosphate receptor agonists.* Science, 2002. **296**(5566): p. 346-9.
376. Siracusa, F., et al., *Maintenance of CD8(+) memory T lymphocytes in the spleen but not in the bone marrow is dependent on proliferation.* Eur J Immunol, 2017. **47**(11): p. 1900-1905.
377. Uddbäck, I., et al., *Long-term maintenance of lung resident memory T cells is mediated by persistent antigen.* Mucosal Immunology, 2021. **14**(1): p. 92-99.

378. Van Braeckel-Budimir, N., et al., *Repeated Antigen Exposure Extends the Durability of Influenza-Specific Lung-Resident Memory CD8+ T Cells and Heterosubtypic Immunity.* Cell Reports, 2018. **24**: p. 3374–3382.
379. van Gisbergen, K., K.D. Zens, and C. Münz, *T-cell memory in tissues.* Eur J Immunol, 2021. **51**(6): p. 1310-1324.
380. Chang, M.-H., et al., *Decreased Incidence of Hepatocellular Carcinoma in Hepatitis B Vaccinees: A 20-Year Follow-up Study.* JNCI: Journal of the National Cancer Institute, 2009. **101**(19): p. 1348-1355.
381. Markowitz, L.E., et al., *Prevalence of HPV After Introduction of the Vaccination Program in the United States.* Pediatrics, 2016. **137**(3).
382. Schiller, J.T., X. Castellsagué, and S.M. Garland, *A review of clinical trials of human papillomavirus prophylactic vaccines.* Vaccine, 2012. **30 Suppl 5**(0 5): p. F123-38.
383. Guo, T., D.W. Eisele, and C. Fakhry, *The potential impact of prophylactic human papillomavirus vaccination on oropharyngeal cancer.* Cancer, 2016. **122**(15): p. 2313-2323.
384. Joshi, V.B., et al., *Tumor lysate-loaded biodegradable microparticles as cancer vaccines.* Expert Review of Vaccines, 2014. **13**(1): p. 9-15.
385. Sun, Y.Y., et al., *Local HPV Recombinant Vaccinia Boost Following Priming with an HPV DNA Vaccine Enhances Local HPV-Specific CD8+ T-cell-Mediated Tumor Control in the Genital Tract.* Clin Cancer Res, 2016. **22**(3): p. 657-69.
386. Purwar, R., et al., *Resident memory T cells (T(RM)) are abundant in human lung: diversity, function, and antigen specificity.* PLoS One, 2011. **6**(1): p. e16245.
387. Koutsakos, M., et al., *Human CD8(+) T cell cross-reactivity across influenza A, B and C viruses.* Nat Immunol, 2019. **20**(5): p. 613-625.
388. Pizzolla, A., et al., *Resident memory CD8+ T cells in the upper respiratory tract prevent pulmonary influenza virus infection.* Science Immunology, 2017. **2**(12): p. eaam6970.
389. Stolley, J.M., et al., *Retrograde migration supplies resident memory T cells to lung-draining LN after influenza infection.* J Exp Med, 2020. **217**(8).
390. Zhao, J., J. Zhao, and S. Perlman, *T Cell Responses Are Required for Protection from Clinical Disease and for Virus Clearance in Severe Acute Respiratory Syndrome Coronavirus-Infected Mice.* Journal of Virology, 2010. **84**(18): p. 9318-9325.
391. Liao, M., et al., *Single-cell landscape of bronchoalveolar immune cells in patients with COVID-19.* Nature Medicine, 2020. **26**(6): p. 842-844.
392. Grau-Expósito, J., et al., *Peripheral and lung resident memory T cell responses against SARS-CoV-2.* Nature Communications, 2021. **12**(1): p. 3010.
393. Gola, A., et al., *Prime and target immunization protects against liver-stage malaria in mice.* Science Translational Medicine, 2018. **10**(460): p. eaap9128.
394. Kingstad-Bakke, B., et al., *Polymeric Pathogen-Like Particles-Based Combination Adjuvants Elicit Potent Mucosal T Cell Immunity to Influenza A Virus.* Frontiers in Immunology, 2021. **11**(3771).
395. Jeyanathan, M., et al., *New Tuberculosis Vaccine Strategies: Taking Aim at Un-Natural Immunity.* Trends in Immunology, 2018. **39**(5): p. 419-433.
396. Shacklett, B.L., A.L. Ferre, and B.E. Kiniry, *Defining T Cell Tissue Residency in Humans: Implications for HIV Pathogenesis and Vaccine Design.* Current HIV/AIDS reports, 2020. **17**(2): p. 109-117.

397. Sabbaghi, A., et al., *Inactivation methods for whole influenza vaccine production.* Reviews in Medical Virology, 2019. **29**(6): p. e2074.
398. Krammer, F., *SARS-CoV-2 vaccines in development.* Nature, 2020. **586**(7830): p. 516-527.
399. Delrue, I., et al., *Inactivated virus vaccines from chemistry to prophylaxis: merits, risks and challenges.* Expert Rev Vaccines, 2012. **11**(6): p. 695-719.
400. Fredenberg, S., et al., *The mechanisms of drug release in poly(lactic-co-glycolic acid)-based drug delivery systems—A review.* International Journal of Pharmaceutics, 2011. **415**(1): p. 34-52.
401. Kim, E.H., G.Y. Han, and H. Nguyen, *An Adenovirus-Vectored Influenza Vaccine Induces Durable Cross-Protective Hemagglutinin Stalk Antibody Responses in Mice.* Viruses, 2017. **9**(8).
402. Tsen, S.W., et al., *Chemical-free inactivated whole influenza virus vaccine prepared by ultrashort pulsed laser treatment.* J Biomed Opt, 2015. **20**(5): p. 051008.
403. Uittenbogaard, J.P., et al., *Reactions of beta-propiolactone with nucleobase analogues, nucleosides, and peptides: implications for the inactivation of viruses.* J Biol Chem, 2011. **286**(42): p. 36198-214.
404. Peter C. Soema, et al., *Current and next generation influenza vaccines: Formulation and production strategies.* European Journal of Pharmaceutics and Biopharmaceutics, 2015. **94**: p. 251-263.
405. Chen, J., et al., *Advances in Development and Application of Influenza Vaccines.* Frontiers in Immunology, 2021. **12**(2740).
406. Hilbert, A.K., U. Fritzsche, and T. Kissel, *Biodegradable microspheres containing influenza A vaccine: immune response in mice.* Vaccine, 1999. **17**(9-10): p. 1065-73.
407. Zhang, W., et al., *Immunopotentiator-Loaded Polymeric Microparticles as Robust Adjuvant to Improve Vaccine Efficacy.* Pharm Res, 2015. **32**(9): p. 2837-50.

8. Record of contributions

All experimental results shown in this work were obtained by me or entirely under my supervision. The identification of the immunization protocol (Figure 8) was performed during the VTK 2017 together with Clarissa Rominger-Baumann. She worked entirely under my supervision.

FACS sorting of the $Ova^{+}Luc^{+}$B16BL6 cells was performed by Ricarda Schwab and Annette Sommershof at the FlowKon Flow Cytometry facility at the University of Konstanz.

The SEM pictures (Figure 27) were taken by Michael Laumann at the Electron microscopy center of the University of Konstanz.

Cloning for generation of the $Ova^{+}Luc^{+}$B16BL6 cells was prepared with major help from Tobias Held.

The graphical abstract was prepared with major help from Dennis Horvath.

The experimental results presented in Figures 8, 9, 10, 11, 12, 13, 20, 22, 24 as well as the M1/CpG image from Figure 27 have been submitted to the “Journal of Controlled Release” for publication. The text accompanying these figures in the results and discussion section of the manuscript has been copied and occasionally modified in this thesis. The manuscript was written by me, with some minor changes by Annette Sommershof and Marcus Groettrup.

9. Acknowledgements

First of all, I would like to express my sincere thanks and appreciation to Prof. Dr. Marcus Groettrup for taking me on as a Fast-Track PhD student and giving me the opportunity to perform my PhD in his group. Thank you also for the many scientific discussions and troubleshooting tips when I was faced with experimental difficulties.

I also want to thank Prof. Dr. Oliver Planz for kindly agreeing to serve as a reviewer of this thesis and for the help and advice concerning the problems I encountered with the IAV experiments.

Moreover, I want to thank Prof. Dr. Thomi Brunner for the scientific input as part of my thesis committee and for agreeing to be part of my PhD defense committee.

Thank you also to Dr. Annette Sommershof, who agreed to be my supervisor in addition to working at the FlowKon. I appreciate the time you took to discuss my project and proofread my manuscript and thesis.

Next, I would like to thank all the members of the Groettrup lab. Thank you especially to Tobi, Richi, Christian and Julia for your help in the lab and for sharing your experimental knowledge with me at the beginning of my thesis. I really would have been lost without your help. As the members of the lab slowly changed with time, the people who I could talk to about difficulties regarding my experiments changed. I'm really grateful to have had the opportunity to discuss my results and problems in the lab with Franzi, Marta and Dennis. Thank you so much! I really enjoyed it.

Thank you also to the other members of the lab: Michi and Gunter for your scientific input, help and lectures on weapons, diving and life in the DDR. I really learnt a lot! :) Thank you also to Heike, Gerardo, Ulli, Tina, Miki, Nico, Gretl, Professor President Dr. Jun Li, Kritika, Natalie and Jinjing.

Moreover, I want to thank my fellow PhD colleagues Franzi, Marta, Katharina, Flo, Dennis and Dennis for the great atmosphere in the lab and for becoming good friends. Thanks especially to my coffee group for the much needed fun breaks. Thanks also to my great office "roommates" for introducing me to the drübergegunterte way of life and Äkta. My life has significantly (****) improved now that I know what my drübergegunterte version looks like. Thanks for that! :)

Thank you to the “Herde” (Alina, Anika, Hane, Kathrin, Lena, Luci, Maria and Nora), the people who I started my scientific career with and who made the Bachelor years in Konstanz the best time of my life so far. I’m so glad to have met you all and, who knows, maybe one day we can start “Hanika Pharma” after all?

Last, but not least, thank you to my family and Tobi for always supporting me and for being there for me when (lab) life kept throwing me lemons. I would not be where I am now without you.